PROTEIN ADSORPTION TO CHEMISORBED POLYETHYLENE OXIDE THIN FILMS

BY

LARRY DAVID UNSWORTH,
B.Sc.

PROTEIN ADSORPTION TO CHEMISORBED PEO THIN FILMS

PROTEIN ADSORPTION TO CHEMISORBED POLYETHYLENE OXIDE THIN FILMS.

By

LARRY DAVID UNSWORTH, B.Sc.

A Thesis
Submitted to the School of Graduate Studies
in Partial Fulfilment of the Requirements
for the Degree
Doctor of Philosophy

McMaster University

DOCTOR OF PHILOSOPHY (2005) McMaster University
(Chemical Engineering) Hamilton, Ontario

TITLE: PROTEIN ADSORPTION TO CHEMISORBED POLYETHYLENE OXIDE THIN FILMS.

AUTHOR: Larry David Unsworth, B.Sc. –With Distinction, Co-op (University of Alberta)

SUPERVISORS: University Professor J.L. Brash
Associate Professor H. Sheardown

NUMBER OF PAGES: xii, 175

ABSTRACT

A major area of biomaterials research is the development of surfaces that reduce or eliminate non-specific protein adsorption. End-tethered PEO has been shown to reduce protein and cell interactions at the tissue-material interface; the effects of polymer chain length, chain density and end-group chemistry are not yet completely understood. To date, there have been few detailed, systematic studies that have attempted to elucidate the effect of end-tethered PEO conformation, surface chain density, molecular weight (MW) and end-group chemistry on protein adsorption at the solid-liquid interface.

In the research described in this thesis PEOs of varying molecular weight (600, 750, 2000 and 5000 MW) and terminal functional group (-OH, -OCH_3) were thiolated and chemisorbed to gold coated silicon wafers for the purpose of characterizing film thickness and surface chain density for direct correlation to protein adsorption behaviour. Tethered chain density was varied by manipulating PEO solubility and chemisorption time, which in principle, should allow for variable, controlled surface chain density from low to very high values. PEO layers were characterized using water contact angles, X-ray photoelectron spectroscopy (XPS), self-nulling ellipsometry and neutron reflectometry (NR). The adsorption of two proteins having widely different molecular weights was examined using radiolabeling and ellipsometry to ascertain the effectiveness of these surfaces in resisting protein adsorption and to provide information about the nature of protein interactions with end-tethered PEO surfaces. These experiments were carried out using single or binary protein solutions in buffer. Adsorption from plasma was also

investigated: (1) by Western Blot analysis of the proteins eluted after plasma contact; (2) *via* experiments using radiolabeled fibrinogen.

The chemisorption of thiolated PEO to gold coated silicon wafers proved to be an effective method for producing surfaces with variable, controlled chain densities. Also, it was apparent that the chain densities obtained were not only among the highest ever reported for these systems, but also that the range of achievable chain density was very broad for all molecular weights studied. Neutron reflectometry and ellipsometry measurements gave values of chain density that were the same within experimental error. For the 750 MW PEO, *in situ* neutron reflectometry yielded novel information about the evolution of layer structure, as the surface filled, for layers formed under high and low solubility conditions. It was concluded from these experiments: (1) that protein adsorption passed through a minimum as PEO volume fraction increased, the minimum occurring at a PEO volume fraction of ~0.39. This is a novel observation for PEO-based inhibition of protein adsorption; (2) that at high chain density there may be regions within the PEO layer where the effective concentration is above the solubility limit of PEO in aqueous solution. It is hypothesized that in these regions the polymer has been "forced" from solution, forming hydrophobic patches that facilitate increased protein adsorption at high chain density.

Initial single protein adsorption experiments using radiolabeled proteins showed that resistance to fibrinogen passed through a maximum as chain density increased and that at a chain density of ~0.5 chains/nm^2 protein adsorption was suppressed to about the same extent (80% decrease in adsorption compared to unmodified gold) for 750 and 2000

MW PEO layers. Further study of single protein adsorption using *in situ* ellipsometry showed similar trends: i.e. adsorption minima for the 750 and 2000 MW systems were similar and occurred at similar chain densities (in this case for both fibrinogen and lysozyme). The observed fibrinogen and lysozyme adsorption trends suggest that chain density, not chain length, is the major determinant of protein resistance. Furthermore, at chain densities of ~ 0.5 chains/nm^2, protein resistance (expressed as fractional reduction compared to the control) seems to be independent of protein size. It is hypothesized that at high chain density, the chemisorbed PEO becomes dehydrated yielding a surface that is less protein resistant. This idea is substantiated by neutron reflectometry data.

Experiments on adsorption from plasma were used to evaluate the surfaces determined to be 'optimal' in reducing single protein adsorption. Vroman effect type experiments, using ^{125}I labeled fibrinogen added to the plasma as a tracer, showed that PEO layers formed from solutions near the cloud point adsorbed the lowest amounts of fibrinogen. Layers of OH-terminated 600 MW PEO showed almost complete suppression (versus controls) of the Vroman peak. Respective Vroman peak amounts of adsorbed fibrinogen for 600-OH, 750-OCH_3 and 2000-OCH_3 were 20 ± 1, 70 ± 20, and 50 ± 3 ng/cm^2 compared to 400 ng/cm^2 for unmodified gold; adsorption levels at higher plasma concentration were 6.7 ± 0.6, 16 ± 9 and 12 ± 3 ng/cm^2 respectively compared to 150 ng/cm^2 for gold. Fibrinogen adsorption from plasma was not significantly different for surfaces prepared with PEO of molecular weight 750 and 2000 when the chain density was the same (~0.5 chains/nm^2) supporting the conclusion that chain density may be the key property for suppression of protein adsorption. Furthermore, the data suggested a

distal chain end group effect such that fibrinogen adsorption was reduced and/or its displacement from the surface facilitated, on hydroxyl-terminated compared to methoxy-terminated PEO layers.

SDS-PAGE gels and immunoblots of the proteins eluted from these surfaces after plasma contact showed that a number of proteins were adsorbed, including fibrinogen, albumin, C3 and apolipoprotein A-I. However, the blot responses were weak for all four proteins of the contact system; some complement activation was observed on all of the surfaces studied.

ACKNOWLEDGEMENTS

I have had the pleasure of working with two excellent supervisors and would like to take this opportunity to thank them both for their guidance, patience and encouragement. I would like to thank Dr. Brash for allowing me enough 'academic-freedom' so that I could control the research project, while knowing when to rein me in. I would like to express my gratitude to Dr. Sheardown for providing encouragement, guidance and the resources to excel.

I would like to continue by acknowledging the researchers of the Brash/Sheardown labs. Although initially Glenn and Rena helped me with experimental techniques and locating things in the lab, over the past few years I have come to value their friendship, encouragement and enthusiasm. Jacques, due to your approachability and intelligence I initially considered you a mentor, but I was glad that we were able to forge a friendship and will always remember our diverse (and some times heated) discussions. I was fortunate to meet and befriend many others during my time at McMaster and would also like to thank them for their friendship/assistance as well: Sarah, Steve, Lindsay, Meghan, Jiahong, ZhanXu, Bettina, Alex, Ella, Ed, Chris, Mark and Brandi.

Without the support of family this project would never have succeeded. That said, I would like to acknowledge the steadfast support, saintly patience and ever-loving spirit of my lovely and beautiful wife. Nancy, if it were possible to co-author a Ph.D. thesis surely you would be included. Without your presence I would never have been able to persevere and succeed in this work, thank you. I would like to acknowledge my two Muses, Matthew and Hannah 'Banana'. May I always be as zealous as they are about learning new things and observing the world around us. I would also like to thank my Mother and Aunt Lorrain for their support in the early years. Finally, I would like to thank my Great-Grandma Francis, Grandpa Louis and Grandma Laura for their sacrifice in providing the required foundation and for daring me to dream: some perhaps being departed, but their contribution will never be forgotten.

TABLE OF CONTENTS

TITLE PAGE I

DESCRIPTIVE NOTE II

ABSTRACT III

ACKNOWLEDGEMENTS VII

TABLE OF CONTENTS VIII

LIST OF FIGURES XI

LIST OF TABLES XII

1.0 INTRODUCTION 1

1.1 REFERENCES 3

2.0 LITERATURE REVIEW 4

2.1 CHEMISORPTION: THIOL-GOLD INTERACTIONS 4
2.2 PEO STRUCTURE AND PROPERTIES 5
2.2.1 PEO IN SOLUTION 6
2.2.1.1 Effect of solvent on PEO structure 6
2.2.1.2 Cloud Point: Definition and effect on PEO Excluded Volume 7
2.3 PROTEINS AND THEIR INTERACTIONS AT INTERFACES 9
2.3.1 PROTEIN STRUCTURE 10
2.3.1.1 Fibrinogen 11
2.3.1.2 Lysozyme 13
2.4 MACROMOLECULAR ADSORPTION AT THE SOLID-LIQUID INTERFACE 15
2.4.1 SURFACE FORCES 15
2.4.1.1 Primary Interactions 15
2.4.1.2 Macromolecular Adsorption 19
2.4.2 POLYMER ADSORPTION AND END-TETHERED POLYMER CONFORMATION 19
2.4.3 DIFFERENCES BETWEEN POLYMER AND GLOBULAR PROTEIN ADSORPTION 23
2.4.4 COMPETITIVE ADSORPTION OF PROTEINS: THE VROMAN EFFECT 24
2.5 PEO MEDIATED PROTEIN REPULSION 25
2.5.1 STERIC STABILIZATION/REPULSION 26
2.5.2 PROPERTIES OF PEO AFFECTING PROTEIN ADSORPTION 29
2.5.2.1 'Masking' of Surface Forces by PEO 33
2.5.2.2 Hydration Forces and Interphase Water 35
2.5.3 PROTEIN ADSORPTION TO OLIGO(ETHYLENE OXIDE) ALKANETHIOLS 37
2.6 REVIEW OF RELEVANT SURFACE ANALYSIS METHODS 39
2.6.1 ELLIPSOMETRY: INTRODUCTION 39
2.6.2 ELLIPSOMETRY: COMPARISON WITH OTHER METHODS 40
2.6.3 ELLIPSOMETRY: ADSORPTION STUDIES 41

2.6.4 NEUTRON REFLECTOMETRY: INTRODUCTION 42
2.6.5 NEUTRON REFLECTOMETRY: COMPARISON WITH OTHER METHODS 44
2.6.6 NEUTRON REFLECTOMETRY: ADSORPTION STUDIES 45
2.7 REFERENCES 46

3.0 OBJECTIVES 60

4.0 METHODS 62

4.1 SESSILE DROP CONTACT ANGLES 62
4.2 X-RAY PHOTOELECTRON SPECTROSCOPY 62
4.3 ELLIPSOMETRY 63
4.3.1 SETUP 63
4.3.2 LAYER REFRACTIVE INDEX ESTIMATION 65
4.3.3 CALCULATION OF MASS IN LAYER 68
4.3.4 ELLIPSOMETRY PROCEDURES 69
4.3.4.1 Ex situ procedure 70
4.3.4.2 In situ procedure 70
4.4 NEUTRON REFLECTOMETRY. 72
4.4.1 SETUP AND PROCEDURE 72
4.4.2 NEUTRON REFLECTOMETRY DATA ANALYSIS 73
4.5 PROTEIN ADSORPTION USING ^{125}I RADIOLABELED PROTEINS 74
4.5.1 PROTEIN LABELING PROCEDURE 74
4.5.2 PROTEIN ADSORPTION FROM BUFFER 74
4.5.3 PROTEIN ADSORPTION FROM PLASMA 75
4.6 PROTEIN ADSORPTION USING SDS-PAGE AND WESTERN BLOTTING 76
4.7 References 77

5.0 CONTRIBUTIONS TO ARTICLES. 80

6.0 PAPER ONE: CHEMISORPTION OF THIOLATED POLY(ETHYLENE OXIDE) TO GOLD: SURFACE CHAIN DENSITIES MEASURED BY ELLIPSOMETRY AND NEUTRON REFLECTOMETRY. 81

7.0 PAPER TWO: PROTEIN RESISTANCE OF SURFACES PREPARED BY SORPTION OF END-THIOLATED POLY(ETHYLENE GLYCOL) TO GOLD: EFFECT OF SURFACE CHAIN DENSITY. 92

8.0 PAPER THREE: POLYETHYLENE OXIDE SURFACES OF VARIABLE CHAIN DENSITY BY CHEMISORPTION OF PEO-THIOL ON GOLD: ADSORPTION OF PROTEINS FROM PLASMA STUDIED BY RADIOLABELLING AND IMMUNOBLOTTING. 99

9.0 PAPER FOUR: PEO-GRAFTED SURFACES FOR SUPPRESSION OF PROTEIN ADSORPTION: EFFECT OF CHAIN DENSITY DETERMINED BY *IN SITU* ELLIPSOMETRY. 119

10.0 PAPER FIVE: *IN SITU* NEUTRON REFLECTOMETRY INVESTIGATION OF CHEMISORBED PEO FILMS OF VARYING CHAIN DENSITY: INSIGHTS INTO PROTEIN ADSORPTION BEHAVIOUR. 138

11.0 SUMMARY AND CONCLUSIONS 160

12.0 RECOMMENDATIONS FOR FUTURE WORK 164

APPENDIX A: EXPERIMENTAL PROCEDURES 166

A.1 THIOLIZATION REACTION 166
A.2 GOLD COATING OF SILICON WAFERS 167
A.3 IN SITU ELLIPSOMETRY SAMPLE CALCULATIONS 167
A.4 PROTEIN LABELING 169
A.5 SDS-PAGE AND WESTERN BLOT PROCEDURE 170

LIST OF FIGURES

FIGURE 2-1. MOLECULAR MODEL OF FIBRINOGEN AND ITS INDIVIDUAL DOMAINS AND CORRESPONDING NET CHARGES AT A PH 7.4 [ADAPTED FROM FENG, 1995]. 12
FIGURE 2-2. STEREOPLOT SHOWING THE CRYSTAL STRUCTURE OF LYSOZYME [ADAPTED FROM HIGO, 2002]. DARK SPHERES REPRESENT TIGHTLY BOUND WATER MOLECULES 13
FIGURE 2-3. ILLUSTRATION OF INTERPHASE STRUCTURE, COMPOSED OF ELECTRONS, IONS AND SOLVENT MOLECULES, NEAR A NEGATIVELY CHARGED SURFACE. I. SCHEMATIC OF ION DISTRIBUTION. II. POTENTIAL AND ION DENSITY PROFILES, WHERE $1/\kappa$ REPRESENTS THE DEBYE LENGTH, AND '**A**' INDICATES LOCATION OF 'FIXED' CHARGES IN STERN LAYER [ADAPTED FROM ISRAELACHVILI, 1991]. 18
FIGURE 2-4. ILLUSTRATION OF END-TETHERED POLYMER CONFORMATION AND LAYER STRUCTURE. FROM TOP TO BOTTOM: DILUTE NON-OVERLAPPING 'MUSHROOMS'; SEMI-DILUTE WEAKLY OVERLAPPING 'MUSHROOMS'; 'EXTENDED MUSHROOMS', DILUTE BRUSH REGIME; HIGHLY EXTENDED CHAINS, DENSE BRUSH REGIME. S = DISTANCE BETWEEN ATTACHMENT POINTS. R_F = FLORY RADIUS. 22
FIGURE 2-5. ILLUSTRATION OF POSSIBLE ENERGY BALANCE DIAGRAMS FOR HYPOTHETICAL HYDROPHOBIC SURFACE (A) AND THE POSSIBLE EFFECTS ASSOCIATED WITH THE PRESENCE OF A PEO LAYER (B) 34
FIGURE 2-6. POSSIBLE ENERGY BALANCE DIAGRAMS ASSOCIATED WITH A HYDROPHOBIC SURFACE THAT HAS BEEN MODIFIED BY AN END-TETHERED PEO FILM. THE NET HYDRATION PRESSURE INDUCED BY THE PRESENCE OF A HYDROPHILIC LAYER IS INCLUDED. 37
FIGURE 2-7. DIAGRAM SHOWING THE SPECULARLY REFLECTED BEAMS IMPINGING ON THE SOLID-SOLUTION INTERFACE [ADAPTED FROM LU, 2003]. 43
FIGURE 4-1. GENERAL ELLIPSOMETRIC LAYOUT. THE LIGHT FROM THE MONOCHROMATIC SOURCE PASSES THROUGH THE POLARIZER PRISM (GENERATING ELLIPTICAL POLARIZATION) TO THE SURFACE. REFLECTION FROM THE SURFACE CHANGES THE POLARIZATION. THE REFLECTED BEAM PASSES THROUGH THE ANALYZER PRISM (WHICH DETECTS THE CHANGE IN POLARIZATION) AND FINALLY THROUGH THE DETECTOR WHICH SENSES THE PRESENCE OF THE ELECTROMAGNETIC WAVE AND ITS INTENSITY. 64
FIGURE 4-2. ILLUSTRATION OF LACK OF SIGNIFICANT CHANGES IN ANALYZER READINGS AMONG VARIOUS MODELS (REFRACTIVE INDEX VALUES) USED TO DESCRIBE THIN LAYERS. FOR LAYERS < 50 Å THICK IT IS IMPOSSIBLE TO DIFFERENTIATE MODELS USING THESE REFRACTIVE INDEX VALUES. (PARAMETERS FOR MODELS SHOWN: SOLUTION REFRACTIVE INDEX OF $1.3355 \pm i0.00$; $N_{Si} = 0.18 \pm i3.1$; WAVELENGTH, 6328 Å; 60.0° INCIDENT ANGLE.) 66
FIGURE 4-3. SCHEMATIC OF NEUTRON REFLECTOMETER SETUP. 73
FIGURE A-1. THIOLIZATION REACTION MECHANISM. 167
FIGURE A-2. REPRESENTATIVE LYSOZYME ADSORPTION PLOT OF POLARIZER ANGLE AND ANALYZER ANGLE AS A FUNCTION OF TIME. LINE REPRESENTS MODELED LAYER OF ADSORBED LYSOZYME. 168

LIST OF TABLES

TABLE A-1: SUMMARY OF MODEL USED TO EVALUATE THE LAYER PROPERTIES OF ADSORBED LYSOZYME. THE INCIDENT ANGLE WAS 70° 169

1.0 INTRODUCTION

Protein adsorption, the initial and fate determining step in all biomaterial applications, is responsible for initiating unwanted host responses that ultimately destroy or isolate 'foreign' material. Biocompatibility has been defined as "the ability of a material to perform with an appropriate host response in a specific application, including acceptance of the material by the host" [Ratner, 1993], which is intimately linked to the adsorption of proteins. As a result, a major area of biomaterials research is the development of surfaces that reduce or eliminate non-specific protein adsorption. Surface physical and chemical characteristics, including chemical surface structure, relative hydrophobicity, ion content, morphology and topography (surface roughness) are all believed to be important in mediating protein adsorption [Wegner, 1985; Ikada, 1994]. It is generally accepted that the hydrophobic effect is a particularly important driving force for protein-surface interactions [Norde, 1998].

The widespread use of polyethylene oxide (PEO) in biomaterial applications is due to its inherently non-cytotoxic and weakly immunogenic nature [Harris, 1992]. End-tethered PEO has been widely shown to reduce protein and cell interactions at the tissue-material interface, without leading to protein denaturation or inactivation [Harris, 1992; Archer, 1964; Zhang, 2001]. However, the mechanisms responsible for these interactions are largely undefined and the effects of end-tethered polymer chain length, chain density and end-group chemistry are not yet completely understood. This is primarily due to the fact that the interpretation of protein adsorption responses to surfaces is uncertain since there is a lack of molecular level definition of both the polymer and adsorbed protein

layer before, during and after adsorption [Ostuni, 2003]. To date, there have been few detailed, systematic studies that have attempted to elucidate the effect of end-tethered PEO conformation, chain density, molecular weight (MW) and end-group chemistry on protein adsorption at the solid-liquid interface. The main difficulty in examining chain density, chain conformation and molecular weight effects on protein adsorption arises from the fact that all of these properties are closely interrelated [Alexander, 1977]. Furthermore, proteins have a wide range of molecular weights and contain many subunits and subdomains with different hydrophobicity, charge and flexibility. The combined complexity of the surface and the protein structure hinders understanding of protein adsorption mechanisms.

In this work, PEO of varying molecular weight (600, 750, 2000 and 5000 MW) and two terminal functional groups (-OH, $-OCH_3$) was thiolated and chemisorbed to gold coated silicon wafers for the purpose of examining the fundamental properties of end-tethered monolayers such as thickness and chain density, and of correlating these properties to protein adsorption. Tethered chain density was varied by manipulating PEO solubility and incubation time, which in principle should allow for controlled chain density ranging from low to very high values. PEO layers were characterized using water contact angles, X-ray photoelectron spectroscopy (XPS), self-nulling ellipsometry and neutron reflectometry (NR). The adsorption of two proteins of widely differing molecular weight was examined using radiolabeling and ellipsometry methods to ascertain the effectiveness of these surfaces in resisting protein adsorption and to provide information about the nature of protein interactions with end-tethered PEO surfaces.

1.1 REFERENCES

Alexander, S., 'Adsorption of chain molecules with a polar head: a scaling description.' *J. de Physique,* **38**, 983 (1977).

Archer, R. J., 'Measurement of the physical adsorption of vapors and the chemisorption of oxygen on silicon by the method of ellipsometry.' *Nat. Bur. Std. Misc. Publ.,* **255ff** (1964).

Harris, J.M., *"Introduction to Biotechnical and Biomedical Applications of Poly(ethylene glycol),"* in Poly(ethylene glycol) Chemistry: Biotechnical and Biomedical Applications, J.M. Harris (ed), Plenum Press, New York, 1992, pp. 1-14.

Ikada, Y., Shalaby, W., 'Polymers of Biological and Biomedical Significance.' *Am.Chem.Soc. Symp. Series,* **540** 135 (1994).

Norde, W., *"Driving forces for Protein Adsorption at Solid Surfaces,"* in Biopolymers at interfaces., M. Malmsten (ed), Marcel Dekker, Inc., New York, New York, 1998; pp 27-54.

Ostuni, E., Grzybowski, B.A., Mrksich, M., Roberts, C.S., Whitesides, G.M., 'Adsorption of proteins to hydrophobic sites on mixed self-assembled monolayers.' *Langmuir* **19**, 1861 (2003).

Ratner, B. D., 'New ideas in biomaterials science. A path to engineered biomaterials.' *J.Biomed.Mat.Res.,* **27**, 837 (1993).

Wegner, G., Polymere Werkstoffe, H. Batzer (ed), Thieme Verlag, Stuttgart, 1985, p 679.

Zhang, F., Kang, E.T., Neoh, K. G., Huang, W., 'Modification of gold surface by grafting of poly(ethylene glycol) for reduction in protein adsorption and platelet adhesion.' *J. Biomater. Sci. Polymer Edn.,* **12**, 515 (2001).

2.0 LITERATURE REVIEW

2.1 CHEMISORPTION: THIOL-GOLD INTERACTIONS

In general adsorption involves three main mechanisms: physical adsorption, chemisorption and chemical bonding. Physical adsorption describes the weak bonding of a molecule to a surface as a result of attractive surface forces (discussed in more detail below) [Clark, 1974]. Chemical bonding involves the sharing of electrons, and thus involves relatively strong interactions. Chemisorption may be defined as an event which occurs when an atom or molecule is bonded to a surface through the overlapping of one or more electron orbitals [Clark, 1974]. While many investigators have tried to characterize the bonding involved in chemisorption, there is as yet no generally accepted description of the phenomenon that applies in all cases [Clark, 1974; Sellers, 1993].

Although generally thought to be inert, gold interacts strongly with sulfur functions including disulfides and thiols, with an approximate bond energy of 44 kcal/mol [Sellers, 1993]. When chemisorbed to face centered cubic (fcc) gold (Au(111)), thiols are thought to reside in the three-fold hollow sites between the gold atoms. The gold-thiol interaction can be written as,

$$\mathbf{RSH + (Au) \rightarrow RS\text{-}Au + H+ + e^{-}(Au)}$$

where the hydrogen ion is assumed to remain in close proximity to the Au interface, and e^{-}(Au) represents an electron that is closely associated with local gold atoms [Paik, 2000].

Electron diffraction studies suggest that the nearest neighbor distance for alkanethiols ($CH_3(CH_2)_{21}SH$) chemisorbed to Au(111) is 4.97 Å corresponding to 21.4

$Å^2$ per thiol group [Strong, 1988; Dubois, 1993]. LEED-Auger studies on silver surfaces showed a minimum S—S distance of 4.41 Å for similar alkanethiol adsorbates [Rovida, 1981; Schwaha, 1979]. These values are important since they set the limit for the maximum attainable surface density of thiol adsorbate (such as the PEO-thiols used in this work) on gold. While the mechanism of the gold-thiol reaction is not fully understood, it can nonetheless be exploited as a method to tether macromolecules such as PEO on gold surfaces. In principle, the gold-thiol method of preparation should yield surfaces with well defined structures.

2.2 *PEO Structure and Properties*

PEO, with repeat unit $-CH_2CH_2O-$, is a linear polymer with a high degree of conformational freedom inherent in the simple -C-C-O- backbone structure. In crystalline PEO the chains adopt a helix structure with internal rotational conformations about the $O-CH_2$, CH_2-CH_2, and CH_2-O bonds that are *trans*, *gauche*, and *trans*, respectively [Molyneux, 1983; Bailey, 1976]. In this conformation, the oxygen atoms are internalized and the methylene groups reside on the periphery of the helix [Molyneux, 1983]. The bulk refractive index for pure 5000 MW PEO is reported to be 1.46 [Brandrup, 1999] although a general refractive index of 1.475 (λ = 620.0 nm) can be estimated using the appropriate Cauchy parameters [Tokumitsu, 2002].

2.2.1 PEO IN SOLUTION

2.2.1.1 EFFECT OF SOLVENT ON PEO STRUCTURE

PEO is soluble in water and a number of common organic solvents. When dissolved in water the PEO chains adopt a conformation consisting of many short helical sections, similar to the crystalline state, connected by segments having a random coil conformation [Molyneux, 1983]. Although this broken helical conformation cannot be considered a true random coil, the equations used to model random coil polymer conformation in solution are still generally considered to be valid [Molyneux, 1983]. PEO conformational entropy, i.e. the entropy associated with a single chain conformation, dictates that, in the absence of external forces, the chain will adopt an overall spherical shape [Malmsten, 2003]. The sphere has a characteristic size (R, radius of gyration) that has been described by Flory for hydrated polymers as follows [de Gennes, 1981],

$$\mathbf{R_F = aN^{\nu}} \qquad \textbf{Eqn. 2-1}$$

where R_F is related through a power law function to the number of monomers (N) per chain, the solvent quality or excluded volume exponent (ν) and a statistical characteristic segment size (a). It is evident that R_F is strongly dependent on the excluded volume exponent, which is directly associated with solvent quality: as solvent quality decreases there is less penetration of solvent into the polymer coil leading to a reduction in polymer swelling and thus decreasing the excluded volume and overall radius of gyration.

2.2.1.2 *Cloud Point: Definition and effect on PEO Excluded Volume*

PEO is unique in that its solubility in water decreases with increasing temperature. The cloud point is defined as the temperature corresponding to the onset of precipitation [Bailey, 1959; Saeki, 1976]. It can be reduced in a controlled manner by changing solution conditions: for example the cloud point of PEO in aqueous solution decreases as ionic strength increases [Bailey, 1976]. The mechanisms involved in "salting out" amphiphilic molecules like PEO are largely undefined. Classically, it is accepted that, for PEO in water, the cloud point exists due to a balance of hydrophobic/hydrophilic forces that can be altered by changing the temperature and/or ionic strength. The switch from hydrophilic to hydrophobic may be associated with the collapse of structured water associated with the PEO [Bailey, 1958; Cook, 1992; Mahler, 1971]. Recent studies suggest that anions can form bridges between amphiphilic, neutral macromolecules directing chain re-arrangement that ultimately facilitates precipitation [Bowron, 2003].

Solvent quality directly affects the PEO excluded volume exponent (ν) and thus is crucial to the radius of gyration calculation. The Gibbs free energy change on mixing a polymer and solvent may be written as,

$$\Delta G_m = k_B T\left[\phi_1 \ln\phi_1 + \frac{\phi_2}{N}\ln\phi_2 + \phi_1\phi_2\chi\right] \qquad \textbf{Eqn. 2-2}$$

where ϕ_1 and ϕ_2 are the respective volume fractions of solvent and polymer, N is the degree of polymerization and χ is the Flory-Huggins interaction parameter [Jones, 1999]. For good solvents, χ is small, making the entropy contribution ($\phi_1 \ln\phi_1$) the dominant term in the equation. This suggests that polymer dissolution is a direct result of solvent

molecules being incorporated throughout the polymer domain [Jones, 1999]. This solvation greatly reduces the accuracy of the random walk statistical model in estimating the radius of gyration. Furthermore, when the polymer concentration becomes such that the distance between molecules is greater than the radius of gyration (R), a gradient of solvent concentration around the center of each molecule leads to a local osmotic pressure [Jones, 1999]. Under these conditions, the volume occupied by the chains is greater than in concentrated solutions, and a self-avoiding random walk model is required. An excluded volume exponent of $\nu = 3/5$ is generally used to describe this case; although it has been shown that a value of 0.588 can be more accurate for some systems [Jones, 1999]. At the cloud point condition, $\chi = ½$, the excluded volume effects that further solvate the polymer molecule in the dilute case are balanced by the unfavourable polymer-solvent interactions [Jones, 1999]. This allows for the use of the random walk model to describe the polymer conformation at the cloud point with an excluded volume exponent of $\nu = ½$. The use of this value in Eqn. 2-1 defines the Flory radius.

Alternatively, the physical meaning of the Flory-Huggins parameter, and the effect of solvent quality on polymer conformation, can be described by the enthalpy contributions upon mixing (Eqn. 2-3):

$$\chi = z(h_{12} - \tfrac{1}{2}h_{11} - \tfrac{1}{2}h_{22})/k_B T \qquad \textbf{Eqn. 2-3}$$

In this equation, z is the coordination number between solvent (1) and polymer (2), h represents the enthalpy associated with the specific interactions, T is temperature and k_B is the Boltzmann constant. It is easily seen that for every 1-1 or 2-2 interaction that is

broken, two (1-2) interactions are formed [Fleer, 1983]. When considering system enthalpy, $\chi > 0$ indicates a poor solvent where 'like' contacts are favoured over 'unlike' contacts. When the system is under unfavourable enthalpy conditions, it can remain thermodynamically stable as long as the entropy of mixing contributions, which are not accounted for in Eqn. 2-3, are favourable [Fleer, 1983].

2.3 PROTEINS AND THEIR INTERACTIONS AT INTERFACES

The adsorption of proteins to surfaces is ubiquitous and is important in fields from food processing to drug manufacture to biomaterials. Three important conclusions have been reached about protein adsorption in biomedical applications: *1.* protein adsorption is ubiquitous and is the initial event at the biomaterial tissue interface that determines all subsequent biointeractions; *2.* the hydrophobic effect is a major driving force for protein adsorption in many systems; *3.* the adsorbed protein layer is dynamic and is subject to both protein conformational change and exchange processes (the Vroman effect) [Andrade, 1987; Zwaal, 1986; Vroman, 1967; Horbett, 1993]. In biomaterials applications, the adsorbed protein layer mediates several host responses including inflammation, blood coagulation, thrombosis, hydrolytic and oxidative processes as well as bacterial adhesion and growth [Bakker, 1988; Williams, 1987; Dankert, 1986; Brash, 2000]. The adsorbed protein layer structure, affecting these interactions, is dependent on the surface properties of the biomaterial.

2.3.1 *PROTEIN STRUCTURE*

Limited to a set of 20 amino acids (monomers) for their make-up, proteins can be considered nonrepetitive biopolymers that are the basis of life. Protein molecular weights span a range of approximately 6,000 to 1,000,000 g/mol. Due to the presence of both acidic (-COOH) and basic ($-NH_2$) groups, proteins can adopt positive, negative or neutral states depending on pH. The isoelectric point (pI) is the pH at which the protein is globally neutral. Characterization of protein structure is difficult due to the variety of forms proteins may take. A four level system is required for their description, *viz.*, primary, secondary, tertiary and quaternary structures. Primary structure refers to the sequential ordering of amino acids in the peptide chain. Secondary structure describes the structural configuration of local amino acid residues as directed by nearest neighbour interactions. It is the amino acid near neighbour constraints that induce secondary structures like α-helices and β-sheets. Tertiary structure accounts for the interactions (folding, bending) within the entire protein due to hydrogen bonding, electrostatic interactions, intramolecular covalent disulphide bonds and hydrophilic/phobic interactions. Quaternary structure describes the interactions of individual polypeptide chains within a single protein. In general, protein structure allows for the precise biological activity required for protein function. Many proteins are also glycosylated, i.e., sugars or polysaccharide chains are attached pendant to the polypeptide backbone. It is also well known that the charged and hydrophobic domains presented by the protein are conformation dependent and can be easily altered upon exposure to a slightly changed environment (pH, temperature, ionic strength) or the presence of a surface.

It is the amphiphilic and macromolecular nature of proteins that makes them surface active, with a strong tendency to concentrate or adsorb nonspecifically at any interface. Inhibition of non-specific protein adsorption is thus difficult since it runs counter to "nature".

2.3.1.1 FIBRINOGEN

Best known for its crucial role in blood coagulation, fibrinogen (Fg), a globular protein that is abundant in plasma (~ 3 mg/mL), has a MW of 330 kDa, a pI of 4.3 and is composed of two sets of three peptide chains (α, β, γ) interconnected by disulfide bonds [Loewy, 1969; Doolittle, 2003]. Structural analysis of Fg has shown protein dimensions of 450 x 90 x 90 Å [Norde, 1995]. Adsorption of Fg as a close packed monolayer would thus give coverage in the range of 0.14 – 0.7 $\mu g/cm^2$ (0.42 – 2.12 $\mu mol/cm^2$). At physiological pH values the various domains and sub-domains (see Figure 2-1) have differing net charges [Feng, 1995], while the net charge on the molecule as a whole is negative. These regional variations in properties result in a multitude of mechanisms by which Fg can adsorb to surfaces.

The primary role of Fg in coagulation is the formation of fibrin through thrombin catalyzed cleavage [Doolittle, 2003]. Fibrin quickly crosslinks and forms a network. In the *in vivo* situation this network traps miscellaneous blood cells, including platelets, forming either a hemostatic plug to seal off vascular defects, or a thrombus. It has been suggested that the highly flexible α chain in the D domain (Figure 2-1, local +2 charge at pH 7.4) acts as the main adsorptive tether for Fg, as it is attracted to negative surfaces and

can easily change conformation and interact with surfaces that present either hydrophobic or hydrophilic domains [Feng, 1995].

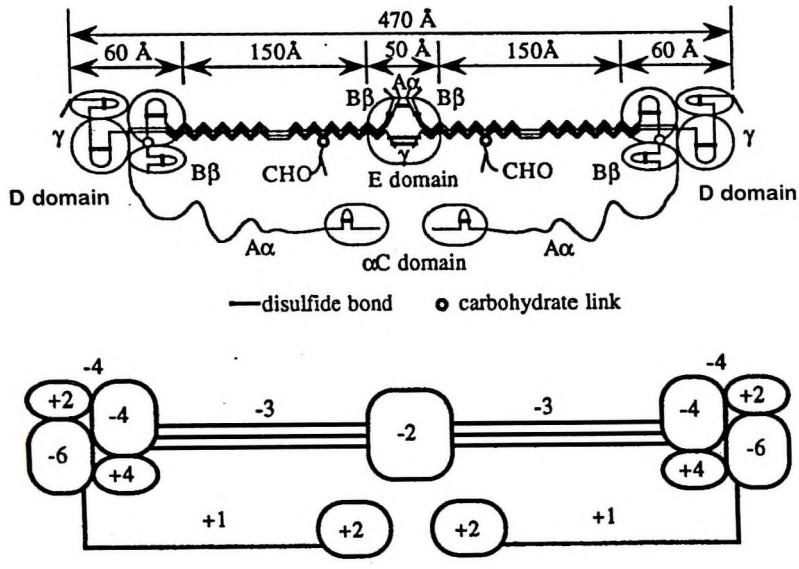

Figure 2-1. Molecular model of fibrinogen and its individual domains and corresponding net charges at a pH 7.4 [Adapted from Feng, 1995].

It has been shown that when Fg is adsorbed to surfaces that are in contact with blood, it is able to bind to the platelet glycoprotein IIb-IIIa integrin receptor [Slack, 1995], thus promoting platelet adhesion, activation, and aggregation [Tsai, 1999; Doolittle, 2003]. It has been suggested that platelet adhesion and activation are reduced to insignificant levels if the Fg adsorbed amount is less than 5 ng/cm^2 [Tsai, 1999]. This may be seen as a design goal for blood contacting biomaterials: it is crucial to prevent platelet adhesion since activated platelets act as a catalyst for several of the coagulation reactions. It has also been shown that adsorbed Fg and fibrin can facilitate macrophage-biomaterial interactions [Hu, 2001]. The denaturation of fibrinogen upon adsorption may reveal two concealed epitopes, P1 and P2, which interact with the β_2 integrin

(CD11b/CD18) on macrophages [Tang, 1996]. Similar epitopes exist for fibrin. This is an excellent example of the multiple structure-function relationships that exist for a single protein: not only does Fg adsorption to a surface play a crucial role in thrombosis but it can also lead to the activation of the inflammatory pathways.

2.3.1.2 LYSOZYME

Found primarily in tear fluid, lysozyme (Lys, Figure 2-2) is a small (14.4 kDa) single-chain globular protein with a pI of 11.1. It has a compact structure with five intramolecular disulphide bridges [Loewy, 1969]. The core of the globule is hydrophobic and the shell, where the charged and polar groups reside (11 arginine, 8 lysine, 1 histidine, 8 aspartic acid, 2 glutamic acid) [Lu, 1998], is hydrophilic.

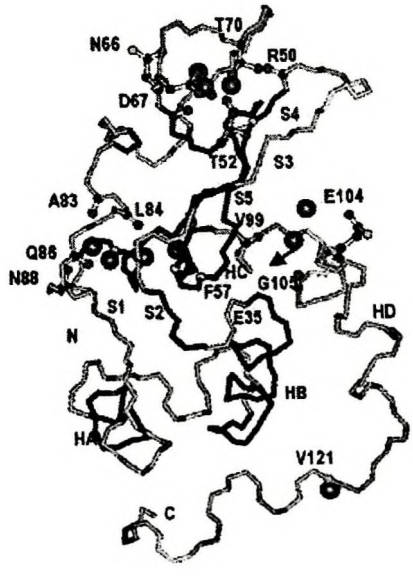

Figure 2-2. Stereoplot showing the crystal structure of lysozyme [Adapted from Higo, 2002]. Dark spheres represent tightly bound water molecules.

The strong internal cohesion of lysozyme should prevent unfolding and other conformational changes when it adsorbs at the solid-liquid interface [Lu, 2003], making this a protein with very low natural entropy. Determination of Lys structure has shown protein dimensions of 46 x 30 x 20 Å [Norde, 1995]. Adsorption of Lys as a close packed monolayer would thus give coverage in the range of 0.17 – 0.26 $\mu g/cm^2$ (11.8 – 18.1 $\mu mol/cm^2$).

Although primarily found in tear fluid, it has been shown that Lys is expressed by epithelial cells throughout the body, including the human eye, lung and intestines [Mason, 1975; Fahlgren, 2003]. It has also been shown that lysozyme is secreted by thrombin activated platelets [Kuijpers, 2000].

Lysozyme sorption from tear fluid to contact lenses plays a key role in lens spoilage and associated clinical complications [Castillo, 1985]. Thus, understanding and reducing lysozyme adsorption to contact lenses is one of the major areas of current ophthalmic biomaterials research. While tear fluid consists of a myriad of materials, including proteins, lipids and mucins, that are also deposited onto contact lenses, lysozyme is the major component of research interest [Senchyna, 2004]. The lysozyme-rich adsorbed protein film precedes a large-scale accumulation of debris on the lens surface facilitating bacterial adhesion, and resulting in reduced lens performance, increased lens discomfort, poor in-eye wettability and increased inflammation [Arciola, 1995]. Despite its structural compactness, it has also been suggested that, upon adsorption, lysozyme may denature and act as an immunological stimulant, possibly

resulting in papillary conjunctivitis and other external ocular surface changes [Porazinski, 1999].

2.4 *Macromolecular Adsorption at the Solid-Liquid Interface*

Macromolecular adsorption events at the solid-liquid interface are similar whether the macromolecule is a synthetic polymer or protein [Malmsten, 2003], although there are differences. Important to the adsorption of proteins and synthetic polymers at aqueous interfaces are surface forces.

2.4.1 *Surface Forces*

Macromolecular adsorption events are largely directed by interfacial forces in the region between the surface and the bulk contacting medium [Ramsden, 2003; Norde, 2003; van Oss, 1994]. For the following discussion the medium is assumed to be aqueous.

2.4.1.1 *Primary Interactions*

van Oss [1994] has described *primary* interactions as including van der Waals, electrostatic, hydrophobic and hydration pressure: the latter two being associated with hydrogen bonding. The associated forces govern the interactions between suspended or dissolved entities and surfaces. *Secondary* interactions, which include those associated with osmotic pressure, are defined as combinations of the fundamental primary interactions.

Approximately 95% of van der Waals interactions in aqueous media are related to dispersion interactions that arise from fluctuating dipole-induced dipole interactions [van

Oss, 1994]. This is not surprising as water is itself highly polar and aqueous solutions usually contain ions. Similar to both orientation and induction forces, dispersion forces are considered to be long range forces that have been shown to decay, for distances less than 100 Å, as a function of distance to the power of negative seven [Overbeek, 1952].

Electrostatic interactions can be repulsive or attractive and, for surfaces in aqueous media, arise from interactions between fixed surface charges and charged particles in solution (Figure 2-3). Once immersed in an aqueous solution containing ions, the charged surface disrupts the ion distribution and, in order to preserve electrical neutrality, drives the accumulation of counter-ions at the surface. It is this preferential segregation of charged ions over this vicinal region that is referred to as the 'electrical double layer'. The electric double layer is characterized by two layers: the Stern layer and the Gouy-Chapman layer. The Stern layer is the closest layer to the surface and consists of 'fixed' counter-ions. The adjacent Gouy-Chapman layer is characterized by a more diffuse ion concentration and extends to the point where the bulk ion distribution resumes. The surface-induced ion segregation leads to the formation of a potential energy gradient, which has been shown, for systems of low potential, to be related to the inverse of the Debye length (κ), the latter being the characteristic dimension of the electrical double layer as defined by Eqn. 2-4 [Israelachvili, 1991].

$$\kappa = \left(2n_O z^2 e^2 / \varepsilon\ kT\right)^{1/2} \qquad \textbf{Eqn. 2-4}$$

The Debye length, being a function of the bulk ion concentration (n_O), ion valence (z), electric charge (e), temperature (T), Boltzmann constant (k) and medium permittivity (ε),

is very sensitive to ionic strength. Systems of low ionic strength tend to have greater Debye length and a more diffuse double layer, than systems of high ionic strength [van Oss, 1994].

Hydrophobic interactions and hydration pressures both arise, in part, from hydrogen bonding interactions and are attractive and repulsive, respectively. Furthermore, these interactions may represent energies that are up to 100 times greater than the energies from combined dispersion and electrostatic forces [van Oss, 1994]. They have been shown to decay with distance from the surface as: $\exp(\ell_o - \ell/\omega)$, where ℓ_o is the minimum equilibrium distance between species (empirically determined to be ~0.157 nm), ℓ is distance and ω is a characteristic length. ω values of 1 and up to 13 nm have been observed for repulsive and attractive interactions, respectively. It is the increase in overall system entropy associated with the 'release' of highly ordered water molecules from the hydration shells present around hydrophobic moieties that drives the interaction between hydrophobic species in aqueous solvents. Repulsive hydrogen bonding interactions can extend several water layers from the 'surface' [Head-Gordon, 1995] and are the result of the high degree of water orientation near the interface which influences subsequent hydration layer ordering [van Oss, 1994].

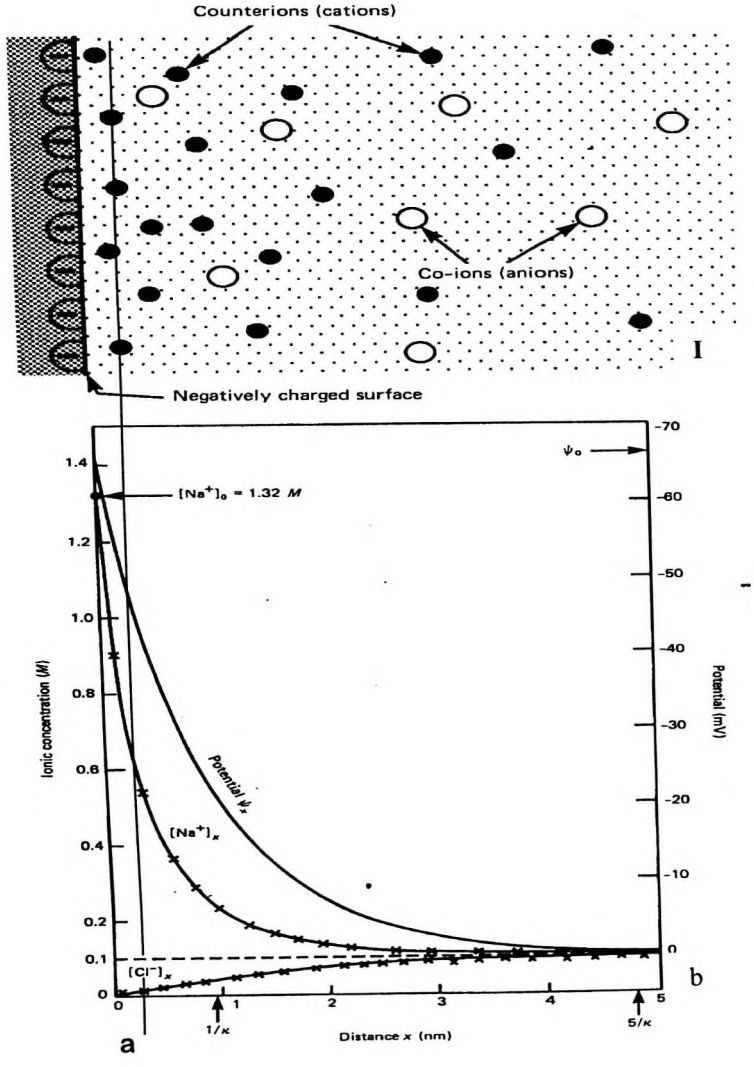

Figure 2-3. Illustration of interphase structure, composed of electrons, ions and solvent molecules, near a negatively charged surface. I. Schematic of ion distribution. II. Potential and ion density profiles, where $1/\kappa$ represents the Debye length, and '**a**' indicates location of 'fixed' charges in Stern layer [adapted from Israelachvili, 1991].

2.4.1.2 *Macromolecular Adsorption*

In the bulk solution (far from the surface), the macromolecule maintains its native conformation. At a particular distance, diffusion becomes the dominant mechanism by which the macromolecule moves toward the interface. The diffusive boundary, for Reynolds numbers in the range of ~1-100, may extend up to tens of micrometers from the surface, well beyond the range of any significant interfacial forces. Surface forces generally begin to affect the macromolecule at distances of approximately 10 nm from the surface [Ramsden, 2003]. The range of hydration forces (extension from the surface) greatly depends on whether they are attractive or repulsive and on the interfacial chemistry. The hydration force generally extends only a few water layers (1 – 5 nm) whereas the hydrophobic 'force' may extend up to tens of nanometers [Ramsden, 2003; van Oss, 1994; Vogler, 1997]. The electrostatic force, whose effective range is well described by the ionic strength dependent Debye length, is usually only 'seen' at distances of less than 1 nm in 0.15 M saline aqueous solutions (blood, tears). However, some reports state that, depending on the aqueous environment, this can be the force of longest range and can be seen up to tens of nanometers from the surface [Israelachvili, 1991]. van der Waals forces, although usually attractive, have been shown to be repulsive in some cases for two materials immersed in aqueous solution [van Oss, 1994].

2.4.2 *Polymer Adsorption and End-tethered Polymer Conformation*

A more complete understanding of polymer adsorption can be developed by considering together the effects of solvent quality (Flory-Huggins parameter), surface forces, and adsorption events. The initial driving force for polymer adsorption is the

balance among the forces on the polymer in solution and the various attractive and repulsive forces associated with the surface. Ultimately, polymer adsorption occurs only if the polymer-surface interactions are favoured over the polymer-solvent or solvent-surface interactions. It is effectively an exchange process such that for every polymer-surface interaction that occurs one solvent-surface and one polymer segment-solvent interaction must be disrupted. Silberberg [1968] first introduced χ_s (Eqn. 2-5) as the adsorption enthalpy parameter which is analogous to the fundamental Flory-Huggins parameter.

$$\chi_S = z'(h_{S1} - h_{S2} + \tfrac{1}{2}h_{22} - \tfrac{1}{2}h_{11})/kT \qquad \textbf{Eqn. 2-5}$$

Here χ_s is a function of the enthalpy associated with polymer-polymer (h_{11}) and solvent-solvent (h_{22}) interactions in the solution and at the surface (h_{S1}, h_{S2}), and the total number of possible surface contacts (z') [Fleer, 1983]. Therefore χ_s is a net enthalpy change which is positive if a polymer segment is preferred over a solvent molecule by the surface. Clearly this argument does not take into account any entropic effects associated with the polymer or solvent being in the solution or at the interface.

Different polymer layer morphologies can be achieved depending on the relative affinity of the polymer for the solvent and the surface. For example, easily deformed polymers that are strongly attracted to the surface usually form a 'pancake' layer: described as a thin layer where there is a high degree of surface-monomer association resulting in a polymer surface concentration that is higher than that of the solution (surface excess). A thicker film, with a polymer concentration that is lower than that of

the bulk, may form if the polymer is unable to deform and only somewhat favors the surface over the solvent. The concentration profile of adsorbed polymers is thus dependent on the balance between the monomer-surface affinity relative to the polymer conformational entropy [Norde, 2003].

While the above is true for polymer adsorption in general, it is possible to design polymers of specific architecture and chemistry such that their interactions with a particular interface would be specific with, for example, formation of a chemical bond. The formation of polymer layers in which the polymer is tethered to the surface, via a chemical bond, is an important example. The chains in an end-tethered polymer layer in a good solvent can assume different conformations as shown in Figure 2-4. When the conditions are such that the net interactions are repulsive ($\chi_s < 0$), and the surface does not interact with the polymer repeat unit, the layer consists of isolated polymer 'mushrooms' [Szleifer, 2000]. Lateral pressure and chemical potential are important factors that influence the final layer structure. The lateral pressure reflects the average repulsion between adjacent chains, and the chemical potential the partial molar free energy change associated with the addition of another chain to the layer [Szleifer, 1996]. As surface chain density increases, the excluded volumes associated with individual chains begin to overlap. This leads to an increase in lateral pressure that forces the chains to stretch normal to the surface until the entropy gain obtained by reducing the excluded volume, through the release of water molecules, is offset by the loss of entropy associated with chain stretching [Jones, 1999]. Thus, by varying chain density, it is theoretically possible to obtain chain conformations ranging from unperturbed random coils to fully-

extended chains (Figure 2-4). Polymer "brushes" are formed when spacing between chains (S) is less than twice the Flory Radius. In practice, it is difficult to achieve extremely high chain densities, when grafting polymers from solution, since tethered polymers form a steric barrier that dramatically increases the energy required for further addition of molecules to the layer [Szleifer, 2000]. For PEO layers, experiment has shown that there is a continuous change from mushroom to brush structure as layer formation proceeds [Szleifer, 1996].

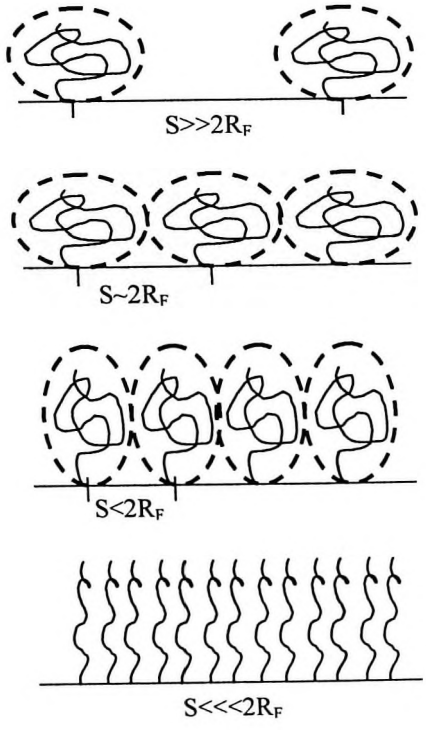

Figure 2-4. Illustration of end-tethered polymer conformation and layer structure. From top to bottom: dilute non-overlapping 'mushrooms'; semi-dilute weakly overlapping 'mushrooms'; 'extended mushrooms', dilute brush regime; highly extended chains, dense brush regime. S = distance between attachment points. R_F = Flory radius.

2.4.3 *Differences Between Polymer and Globular Protein Adsorption*

Although there are many similarities between globular protein and synthetic polymer adsorption at the solid-liquid interface, proteins exhibit unique adsorption properties arising from their specific structure. Proteins are innately amphipathic, and consequently are highly surface active molecules [Norde, 2003]. Contributing to their amphipathic nature is the fact that proteins are usually highly spatially organized, with various substructures that have both differing stabilities and different charges at a given pH. Nevertheless, the basic adsorption mechanisms remain the same for globular protein and polymer adsorption.

Proteins that have a native conformation described as compact and highly ordered (e.g. lysozyme), where native volumetric packing densities in solution can be as high as 70-80% v/v [Norde, 2003], are considered low entropy or hard proteins. These proteins adsorb somewhat differently than either soft proteins or polymers. Although these proteins can attach to the surface with multiple contacts, their strong internal cohesion reduces the rate at which they change conformation and spread, usually yielding layers with higher adsorbed masses [Norde, 2003]. Another important difference between flexible and low entropy molecules is the conformational entropy change upon adsorption. When highly ordered proteins adsorb, their conformational entropy may increase, something that is rarely observed for flexible polymers [Norde, 2003]. This entropy gain may be sufficient to cause adsorption to surfaces otherwise considered non-biofouling, and to hydrophilic, electrostatically repelling surfaces [Norde, 2003]. This is

another aspect of protein structure that makes it more difficult to design truly non-fouling surfaces.

2.4.4 *Competitive Adsorption of Proteins: the Vroman Effect*

The initial observation by Vroman and colleagues [Vroman, 1964] that the antibody binding activity of fibrinogen, when adsorbed to surfaces from plasma, appeared to decrease with increasing adsorption time was later shown to be due to the displacement of initially adsorbed fibrinogen by proteins of higher affinity and lower concentration [Brash, 1984; Horbett, 1984]. This is a manifestation of competitive adsorption and is now known as the Vroman effect. Questions regarding the Vroman effect still remain, including its overall physiological significance and identification of the proteins responsible for Fg displacement [Slack, 1995]. It was hypothesized that the spatiotemporal protein layer composition should depend largely on protein properties relative to those of the surface. This is mainly due to the abundance of plasma proteins and the limited number of surface sites [Andrade, 1985]. Generally, it is thought that the Vroman effect is not unique to Fg, but is a general phenomenon involving all surface active proteins, and that the main driving force for protein exchange are the differences in affinity of the different proteins.

Subsequent to the discovery of the Vroman effect, studies of blood coagulation mechanisms demonstrated that surface dependent autoactivation of Factor XII led to the cleavage of high molecular weight kininogen (HK) into the more surface active form, HKa [Wiggins, 1983]. Several studies, mostly involving negatively charged surfaces (i.e. glass and kaolin), seem to suggest that HKa is largely responsible for Fg displacement

[Brash, 1988; Slack, 1995; Colman, 1997]. However, Brash and colleagues, using plasma deficient in HK in studies of adsorption to glass, found that a weak Vroman peak persisted [Brash, 1988]. Studies involving materials that do not aggressively activate the coagulation cascade, however, such as polyethylene and silicone rubber, and surfaces of varying hydrophobicity, suggested that HKa has no significant effect on Fg displacement [Slack, 1995]. Other proteins that have been implicated in the displacement of Fg include oxyhemoglobin and albumin [Horbett, 1984; Malmsten, 1997]. It has been shown that the highly flexible αC chain of fibrinogen (local charge of +2 at pH 7.4) may act as the main adsorptive "tether" [Feng, 1995]. It has recently been shown that at neutral pH, the αC chain interacts electrostatically with silicon surfaces (and thus probably with negatively charged glass and kaolin as discussed previously), preventing the rest of the Fg molecule from forming intimate contacts with the surface [Jung, 2003]. Under acidic conditions, the αC chain no longer interacts electrostatically with the silicon surface, allowing the rest of the molecule to form strong hydrogen bonds with the surface. This reduces Fg elutability by 170 fold [Jung, 2003]. This suggests that the conformation of adsorbed Fg may play role in the Vroman effect.

2.5 PEO MEDIATED PROTEIN REPULSION

It is well known that both protein adsorption and platelet adhesion are reduced significantly when surfaces are modified with hydrophilic, water soluble polymers like poly(ethylene oxide) [McPherson, 1994]. Although this strategy has been extremely successful, the underlying anti-fouling mechanisms have yet to be fully understood.

2.5.1 *Steric Stabilization/Repulsion*

The steric repulsion theory is a relatively basic model that accounts for the inhibition of protein adsorption due to the presence of end-tethered PEO or other surface bonded, long chain hydrophilic molecules [Napper, 1983]. According to this theory, the PEO layer is compressed and the protein molecules dehydrate as they approach the surface. Compression decreases the PEO chain conformational entropy, thereby pushing the system into an unfavorable thermodynamic state [McPherson, 1995; van Oss, 1994]. Compression also leads to a local increase in PEO volume fraction (density) that lowers the rate of protein transport through the layer to the underlying surface. Furthermore, local osmotic pressures increase due to regional dehydration, thus forcing water back into both the PEO layer and the proteins near the interface, and increasing the conformational entropy. It is the movement of water back into the PEO and protein that is credited with facilitating decreased protein-surface interactions [McPherson, 1995]. As can be inferred from the above discussion, steric repulsion is considered an osmotic-entropy effect [McPherson, 1995].

In a sense this conclusion is somewhat surprising for as early as 1967 researchers were viewing steric stabilization as resulting from three main interactions: chain elasticity, Brownian movement and osmotic pressure [Ottewill, 1967]. Chain elasticity refers to the deformation energy associated with layer compression due to elastic collisions and is estimated using the elastic modulus of the layer [van Oss, 1994]. It has been suggested [van Oss, 1994] that in an aqueous environment, the Brownian movement

and osmotic contribution to steric stabilization is small. In this case the main mechanism arises from hydrogen bonding interactions.

The notion that the conformational entropy of the polymer is of major importance for steric stabilization may be flawed, since protein adsorption should result in an increase in overall entropy due to both the release of PEO-bound water *via* chain compression and protein-bound water during protein spreading on the surface. In fact, it appears that the role of water is entirely neglected in most discussions of protein adsorption [Morra, 2000]. It can be argued that the entropy loss associated with PEO compression is compensated by the entropy gain due to the 'freeing' of the 2-3 water molecules associated with each monomer [Antonsen, 1992]. As Morra [2000] points out, the putative importance of polymer conformational entropy may arise from assumptions in some of the earliest models of steric repulsion. Water interactions in these models are only considered with respect to polymer solubility *via* the Flory-Huggins parameter, and always define the polymer as being soluble. While PEO must remain soluble in order to remain an effective inhibitor of protein adsorption, its solubility may range from high to only slight. In fact, PEO solubility may even change as proteins approach the surface, for as compression occurs the polymer may become locally insoluble. If this effect is not reversible, the steric repulsion mechanism may break down.

In early descriptions of steric repulsion due to terminally attached polymers [Makor, 1951; Makor, 1952] the polymer chains were modeled as rigid rods and only entropic effects were considered, with the number of accessible conformations being defined by the footprint of the rods [Morra, 2000]. Under these conditions, the approach

of another molecule (polymer or protein) to the surface results in a reduction in the conformational entropy. In more recent work by Szleifer [2000] and Halperin [1999], the contributions of graft density, solvent quality, and molecular weight have been considered; this work has led to significant advances in modeling the interactions within the layer and between the layer and 'idealized' proteins. In other theoretical work, Tang [1995] initially focused on single chain mean field theory to model the transition from 'mushroom' to 'brush' layers in poor solvents. The main conclusion of this study was that the mushroom-brush transition corresponds to the shift from a dilute to a semi-dilute system. In papers by Szleifer [Szleifer, 1996; 1997a; 1997b; 1997c], proteins in solution were modeled as hard spheres and all protein-polymer, protein-solvent and polymer-solvent interactions were considered to be equal. Although they were able to model accurately some of the experimental results of the Whitesides group [Prime, 1993], where it was shown that a few oligo-ethylene oxide units were enough to reduce protein adsorption significantly, these models have shown only repulsive protein-polymer interactions [Morra, 2000].

In recent work Fang and Szleifer [Fang, 2002] have tried to address the shortcomings of these previous models, specifically by investigating the effects of protein-surface and polymer-surface interactions as well segment volume and types of polymer conformation that can be achieved during adsorption. This work demonstrated that protein adsorption depends strongly on the polymer surface density, protein-surface and polymer-surface interactions, the size of the polymer segments and the protein conformational freedom. It represents perhaps the first attempt to model proteins with

limited conformational freedom. However, the effects of solvent quality and possible phase transitions were still largely ignored. Related to this, Halperin [1999] tried to link primary interaction energies directly to protein adsorption. Although he considered an idealized case that only accounts for attractive surface-protein interactions and repulsive brush-protein interactions, his model is one of the first to try to explain protein resistance by considering surface forces. However, as in previous work, no repulsive forces other than those caused by brush compression were considered.

2.5.2 *Properties of PEO Affecting Protein Adsorption*

Stemming from the rigid rod approximation for end-tethered polymeric chains, it is commonly held that in order for surface bonded polymers to inhibit protein adsorption, they must be flexible, tightly anchored to the surface, and must cover the surface completely [McPherson, 1995]. Most studies investigating protein adsorption to PEO modified surfaces have tried to determine and correlate the effects of PEO chain length (MW), chain density and end-group chemistry to protein adsorption.

The effect of PEO chain length on protein adsorption has been widely studied [Kingshott, 2002a; Kingshott, 2002b; Zhu, 2001; Holmberg, 2003]. Kingshott [2002a/b] showed that when PEO of 3400 and 5000 MW was grafted under cloud point conditions, lysozyme and fibronectin adsorption were reduced below the detection limits of both XPS and matrix assisted laser desorption/ionization time-of-flight mass spectrometry (MALDI-ToF-MS). In contrast, protein adsorption was evident on surfaces formed under conditions away from the cloud point. This work led to the suggestion that the optimization of chain density is the key factor in reducing protein adsorption.

Holmberg [2003] showed that when PEO was grafted to polystyrene, *via* a pre-adsorbed polyethylenimine (PEI) layer, fibrinogen adsorption was the same for MWs between 1,500 and 19,000 but was greater for MWs less than 1,000. Zhu [2001], using surface plasmon resonance (SPR) to measure adsorption, studied the effect of PEO chain length on protein and cell resistance using PEO terminated alkanethiol self assembled monolayers on gold. All of the PEO layers were shown to be protein resistant to the same degree, suggesting little or no effect of chain length on protein adsorption.

Considerable discussion has focused on the minimum PEO chain length required to repel proteins. Prime and Whitesides [1993] demonstrated that chain lengths of as few as 1-3 ethylene oxide units are sufficient for 'total' protein inhibition as determined using XPS. However, it has been shown that XPS is not sufficiently sensitive to detect trace amounts of adsorbed protein [Kingshott, 2002b]. Others have reported that a minimum of 35 to 100 ethylene oxide units is required for effective protein repulsion [Malmsten, 2003].

Kingshott [2002a] prepared layers of tethered PEO by grafting on polymeric substrates using various MWs under different solubility conditions (including cloud point grafting) and studied the effects of chain density on protein adsorption behaviour. They showed that dense PEO films could be obtained by grafting near the cloud point. Subsequent work by this group [Kingshott, 2002b] demonstrated that only the surfaces with the highest PEO chain density showed "zero" adsorption of fibrinogen or lysozyme as assessed by MALDI-ToF-MS.

One problem that has hampered work in this area is the difficulty of designing experiments that decouple the effects of chain density and chain length, leading Holmberg [2003] to suggest that there has been no systematic study correlating PEO chain density and protein resistance. Nonetheless, there have been some attempts to investigate chain density (and the associated chain conformation) for correlation to protein adsorption. Theoretical studies were carried out by Harder [1998] and Wang [1997] to investigate how closely packed layers of slightly different chain density, but similar chain length, could lead to different molecular structures and different protein adsorption behavior. Harder [1998] investigated oligo(ethylene oxide) terminated alkanethiolates adsorbed to <111> Au and Ag. Different chain densities were possible due to the fact that the three fold hollow separation is less on Ag than Au. This difference in spacing results in a predominantly helical and amorphous conformation on the Au surface and an all *trans* conformation on the Ag surface. The silver surface was found to adsorb more fibrinogen than the gold, a result that was attributed to the different PEO conformations. Wang [1997] studied water binding to PEO layers in helical and all trans conformations and concluded that the helical oligo(ethylene oxide) system provides a template that promotes water nucleation. This was one of the first investigations where an attempt was made to correlate solvent-polymer interactions to protein adsorption trends. The studies of both Wang and Harder suggest that the stability of the water layer associated with helical oligo(ethylene oxide) prevents proteins and other molecules from adsorbing.

However, in none of these studies was the chain density quantified. Rather, systems were compared based on differences in how the surfaces were formed. In fact there have been very few studies where chain density has been determined accurately for the purpose of correlation to protein adsorption. Malmsten [1998] used ellipsometry to determine the chain density of 5000 MW PEO adsorbed to silica from solution. These layers were then exposed to solutions containing fibrinogen, human serum albumin, IgG, fibronectin and cleaved complement factor C1q. Chain densities in the range of 0.004 - 0.12 chains/nm^2 were obtained for CH_3-EO_{113} layers. These surfaces showed fibrinogen adsorbed amounts from 0.28 to 0.015 μg/cm^2. Sofia [1997] prepared surfaces with chain densities ranging up to $1.8x10^{-4}$, $6.8x10^{-5}$ and $2.5x10^{-5}$ chains/nm^2 for PEO MWs 3400, 10000 and 20000, respectively. These lower chain densities were presumably due to the relatively high molecular weights. It was shown that minimum chain densities of $1.2x10^{-7}$, $4.2x10^{-5}$ and $2.2x10^{-5}$ chains/nm^2 for the 3400, 10000 and 20000 PEO respectively, were required to reduce fibrinogen adsorption to levels below the XPS detection limit.

Only a few studies of the effect of end-group chemistry on protein adsorption have been reported. Prime and Whitesides [1993] reported no significant difference in adsorbed protein for tethered OEO layers with hydroxyl or methoxy end groups. However, Du [2001] observed that chemisorbed hydroxyl terminated PEO adsorbed significantly less fibrinogen than the methoxy analog. Similarly, Benesch [2001] found that methoxy terminated EO_3-alkanethiols adsorbed significantly more fibrinogen than the hydroxyl analog. Lindblad [1997] studied the effect of end group on protein, cell and soft tissue interactions. They found that fibrinogen adsorption was lower on the hydroxyl

terminated alkane thiol surfaces than on the methoxy analogs. They also observed, perhaps surprisingly, that cell adhesion was less on the methylated surfaces, but the cells in the fluid space around the methylated surfaces contained higher numbers of inflammatory cells compared to the hydroxyl-terminated ones.

2.5.2.1 'MASKING' OF SURFACE FORCES BY PEO

In addition to the intrinsic properties of PEO that may be considered important in imparting protein resistance, is the idea that the presence of end-tethered PEO has a significant effect on the underlying interfacial forces. Assuming that the interactions are averaged over the entire surface and that the surface roughness is zero, the effect of PEO on the resulting surface may be dramatic as illustrated in Figure 2-5 [Malmsten, 2003]. Figure 2-5A illustrates the case of a surface exhibiting attractive forces arising from hydrophobic and van der Waals interactions. The effect of adding a PEO layer to this "substrate" is shown in Figure 2-5B.

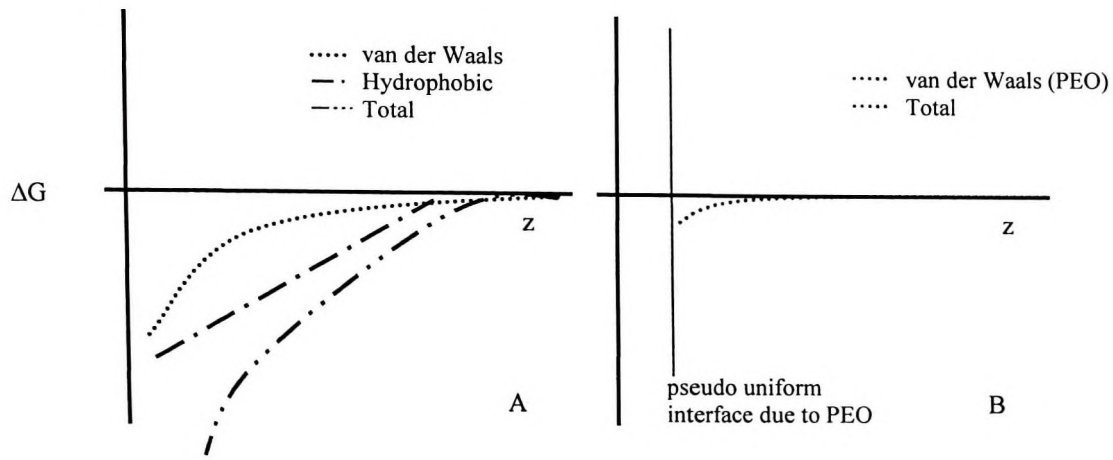

Figure 2-5. Illustration of possible energy balance diagrams for hypothetical hydrophobic surface (A) and the possible effects associated with the presence of a PEO layer (B).

In effect a new 'pseudo' interface is formed, whereby the PEO layer not only destroys the water structure responsible for the strong long-range hydrophobic interactions but also effectively masks the van der Waals interactions associated with the substrate [Israelachvili, 1996]. Although the tethered PEO film will have its own associated van der Waals interactions, these are expected to be relatively weak as the PEO film is usually well hydrated (~90%): provided that the solvent is "good" [Malmsten, 2003]. Another important PEO-induced modification is the attenuation or elimination of the surface induced electrostatic force, whether attractive or repulsive, through the disruption of the electrical double layer [Burns, 1995]. Recent studies have shown that for oligo(ethylene oxide) alkanethiol surfaces there is a unique repulsive electrostatic force that is strongly dependent on ionic strength, and which extends tens of

nanometers from the surface [Feldman, 1999; Dicke, 2002a; Dicke, 2002b]. Feldman [1999] showed that this force was not present for thin films composed of 2000 MW PEO chains.

2.5.2.2 Hydration Forces and Interphase Water

Potentially the most important interaction associated with the presence of tethered PEO at interfaces, depending on the model, is the highly controversial repulsive hydration force. While hydrophobic forces (attractive hydration forces) are commonly accepted, the existence of repulsive hydration forces has yet to be established, and it is considered by some researchers that this concept is only employed to account for repulsive forces at the interface that can not be easily described in any other way [Israelachvili, 1996]. Israelachvili [1996] suggested that short range repulsive forces arise from entropic repulsion due to the confinement of mobile surface groups at the interface and that the effect of water structure may be oscillatory or attractive only. On the other hand, Besseling [1997] and van Oss [1994] consider this repulsive force to be important and to be related to the total concentration of hydrogen bonds and to the hydrogen bond acceptor to donor ratio at the interface. Besseling [1997] developed models suggesting that if the hydrogen bond acceptor to donor ratio was close to one, the resulting water structure would give rise to long range attractive forces. If however, it was far from one, short range repulsive forces would be present.

Vogler [1999] proposed that water association at the biomaterial surface is the first step in biomaterial-tissue interactions and that designing for appropriate surface-

water interactions is more important than trying to control secondary biological responses such as protein adsorption that are only a consequence of water interactions.

It is well known, through experiments conducted with the surface forces apparatus (SFA) and the atomic force microscope (AFM), that hydrophilic surfaces repel each other as they approach within the contact limit [Morra, 1999]. Also, recent experimental work by Hyun [2003] and Feibelman [2004] has shown the presence of a viscous water interphase adjacent to oligo(ethylene oxide) alkanethiol monolayers. It seems likely that an oriented, dense vicinal water region with a collapsed hydrogen bonded network forms near hydrophilic surfaces [Vogler, 1999]. Including the hydration force at the effective PEO interface (Figure 2-5B), and given that its overall energy can be up to 100 times greater than either the van der Waals or electrostatic forces that are induced by either the substrate or PEO film [van Oss, 1994], a profile as depicted in Figure 2-6 may reasonably represent the interface on introduction of a PEO layer.

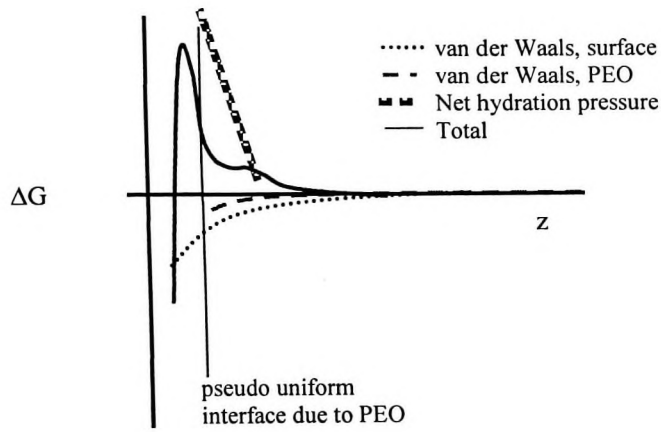

Figure 2-6. Possible energy balance diagrams associated with a hydrophobic surface that has been modified by an end-tethered PEO film. The net hydration pressure induced by the presence of a hydrophilic layer is included.

2.5.3 *Protein adsorption to Oligo(ethylene oxide) Alkanethiols*

It is generally accepted that the osmotic pressure-entropy effect exists for films composed of relatively high PEO MWs. Hence this effect cannot explain the protein resistance of oligo(ethylene oxide) terminated alkanethiol layers observed by Prime and Whitesides [1993]; these layers are too thin and densely packed for steric stabilization mechanisms to be applicable. It may be that these dense oligo(ethylene oxide) layers represent the extreme limit of steric repulsion mechanisms or that other, as yet undiscovered, PEO mediated repulsion mechanisms are in play, as further discussed below. Though these surfaces showed low protein adsorption, the EO chains are not long enough for resistance to be accounted for by the steric stabilization mechanism.

It has been suggested that electrostatic effects [Feldman, 1999; Dicke, 2002a; Dicke, 2002b], vicinal and interphase water structure [Kim, 2003; Feibelman, 2004; Ostuni, 2003; Herrwerth, 2004], reduction of substrate induced attractive forces [Malmsten, 2003; Israelachvili, 1996], internal and terminal hydrophilicity [Herrwerth, 2003] and hydration forces [Vogler, 1999; van Oss, 1994; Besseling, 1997; Morra, 1999] play a dominant role in inhibiting protein adsorption. Therefore novel mechanisms, particularly for the case of oligo(ethylene oxide) SAMs, must be considered: for example these surfaces may be indicative of a 'regime' whereby inherent EO properties, which are masked in the case of long EO chains, become important.

In experiments to measure the forces between functionalized scanning force microscopy tips and gold or silver surfaces modified with $(EO)_3$-alkanethiols, Feldman [1999] observed repulsive forces on Au and attractive forces on Ag. It was concluded that the difference was related to the chain conformation: *helical* on gold and all-*trans* on silver. This work also suggests that if the chain density is too great, protein adsorption may increase. Furthermore, it was observed that the repulsive force seen for the modified gold surface was strongly affected by ionic strength, suggesting electrostatic involvement in the repulsive force. On the other hand, while it has been observed that 2000 MW PEO directly grafted to gold via a thiol anchor is predominantly helical in conformation [Tokumitsu, 2002], Feldman [1999] found that the repulsive force did not depend on ionic strength. Recent work [Wang, 2000; Zolk, 2000] has suggested that the orientation of interfacial dipole moments and the resulting structure of water at the interface are important determinants for an inert surface. A similar mechanism has been postulated by

van Oss [1994] and the associated phenomenon is referred to as hydration pressure. Force spectroscopy studies conducted by Dicke [2002a/b] on similar modified gold surfaces showed that a negative surface charge was associated with the adsorption of hydroxyl ions at the EO-solution interface and that the resulting electrostatic repulsive force extends up to several tens of nanometers from the surface. These results suggest that these layers act as a template for water nucleation and emphasize that they must be hydrogen bond acceptors and not hydrogen bond donors in order to generate effective repulsive forces [Ostuni, 2003].

Kim [2003] investigated the forces between OEO-alkanethiol surfaces and modified (various alkanethiol chemistries) probe tips. It was found that $(EO)_3$-OH terminated monolayers generated an aqueous interphase layer with a viscosity 6 orders of magnitude greater than bulk water that extended up to 5 nm from the surface. This distance accounts for a layer that is ~30 water molecules thick. It was proposed that EO-mediated protein repulsion may be due to a diffusion barrier that is imposed by this thick, viscous interphase layer coupled with a neighbouring tightly bonded water monolayer. Neutron reflectometry studies have shown the existence of a vicinal water layer that is ~4 nm thick with a density 85-90% that of bulk water [Schwendel, 2003].

2.6 *Review of Relevant Surface Analysis Methods*

2.6.1 *Ellipsometry: Introduction*

Ellipsometry is a valuable optical technique that uses the properties of polarized light to investigate interfacial phenomena non-destructively by measuring changes in the

state of polarization of light upon reflection from the interface [Drude, 1889; Azzam, 1977]. The quantities derived from ellipsometry measurements are layer thickness and refractive index. Information on adsorbed quantity can be derived. Ellipsometry can be used to monitor the growth and evolution of thin films in real time (*in situ* monitoring). Thickness values on the order of nanometers can be measured with a precision of ~2Å [Rabe, 1988]. Limitations of this method are that at the wavelength of interest there must be a significant refractive index discontinuity at the interface and the surface must be smooth.

2.6.2 *Ellipsometry: Comparison With Other Methods*

Many studies have been conducted to evaluate the effectiveness of different techniques in measuring surfactant adsorption at the solid-liquid interface. Surfactant adsorption studies have shown that ellipsometry gives values of adsorbed amount and adsorbed layer thickness (to within a few Angstroms) similar to values obtained using neutron and x-ray scattering, neutron reflectometry and surface force measurements [Bohmer, 1992; Gellan, 1985; Lee, 1989; McDermott, 1992; Rutland, 1993; Tiberg, 1996]. However, as film thickness decreases it is increasingly difficult to unambiguously determine thickness and refractive index values simultaneously; this is due to the fact that there is a strong correlation that exists between these parameters at very small thickness values [Dura, 1998]..

2.6.3 *Ellipsometry: Adsorption Studies*

Ellipsometry has been widely used in biomaterials research to study protein adsorption [Vroman, 1964; Vroman, 1969; Tengvall, 2001; Benesch, 2001; Olivieri, 1999; Elwing, 1987; Liu, 1994], antigen-antibody reactions at surfaces [Rothen, 1945; Elwing, 1981], and cell surface interactions [Poste, 1972; Tegoulia, 2000]. It has also been used to investigate PEO layers and their effect on protein adsorption. Tiberg [1992] studied the effect of temperature on the thickness of surface grafted poly(ethylene oxide)-poly(propylene oxide) copolymers. IgG adsorption to these surfaces was also studied. It was found that increasing temperature caused a collapse of the film which resulted in an increase in protein adsorption. Although no explanation was given for this result, it may have been due to a loss of PEO solvation, consequent increase in PEO film related van der Waals forces, and loss of steric repulsion.

Ellipsometry experiments reported by Malmsten [1998], showed that the critical chain density of monomethoxy-PEG 5000 MW at the silica interface required to reduce fibrinogen adsorption to 0.02 mg/m^2, was 0.066 chains/nm^2. Malmsten [1994] also studied lysozyme adsorption at the silica-solution interface, and showed that the molecules adopt a side-on orientation with minimal conformational change [Oppenheim, 1996]. It has also been observed that in the adsorption of lysozyme at the solid-liquid interface multilayers may form at higher solution concentrations [Malmsten, 1994; Su, 1998].

Measurement of protein adsorption by ellipsometry and radioisotope labeling techniques have been shown to give similar values of adsorbed amount [Wojciechowski,

1993; Lensen, 1984; Benesch, 2000], although it should be kept in mind that phenomena unique to protein adsorption including conformational changes and effects of electrolyte concentration and pH, may introduce complications. Benesch [2000] showed that human serum albumin (HSA) adsorption measurements using ellipsometry and ^{125}I labeling procedures gave similar data.

2.6.4 Neutron Reflectometry: Introduction

The specular reflection of neutrons at an interface yields information about interfacial properties perpendicular to the interface (z-direction) at high resolution. Fundamentally, neutron reflection (NR) experiments are performed in a similar manner to light reflection. A parallel beam, with incident angle θ, is specularly reflected from the interface under study (Figure 2-7). The basic measurement is the variation of specular reflectivity as a function of the wave vector transfer function, Q:

$$Q = 4 \pi \sin\theta/\lambda \qquad \textbf{Eqn. 2-6}$$

where λ is the neutron de Broglie wavelength. Since λ is fixed, Q varies effectively as the sine of the angle of incidence. The intensity and shape of the reflectivity profile is determined by the layer thickness and the variation of the film density normal to the interface. Therefore the evaluation of interfacial properties, *viz.*, thickness and density, is possible because the variation in neutron reflectivity with Q is related to the scattering length density profile, $\rho(z)$:

$$\rho(z) = \sum_i b_i n_i(z) \qquad \textbf{Eqn. 2-7}$$

where $\rho(z)$ is a function of the unique neutron scattering length (b_i) of the individual atoms (readily available reference values, see Sears [1992]) within the film and their number density (n_i) which may vary with distance (z) from the interface [Russell, 1990; Penfold, 1990; Zhou, 1995]. Briefly, the presence of a thin layer (eg. adsorbed species) at the interface produces oscillations in the reflectivity profile (reflectivity vs. Q) with a period that is inversely proportional to the layer thickness. The basic principle can be understood by considering an isotropic thin film in contact with a surface on one side and a fluid on its other. In this case, the characteristic feature is the difference in path length between the beams reflected at the solid-film and film-liquid interface. Here the phase shift is a function of θ, which leads to alternating constructive and destructive interference as the reflected beams move in and out of phase. The constructive peaks of the interference fringes are related to θ by,

$$n\lambda = 2\,d\sin\theta \qquad \textbf{Eqn. 2-8}$$

where n is an integer, λ is the wavelength and d is film thickness [Lu, 2003].

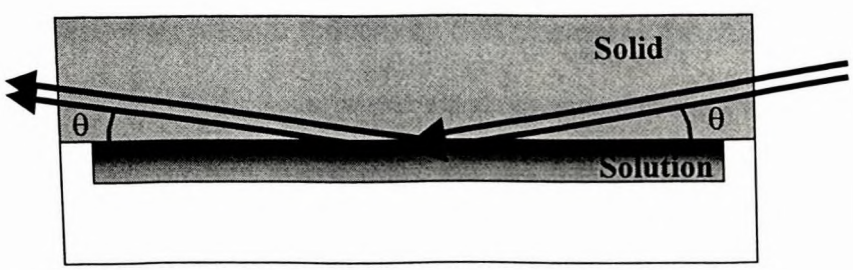

Figure 2-7. Diagram showing the specularly reflected beams impinging on the solid-solution interface [Adapted from Lu, 2003].

Neutrons are particularly suited for reflectivity studies since they are highly penetrating and their interactions with matter are atom specific. High penetration facilitates *in situ* measurements, since the neutrons are able to pass easily through the adjacent contacting media before reaching the interface under scrutiny. Limitations of the neutron method include the lack of contrast between most polymers (including PEO) and air or water (the relevant contacting fluid media in the present work) the inherent uncertainty associated with modeling the interface under study and the fact that the surface must be 'relatively' smooth.

2.6.5 *Neutron Reflectometry: Comparison with other methods*

Although optical techniques are readily available, non-destructive to the interface, relatively inexpensive and can be used under ambient conditions, their resolution is limited. Thus the resolution in concentration profiles normal to the surface is generally of the order of several tenths of a micrometer [Russell, 1990]. In the case of ellipsometry accurate thickness values down to ~10 Å [Brunner, 1998] can be achieved, with an associated error of ~2 Å [Rabe, 1986]. Neutron (and X-ray) reflectivity are more powerful methods. X-ray reflectivity indicates the variation in electron density in the z-direction [Jark, 1989], while neutron reflectivity (NR) measures the change in scattering length density [Fernandez, 1988]. Some major disadvantages that limit the application of X-ray reflectivity include surface degradation, the requirement of labeling for contrast (case specific) and beam attenuation.

The main problem associated with NR, as indicated, is the inherent lack of contrast between most polymers and either air or water. However, in the case of aqueous

contact, matching of the solution scattering length density to that of the substrate (contrast matching) using D_2O, has been shown to provide sufficient contrast to allow for the characterization of even minute traces of adsorbent [Penfold, 1991]. Lu [1995] demonstrated that thicknesses of the order of 2 Å can be accurately measured by contrast matching using D_2O.

2.6.6 Neutron Reflectometry: Adsorption Studies

NR has been used to study adsorption at various interfaces. Included in these investigations are time dependent processes [Gentle, 1993], adsorption of surfactants used in colloidal dispersions [Staples, 1999], copolymer adsorption at the liquid/liquid interface [Cosgrove, 1992; Li, 1998], and protein adsorption at various interfaces [Lu, 1999; Harzallah, 1998; Lu, 1998; Lee, 1999; Su, 1998; Su, 1999]. Studies have also been done on the adsorption of star-type and deuterated polyethylene oxide (PEO) at the solid liquid interface [Lee, 1990; Irvine, 1998] and on lipidated PEO at the air/water interface [Bianco-Peled, 2001]. In the latter study, the structure of monolayers of PEO-lipid complexes with PEO molecular weights of 120, 750, 2000, and 5000 was examined. It was shown that surface density and the resulting layer profile were related: higher molecular weight PEO chains formed parabolic monomer density profiles normal to the interface. 'Brush' layer configurations were seen at lower molecular weight. Lee [1990] studied the adsorption of PEO (145,000 MW) to quartz from H_2O-D_2O and $MgSO_4$ contrast matched solutions. By adding ions to vary polymer solubility it was found that the polymer layers were denser and thicker when formed under poor solubility conditions.

Specifically applied to studies of protein adsorption, NR has been used to examine the adsorption of HSA and BSA at the aqueous/hydrophilic silica interface. Su [1999] showed that bovine serum albumin (BSA) adsorption at the silica/water interface was strongly dependent on pH, and that it was reversible depending on the pH cycle used. Su [1998] investigated the effect of pH on lysozyme adsorption and concluded that the orientation and adsorbed amount are dominated by the intermolecular electrostatic interactions within the adsorbed protein layer, rather than surface-protein interactions. Lu [2003] observed that when the pH cycles from 4 to 8 to 4, lysozyme adsorption to SiO_2 surfaces is totally reversible. In contrast, for hydrophobic OTS films formed on silicon, lysozyme adsorption was found to be irreversible [Lu, 2003].

2.7 REFERENCES

Andrade, J.D. "Principles of protein adsorption," in *Surface and Interfacial Aspects of Biomedical Polymers*, J.D. Andrade (ed), Plenum Press, New York, 1985.

Andrade, J. D., Nagaoka, S., Cooper, S., Okano, T., Kim, S. W., 'Surfaces and blood compatibility. Current hypotheses.' *Am. Soc. Artif. Intern. Org. J.*, **33**, 75 (1987).

Antenson, K. P., Hoffman, A. S., "Water structure of PEG solutions by differential scanning calorimetry measurements," in *Poly(ethylene glycol) chemistry: Biotechnical and Biomedical Applications,* J.M. Harris (ed.), Plenum Press, New York, 1992, pp. 15-28.

Arciola, C.R., Maltarello, M.C., Cenni, E., Pizzoserrapo, A., 'Disposable contact lenses and bacterial adhesion. In vitro comparison between ionic/high-water-content and non-ionic/low-water-content lenses.' *Biomaterials*, **16**, 685 (1995).

Azzam, R. M. A., Bashara, N. M., *Ellipsometry and Polarized Light,* North-Holland Publishing Company, New York, 1977, pp 2-10.

Bailey, F. E., Callard, R. W., 'Properties of poly(ethylene oxide) in aqueous soln.' *J. App. Poly. Sci.*, **1**, 56 (1959).

Bailey, F. E., Koleske, J. V., *Poly(Ethylene Oxide)*, Academic Press: London, England, 1976, pp 105-150.

Bailey, F. E., Powell, G. M., Smith, K. L., 'Solution properties.' *J. Ind. Eng. Chem.*, **50**, 8 (1958).

Bakker, D., van Blitterswijk, C. A., Hessling, S. C., Grote, J. J., Daems, W. T., 'Effect of implantation site on phagocyte/polymer interaction and fibrous capsule formation.' *Biomaterials*, **9**, 14 (1988).

Bashara N. M., Buckman, A. B., Hall, A. C., *Proceedings of the Symposium on Recent Developments in Ellipsometry. Surface Sci.*, **16**, 85 (1969).

Benesch J., Askendal, A., Tengvall P., 'Quantification of adsorbed human serum albumin at solid interfaces: a comparison between radioimmunoassay (RIA) and simple null ellipsometry. ' *Colloids and Surf. B: Biointerfaces*, **18**, 71 (2000).

Benesch J., Svedhem S., Svensson S. C., Valiokas R., Liedberg B., Tengvall P., 'Protein adsorption to oligo(ethylene glycol) self-assembled monolayers: experiments with fibrinogen, heparinized plasma, and serum.' *J. Biomater. Sci., Polymer Ed.*, **12**, 581 (2001).

Besseling, N. A. M., 'Theory of Hydration Forces between Surfaces.' *Langmuir*, **13**, 2113 (1997).

Bianco-Peled, H., Dori, Y., Schneider, J., Sung, L.P., Satija, S., Tirrell M., 'Structural study of Langmuir monolayers containing lipidated poly(ethylene glycol) and peptides.' *Langmuir*, **17**, 6931 (2001).

Bohmer, M. R., Koopal, L. D., Janssen, R., Lee, E. M., Thomas, R. K., Rennie, A. R., 'Adsorption of nonionic surfactants on hydrophilic surfaces. An experimental and theoretical study on association in the adsorbed layer.' *Langmuir*, **8**, 2228 (1992).

Born, M., Wolf, E., *Principles of Optics*; Pergamon, New York, 1969, pp 614.

Bowron, D. T. and Finney, J. L., 'Structure of a salt-amphiphile-water solution and the mechanism of salting out. ' *J. Chem. Phys.*, **118**, 8357 (2003).

Brandrup, J., Immergut, E. H., Grulke, E.A., *Polymer Handbook*, John Wiley and Sons, New York, 1999, pp IV33

Brash, J.L., 'Exploiting the current paradigm of blood-material interactions for the rational design of blood-compatible materials.' *J. Biomater. Sci. Polymer Ed.*, **11**, 1135 (2000).

Brash, J.L., Scott, C.F., ten Hove, P., Wojciechowski, P., Colman, R.W., 'Mechanism of transient adsorption of fibrinogen from plasma to solid surfaces: role of the contact and fibrinolytic systems.' *Blood*, **71**, 932 (1988).

Brash, J. L., ten Hove, P., 'Effect of plasma dilution on adsorption of fibrinogen to solid surfaces.' *Thromb.Hemost.*, **51**, 326 (1984).

Brunner, H., Vallant, T., Mayer, U., Hoffmann, H., 'Formation of Ultrathin Films at the Solid–Liquid Interface Studied by *In Situ* Ellipsometry.' *J.Coll.and Inter.Sci.*, **212**, 545 (1998).

Burns, N.L., van Alstine, J.M., Harris, J.M., 'Poly(ethylene glycol) Grafted to Quartz: Analysis In Terms Of A Site-Dissociation Model of Electroosmotic Fluid Flow.' *Langmuir*, **11,** 2768 (1995).

Castillo, E.J., Koenig, J.L., Anderson, J.M., Lo, J., 'Protein adsorption on hydrogels. II. Reversible and irreversible interactions between lysozyme and soft contact lens surfaces.' *Biomaterials*, **6**, 338 (1985).

Clark, A., *The Chemisorptive Bond: Basic Concepts*. Academic Press, New York, New York, 1974.

Colman, R.W., Schmaier, A.H., 'Contact system: a vascular biology modulator with anticoagulant, profibrinolytic, antiadhesive, and proinflammatory attributes.' *Blood*, **90**, 3819 (1997).

Cook, R. L., King, H. E. jr., Peiffer, D. G., 'High-pressure viscosity of dilute polymer solutions in good solvents.' *Macromolecules,* **25**, 2928 (1992).

Cosgrove, T., Phipps, J. S., Richardson, R.M., 'Neutron reflection from a liquid/liquid interface.' *Coll.and Surf.*, **62**, 199 (1992).

Dankert, J., Hogt, A.H., Feijen, J., 'Biomedical polymers: bacterial adhesion, colonization, and infection.' Critical Reviews in Biocompatibility **2,** 219 (1986).

de Gennes, P.G., 'Polymer solutions near an interface. 1. Adsorption and depletion layers.' Macromolecules **14**, 1637 (1981).

Dicke, C., Hahner, G., 'pH-Dependent Force Spectroscopy of Tri(ethylene Glycol)- and Methyl-Terminated Self-Assembled Monolayers Adsorbed on Gold.' *J. Am. Chem. Soc.*, **124**, 12619 (2002a).

Dicke, C., Hahner, G., 'Interaction between a Hydrophobic Probe and Tri(ethylene glycol)-Containing Self-assembled Monolayers on Gold Studied with Force Spectroscopy in Aqueous Electrolyte Solution.' *J. Phys. Chem. B,* **106**, 4450 (2002b).

Doolittle, R.F., 'X-ray crystallographic studies on fibrinogen and fibrin.' *J. Throm. Haemost.*, **1**, 1559 (2003).

Doolittle, R.F. "Structural basis of signaling events involving fibrinogen and fibrin." Bradshaw, R., Dennis, E. (eds). Academic Press, New York, New York, 2003.

Drude, P., 'Measurement of the dielectric constant by means of electric waves.' *Ann. Phys. Chem.*, **39**, 481 (1890).

Du, Y.-J., *Ph.D. Thesis*, McMaster University, Hamilton ON, 2001.

Dubois, L. H., Zegarski, B. R., Nuzzo, R. G., 'Molecular ordering of organosulfur compounds on gold(111) and gold(100): adsorption from solution and in ultrahigh vacuum.' *J. Chem. Phys.*, **98**, 678 (1993).

Dura, J.A., Richter, C.A., Majkrzak, C.F., Nguyen, N.V., 'Neutron reflectometry, x-ray reflectometry, and spectroscopic ellipsometry characterization of thin SiO2 on Si.' *App. Phys. Lett.*, **73**, 2131 (1998).

Elwing, H., Ivarsson, B., Lundstrom, I., 'Serum complement deposition on platinum and titanium oxide surfaces measured by ellipsometry at liquid-solid interface.' *J. Biomed. Mater. Res.*, **21**, 263, (1987).

Elwing, H., Stenberg, M., 'Biospecific bimolecular binding reactions - a new ellipsometric method for their detection, quantification and characterization.' *J. Immunological Methods*, **44**, 343 (1981).

Faber, T. E., Smith, N. V., 'Optical measurements on liquid metals using a new ellipsometer.' *J. Opt. Soc. Am.*, **58**, 102 (1968).

Fahlgren, A., Hammarstrom, S., Danielsson, A., Hammarstrom, M-L., 'Increased expression of antimicrobial peptides and lysozyme in colonic epithelial cells of patients with ulcerative colitis.' *Clin. Exp. Immunol.*, **131**, 90 (2003).

Fang, F., Szleifer, I., 'Effect of Molecular Structure on the Adsorption of Protein on Surfaces with Grafted Polymers.' *Langmuir*, **18**, 5497 (2002).

Fernandez, M.L., Higgins, J.S., Penfold, J., Ward, R.C., Shackleton, C., Walsh, D.J., 'Neutron reflection investigation of the interface between an immiscible polymer pair.' *Polymer*, **29**, 1923 (1988).

Feldman, K., Hahner, G., Spencer, N.D., Harder, P., Grunze, M., 'Probing Resistance to Protein Adsorption of Oligo(ethylene glycol)-Terminated Self-Assembled Monolayers by Scanning Force Microscopy.' *J. Am. Chem. Soc.*, **121**, 10134 (1999).

Feng, L., Andrade, J.D., *"Structure and adsorption properties of fibrinogen,"* in Proteins at interfaces II: Fundamentals and Applications. T.A. Horbett, J.L. Brash, J.L. (eds), American Chemical Society, Washington, DC, 1995.

Gellan, A., Rochester, C.H., 'Adsorption of n-alkylpolyethylene glycol nonionic surfactants from aqueous solution on to silica.' *J. Chem. Soc. Faraday Trans.*, **181,** 2235 (1985).

Gentle, I.R., Hillman, A. Robert; Saville, Paul M.; Glidle, Andrew; Richardson, Robert M.; Roser, Stephen J.; Swann, Marcus J.; Webster, John R. P. 'Neutron Reflectivity Determination of Buried Electroactive Interface Structure: PBT/PPy and PBT/PXV Bilayers.' *J. Am. Chem. Soc.*, **120**, 12882, (1998).

Goedel, W.A., Luap, C., Oeser, R., Lang, P., Braun, C. Steitz, R., 'Stratification in Monolayers of a Bidisperse Melt Polymer Brush As Revealed by Neutron Reflectivity.' *Macromolecules*, **32**, 7599 (1999).

Halperin, A., 'Polymer Brushes that Resist Adsorption of Model Proteins: Design Parameters.' *Langmuir*, **15**, 2525 (1999).

Harzallah, B., Aguie-Beghin, V., Douillard, R., Bosio, L., 'A structural study of b-casein adsorbed layers at the air-water interface using X-ray and neutron reflectivity.' *Int. J. Biological Macromolecules,* **23**, 73 (1998).

Head-Gordon, T., 'Is water structure around hydrophobic groups clathrate-like?' *Proc. Natl. Acad. Sci. USA*, **92**, 8308 (1995).

Herrwerth, S., Eck, W., Reinhardt, S., Grunze, M., 'Factors that Determine the Protein Resistance of Oligoether Self-Assembled Monolayers - Internal Hydrophilicity, Terminal Hydrophilicity, and Lateral Packing Density.' *J. Am. Chem. Soc.*, **125**, 9359 (2003).

Higo, J., Nakasako, M., 'Hydration structure of human lysozyme investigated by molecular dynamics simulation and cryogenic X-ray crystal structure analyses: On the correlation between crystal water sites, solvent density, and solvent dipole.' *J. Comp. Chem.* **23**, 1323 (2002).

Holmberg, K., Quash, G., *"Control of Protein Adsorption in Solid-Phase Diagnostics and Therapeutics,"* in Biopolymers at Interfaces. 2nd Ed., M. Malmsten (ed), Marcel Dekker, Inc., New York, New York, 2003.

Horbett, T.A., 'Mass action effects on competitive adsorption of fibrinogen from hemoglobin solutions and from plasma.' *Throm. Haemostas.*, **51**, 174 (1984).

Horbett, T.A., 'Principles underlying the role of adsorbed plasma proteins in blood interactions with foreign materials.' *Cardiovasc. Pathol.*, **2**, 1375 (1993).

Huglin, M.B. Light Scattering from Polymer Solutions, M.B. Huglin (ed), Academic Press, Aberdeen, London, 1972, pp 165.

Irvine, D.J., Mayes, A.M., Satija, S.M., Barker, J.G., Sofia-Allgor S.J., Griffith, L.G., 'Comparison of tethered star and linear poly(ethylene oxide) for control of biomaterials surface properties.' *J. Biomed. Mater. Res.*, **40**, 498 (1998).

Israelachvili, J.N., Intermolecular and Surface Forces, Academic Press, London, 2nd Ed. 1991.

Israelachvili, J.N., Wennerstrom, H., 'Role of hydration and water structure in biological and colloidal interactions.' *Nature*, **379**, 219 (1996).

Jark, W., Comelli, G., Russell, T. P., Stoehr, J., 'Structural studies of Langmuir-Blodgett multilayers by means of soft x-ray diffraction.' *Thin Solid Films*, **170**, 309 (1989).

Jones, R.A.L., Richards, R.W., Polymers at Surfaces and Interfaces. Cambridge University Press, Cambridge, UK, 1999.

Johnson Jr., R.E., Dettre, R.H., 'Contact angle hysteresis. I. Idealized rough surface.' *Adv. in Chem. Series*, **43**, 112 (1964a).

Johnson Jr., R.E., Dettre, R.H., 'Contact angle hysteresis. III. Study of an idealized heterogeneous surface.' *J. Phys. Chem.*, **68**, 1744 (1964b).

Jung, S-Y., Lim, S.-M., Albertorio, F., Kim, G., Gurau, M. C., Yang, R.D., Holden, M.A., Cremer, P.S., 'The Vroman Effect: A Molecular Level Description of Fibrinogen Displacement.' *J. Am. Chem. Soc.*, **125**, 12782 (2003).

Kim, H.I., Kushmerick, J.G., Houston, J.E., Bunker, B.C., 'Viscous "Interphase" Water Adjacent to Oligo(ethylene glycol)-Terminated Monolayers.' *Langmuir*, **19**, 9271 (2003).

Kingshott, P., Thissen, H., Griesser, H.J., 'Effects of cloud-point grafting, chain length, and density of PEG layers on competitive adsorption of ocular proteins.' *Biomaterials*, **23**, 2043 (2002a).

Kingshott, P., McArthur, S., Thissen, H., Castner, D.G., Griesser, H.J., 'Ultrasensitive probing of the protein resistance of PEG surfaces by secondary ion mass spectrometry.' *Biomaterials*, **23**, 4775 (2002b).

Kruger, J., Ambs, W. J., 'Optical measurements on thin films of condensed gases at low temperatures.' *J.Opt.Soc.Am.*, **49**, 1195 (1959).

Kuijpers, A.J., van Wachem, P.B., van Luyn, M.J.A., Engbers, G.H.M., Krijgsveld, J., Zaat, S.A.J., Dankert, J., Feijen, J., 'In vivo and in vitro release of lysozyme from cross-

linked gelatin hydrogels: a model system for the delivery of antibacterial proteins from prosthetic heart valves.' *J. Controlled Release,* **67**, 323 (2000).

Lee, L.-T., Jha, B.K., Malmsten, M., Holmberg, K., 'Lipase-Surfactant Interactions Studied by Neutron Reflectivity and Ellipsometry.' *J.Phys.Chem.B,* **103**, 7489 (1999).

Lee, E.M., Thomas, R.K., Cummings, P.G., Staples, E.J., Penfold, J., Rennie, A.R., 'Determination of the structure of a surfactant layer adsorbed at the silica/water interface by neutron reflection.' *Chem. Phys. Lett.,* **162**, 196 (1989).

Lee, E.M, Thomas, R.K., Rennie, A.R., 'Reflection of neutrons from a polymer layer adsorbed at the quartz-water interface.' *Europhyx. Lett.,* **13**, 135 (1990).

Lensen, H.G.W., Bargeman, D., Bergveld, P., Smolders, C.A., Feijen, J., 'High-performance liquid chromatography as a technique to measure the competitive adsorption of plasma proteins onto latices.' *J. Colloid Interface Sci.,* **99**, 1 (1984).

Leslie, J. D., Tran, H. X., Buchanan, S., Dubowski, J. J., Das, S. R., LeBrun, L., Personal Communication, 2000.

Li, W. B., Segre, P. N., Gammon, R. W., Sengers, J. V., 'Determination of the temperature and concentration dependence of the refractive index of a liquid mixture' *J.Chem.Phys.,* **101**, 5058 (1994).

Li, Z.X., Fragneto, G., Thomas, R.K., Binks, B.P., Fletcher, P.D.I., Penfold, J., 'Neutron reflectivity studies of Aerosol-OT monolayers adsorbed at the oil/water, air/water and hydrophobic solid/water interfaces.' *Coll. Surf. A: Physiochemical and Engineering Aspects,* **135**, 277 (1998).

Lindblad, M., Lestelius, M., Johansson, A., Tengvall, P., Thomsen, P., 'Cell and soft tissue interactions with methyl- and hydroxyl-terminated alkane thiols on gold surfaces.' *Biomaterials*, **18**, 1059 (1997).

Lindh, L., Arnebrant, T., Isberg, P.-E., Glantz, P.-O., 'Concentration dependence of adsorption from human whole resting saliva at solid/liquid interfaces--an ellipsometric study .' *Biofouling* **14**, 189 (1999).

Liu, L., Elwing, H., 'Complement activation on solid surfaces as determined by C3 deposition and hemolytic consumption.' *J. Biomed. Mater. Res.,* **28**, 767 (1994).

Loewy, A.G. and Siekevitz, P., Cell Structure and Function, Holt, Rinehart and Winston, Inc., New York, pp. 221, 1969.

Lu, J.R., Li, Z.X., Smallwood, J., Thomas, R.K., Penfold, J., 'Detailed Structure of the Hydrocarbon Chain in a Surfactant Monolayer at the Air/Water Interface: Neutron

Reflection from Hexadecyltrimethylammonium Bromide.' *J.Phys.Chem.*, **99**, 8233 (1995).

Lu, J.R., Su, T.J., 'Adsorption of Serum Albumins at the Air/Water Interface' *Langmuir,* **15**, 6975 (1999).

Lu, J.R, Su, T.J., Thomas, R.K., Penfold, J., Webster, J., 'Structural conformation of lysozyme layers at the air/water interface studied by neutron reflection '*J. Chem. Soc., Faraday Trans.,* **94**, 3279 (1998).

Lu, J.R. *"Neutron Reflection Study of Protein Adsorption at the Solid-Liquid Interface,"* in Biopolymers at interfaces, 2nd edition, M. Malmsten (ed), Marcel Dekker, Inc., New York, New York, 2003.

Mahler, H.R., Cordes, E.H., Biological Chemistry, Harper and Row, New York, 1971.

Malmsten, M., 'Competitive adsorption at hydrophobic surfaces from binary protein systems.' *J. Coll. Interfacial Sci.,* **166,** 333 (1994).

Malmsten, M., *"Macromolecular Adsorption: A Brief Introduction,"* in Biopolymers at Interfaces. 2nd Ed., M. Malmsten (ed), Marcel Dekker, Inc., New York, New York, 2003.

Malmsten, M., Emoto, K., van Alstine, J.M., 'Effect of chain density on inhibition of protein adsorption by poly (ethylene glycol) based coatings' *J. Coll. Interfacial Sci.,* **202,** 507 (1998).

Malmsten, M., Muller, D., Lassen, B., 'Sequential adsorption of human serum albumin (HSA), immunoglobulin G (IgG), and fibrinogen (Fgn) at HMDSO plasma polymer surfaces.' *J. Coll. Interfacial Sci.,* **193**, 88 (1997).

Mason, D.Y., Taylor, C.R., 'The distribution of muramidase (lysozyme) in human tissues.' *J. Clin. Pathol.,* **28**, 124 (1975).

McDermott, D.C., Lu, J.R., Lee, E.M., Thomas, R.K., Rennie, A.R., 'Study of the adsorption from aqueous solution of hexaethylene glycol monododecyl ether on silica substrates using the technique of neutron reflection.' *Langmuir,* **8,** 1204 (1992).

McFarlane, A. S., 'Efficient trace-labeling of proteins with iodine.' *Nature,* **182**, 53 (1958).

McPherson, T.B., Lee, S.J., Park, K., *"Analysis of the prevention of protein adsorption by steric repulsion theory,"* in Proteins at interfaces II: Fundamentals and Applications, T.A. Horbett and J.L. Brash (eds), American Chemical Society, Washington, DC, 1995.

Molyneux, P. 'Water soluble synthetic polymers: properties and behavior.' CRC Press Inc., Boca Baton, Florida, pp. 23-38.

Morra, M., 'On the molecular basis of fouling resistance.' *J.Biomater.Sci.Polymer Edn.* **11**, 547 (2000).

Napper, D.H., Polymeric stabilization of colloidal dispersions. Academic Press, New York, 1983.

Nee, S. F., 'Error Analysis of Null Ellipsometry with Depolarization.' *Appl.Opt.*, **38**, 5388 (1999).

Norde, W., Haynes, C.A., Protein at Interfaces II: Fundamentals and Applications, T.A. Horbett and J.L. Brash (eds), American Chemical Society, Washington, DC, 1995.

Norde, W., *"Driving forces for Protein Adsorption at Solid Surfaces,"* in Biopolymers at interfaces, 2nd edition., M.Malmsten (ed), Marcel Dekker, Inc., New York, New York, 2003.

Nylander, T., Arnebrant, T., Glantz, P.-O., 'Interactions between salivary films adsorbed on mica surfaces.' *Colloids Surf. A.*, **129-130,** 339 (1997).

O'Bryan, H. M., 'The optical constants of several metals in vacuum.' *J.Opt.Soc.Am.*, **20**, 122 (1936).

Olivieri M.P., Tweden K.S., 'Human serum albumin and fibrinogen interactions with an adsorbed RGD-containing peptide.' *J.Biomed.Mater.Res.*, **46**, 355 (1999).

Ostuni, E., Grzybowski, B.A., Mrksich, M., Roberts, C.S., Whitesides, G.M., 'Adsorption of proteins to hydrophobic sites on mixed self-assembled monolayers.' *Langmuir* **19**, 1861 (2003).

Ottewill, R.H., Nonionic surfactants, M.J. Schick (ed.), Marcel Dekker, New York, 1967.

Overbeek, J.Th.G., Colloid Science, vol 1, H.R. Kruyt (ed.) Elsevier, Amsterdam, 1952.

Paik, W-k., Eu, S., Lee, K., Chon, S., Kim, M., 'Electrochemical Reactions in Adsorption of Organosulfur Molecules on Gold and Silver: Potential Dependent Adsorption.' *Langmuir*, **16**, 10198 (2000).

Penfold, J., Thomas, R.K., 'The application of the specular reflection of neutrons to the study of surfaces and interfaces.' *J.Phys.: Condens.Matter,* **2**, 1369 (1990).

Penfold, J., 'Instrumentation for neutron reflectivity.' *Physica B*, **173**, 1 (1991).

Pliskin, W. A., 'Refractive index dispersion of dielectric films used in the semiconductor industry.' *J.Electrochem.Soc.*, **134**, 2819 (1987).

Porazinski, A.D., Donshik, P.C., 'Giant papillary conjunctivitis in frequent replacement contact lens wearers: a retrospective study.' *CLAO J.*, **25**, 142 (1999).

Poste, G., Moss, C. Progress in Surface Science, North-Holland, Amsterdam, 1972.

Prime, K.L., Whitesides, G.M., 'Adsorption of proteins onto surfaces containing end-attached oligo(ethylene oxide): a model system using self-assembled monolayers.' *J. Am. Chem. Soc.*, **115**, 10714 (1993).

Rabe, J. P., Knoll, W. K., 'An ellipsometric method for the characterization of macroscopically heterogeneous films.' *Opt.Commun.*, **57**, 189 (1986).

Rabe, J. P., Novotny, V., Swalen, J. D., Rabolt J.F., 'Structure and dynamics in a Langmuir-Blodgett film at elevated temperatures.' *Thin Solid Films,* **159**, 359 (1988).

Ramsden, J.J., *"Protein adsorption kinetics,"* in Biopolymers at interfaces, 2nd Edn.. M.Malmsten (ed), Marcel Dekker, Inc., New York, New York, 2003.

Rothen, A., 'The ellipsometer, an apparatus to measure thicknesses of thin surface films.' *Rev.Sci.Instr.*, **16**, 26 (1945).

Rovida, G.; Pratesi, F., 'Sulfur overlayers on the low-index faces of silver.' *Surf. Sci.*, **104**, 609, 1981.

Russell, T.P., 'X-ray and neutron reflectivity for the investigation of polymers.' *Mater.Sci.Rep.*, **5**, 171 (1990).

Rutland, M.W., Senden, T.J., 'Adsorption of the poly(oxyethylene) nonionic surfactant C12E5 to silica: a study using atomic force microscopy.' *Langmuir,* **9**, 412 (1993).

Saeki, S., Kuwahara, N., Nakata, M., Kaneko, M., 'Pressure dependence of upper critical solution temperatures in the polystyrene-cyclohexane system.' *Polymer*, **17**, 685 (1976).

Schwaha, K., Spencer, N. D., Lambert, R. M., 'A single crystal study of the initial stages of silver sulfidation: The chemisorption and reactivity of molecular sulfur (S2) on silver(111).' *Surf. Sci.*, **81**, 273 (1979).

Schwendel, D., Hayashi, T., Dahint, R., Pertsin, A.J., Grunze, M., Steintz, R., Schreiber, F., 'Interaction of Water with Self-Assembled Monolayers: Neutron Reflectivity Measurements of the Water Density in the Interface Region.' *Langmuir,* **19**, 2284 (2003).

Sears, V.F. 'Neutron scattering lengths and cross sections.' Neutron News, **3**, 26 (1992).

Sellers, H., Ulman, A., Shnidman, Y., Eilers, J. E. 'Structure and binding of alkanethiolates on gold and silver surfaces: implications for self-assembled monolayers.' *J.Am.Chem.Soc.*, **115**, 9389 (1993).

Senchyna, M., Jones, L., Louie, D., May, C., Forbes, I., Glasier, M-A., 'Quantitative and conformational characterization of lysozyme deposited on balafilcon and etafilcon contact lens materials.' *Current Eye Research*, **28**, 25 (2004).

Sheardown, H., Cornelius, R. M., Brash, J. L., 'Measurement of protein adsorption to metals using radioiodination methods: a caveat.' *Coll.and Surf.B: Biointerfaces*, **10**, 29 (1997).

Silberberg, A., 'The adsorption of flexible macromolecules. II. The shape of the adsorbed molecule; the adsorption isotherm, surface tension, and pressure.' *J.Phys.Chem.*, **66**, 1884 (1962).

Silberberg, A., 'Adsorption of flexible macromolecules. IV. Effect of solvent-solute interactions, solute concentration, and molecular weight.' *J. Chem. Phys.*, **48**, 2835 (1968).

Silberberg, A., 'Behavior of macromolecules at phase boundaries.' *Pure Appl.Chem.*, **26**, 583 (1971).

Slack, S.M., Horbett, T.A., *"The Vroman Effect,"* in Proteins at interfaces II: Fundamentals and Applications. T.A. Horbett J.L. Brash (eds), American Chemical Society, Washington, DC, 1995.

Sofia, S.J., Kuhl, P.R., Griffith, L.G., Tissue Engineering Methods and Protocols, J.R. Morgan and M.L. Yarmush (eds), Humana Press Inc., Totowa, 1995, pp 19.

Sofia, S.J., Merrill, E.W., *"Protein adsorption on poly(ethylene oxide) grafted silicon surfaces,"* in Poly(ethylene glycol): Chemistry and Biological Applications. J.M. Harris and S. Zalipsky (eds), American Chemical Society, Washington, DC. 1997.

Spottiswoode, W., Polarisation of Light, Macmillan, London, UK, 1874, pp 11

Staples, E.J., Gilchrist, V. A., Lu, J. R., Garrett, P.; Penfold, J. 'Adsorption of Pentaethylene Glycol Monododecyl Ether at the Planar Polymer/Water Interface Studied by Specular Neutron Reflection.' *Langmuir*, **15**, 250 (1999).

Stone, J.M., Radiation and Optics, McGraw-Hill, New York, 1963.

Strong, L., Whitesides, G. M., 'Structures of self-assembled monolayer films of organosulfur compounds adsorbed on gold single crystals: electron diffraction studies.' *Langmuir*, ***4***, 546 (1988).

Su, T.J., Lu, J.R., Thomas, R.K., Cui, Z.F., 'Effect of pH on the Adsorption of Bovine Serum Albumin at the Silica/Water Interface Studied by Neutron Reflection.' *J.Phys.Chem.B,* **103**, 3727 (1999).

Su, T.J., Lu, J.R., Thomas, R.K., Cui, Z.F. Penfold, J., 'Application of Small Angle Neutron Scattering to the in situ Study of Protein Fouling on Ceramic Membranes.' *Langmuir,* **14**, 438 (1998).

Szleifer, I., 'Statistical thermodynamics of polymers near surfaces.' *Curr. Opin. Colloid Interface Sci.,* **1**, 416 (1996).

Szleifer, I., 'Protein adsorption on surfaces with grafted polymers: a theoretical approach.' *Biophys. J.,* **72**, 595 (1997a).

Szleifer, I., 'Protein adsorption on tethered polymer layers: effect of polymer chain architecture and composition.' *Physica A*, **244**, 370 (1997b).

Szleifer, I., 'Polymers and proteins: interactions at interfaces.' *Curr. Opin. Solid State Mater. Sci.,* **2**, 337 (1997c).

Szleifer, I., Carignano, M.A., 'Tethered polymer layers.' *Adv. Chem. Phys.,* **94,** 165 (1996).

Szleifer, I., Carignano, M.A., 'Tethered polymer layers: phase transitions and reduction of protein adsorption.' *Macromol. Rapid Commun.*, **21**, 423 (2000).

Tang, H., Carignano, M.A., Szleifer, I., 'Phase behavior of tethered polymers with lateral mobility in poor solvents.' *J. Chem. Phys.,* **102**, 3404 (1995).

Tiberg, F., 'Physical characterization of non-ionic surfactant layers adsorbed at hydrophilic and hydrophobic solid surfaces by time-resolved ellipsometry.' *J. Chem. Soc. Faraday Trans.,* **92**, 531 (1996).

Tiberg, F., Brink, C., Hellsten, M., Holmberg, K., 'Immobilization of protein to surface-grafted PEO/PPO block copolymers.' *Colloid Polym. Sci.*, **270,** 1188 (1992).

Tillman, N., Ulman, A., Schildkraut, J. S., Penner, T. L., 'Incorporation of phenoxy groups in self-assembled monolayers of trichlorosilane derivatives. Effects on film thickness, wettability, and molecular orientation.' *J.Am.Chem.Soc.,* **110**, 6136 (1988).

Tegoulia, V.A., Cooper S.L., 'Leukocyte adhesion on model surfaces under flow: effects of surface chemistry, protein adsorption, and shear rate.' *J.Biomed.Mater.Res.,* **50**, 291 (2000).

Tengvall P., Askendal A., Lundstrom I., 'Ellipsometric in vitro studies on the activation of complement by human immunoglobulins M and G after adsorption to methylated silicon.' *Colloids and Surfaces B: Biointerfaces,* **20**, 51 (2001).

Tokumitsu, S., Liebich, A., Herrwerth, S., Eck, W., Himmelhaus, M., Grunze, M., 'Grafting of Alkanethiol-Terminated Poly(ethylene glycol) on Gold.' *Langmuir,* **18**, 8862 (2002).

Tompkins, H.G., A User's Guide to Ellipsometry, Academic Press, Inc., London, UK, 1993, pp 6.

Tsai, W.B., Grunkemeier, J.M., McFarland, C.D., Horbett, T.A., Selectively depleted plasmas to study the role of four plasma proteins in platelet adhesion to biomaterials. M. LeBerge and C.M. Agrawal (eds), *Society for Biomaterials,* Providence, Rhode Island, Vol. **22**, 266. (1999).

Ulman, A., An Introduction to Ultrathin Organic Films, Academic Press, Inc., San Diego, Calif., 1991.

van Oss, C.J., Interfacial Forces in Aqueous Media. Marcel Dekker, Inc., New York, New York, 2003.

Vogler, E.A., 'Water and the acute biological response to surfaces.' *J. Biomater. Sci. Polymer Ed.,* **10**, 1015 (1999).

Vroman, L., Blood, Natural History Press, New York, New York, 1967.

Vroman, L., Adams, A. C., 'Blood coagulation studies with the recording ellipsometer.' *Nat.Bur.Std.Misc.Publ.,* 335ff (1964).

Vroman, L., Adams, A.C., Proceedings of the Symposium on Recent Developments in Ellipsometry, North-Holland, Amsterdam, 1969, pp 335ff.

Wang, R.L.C., Kreuzer, H., Grunze, M., 'The interaction of oligo(ethylene oxide) with water: a quantum mechanical study.' *Phys. Chem. Chem. Phys.,* **2**, 3613 (2000).

Ward, L., The Optical Constants of Bulk Materials and Films, Adam Hilger, Philadelphia, 1988.

Wasserman, S. R., Whitesides, G. M., Tidswell, I. M., Ocko, B. M., Pershan, P. S., Axe, J. D., 'The structure of self-assembled monolayers of alkylsiloxanes on silicon: a comparison of results from ellipsometry and low-angle x-ray reflectivity.' *J.Am.Chem.Soc.,* **111**, 5852 (1989).

Williams, D. F., 'Tissue-biomaterial interactions.' *J. Mater.Sci.,* **22**, 3421 (1987).

Williams, D.F., Progress in biomedical engineering, Elsevier, Amsterdam, 1987b.

Wiggins, R.C., 'Kinin release from high molecular weight kininogen by the action of Hageman factor in the absence of kallikrein.' *J. Biol. Chem.*, **258**, 8963 (1983).

Zhou, X.L., Chen, S.H., 'Theoretical foundation of X-ray and neutron reflectometry.' *Phys.Rep.*, **257**, 223 (1995).

Zhu, B., Eurell, T., Gunawan, R., Leckband, D.,' Chain-length dependence of the protein and cell resistance of oligo(ethylene glycol)-terminated self-assembled monolayers on gold.' *J.Biomed.Mater.Res.* **56,** 406 (2001).

Ziats, N. P., Miller, K. M., Anderson, J. M., '*In vitro* and *in vivo* interactions of cells with biomaterials.' *Biomaterials*, **9**, 5 (1988).

Zolk, M., Eisert, F., Pipper, J., Herrwerth, S., Eck, W., Buck, M., Grunze, M., 'Solvation of Oligo(ethylene glycol)-Terminated Self-Assembled Monolayers Studied by Vibrational Sum Frequency Spectroscopy.' *Langmuir,* **16**, 5849 (2000).

Zwaal, R.F.A., Hemker, H.C., Blood Coagulation, R.F.A. Zwaal and H.C. Hemker (eds), Elsevier, Amsterdam, 1986.

3.0 OBJECTIVES

From the above discussions of end-tethered PEO structure and protein adsorption to PEO modified surfaces, it is clear that while it is well accepted that PEO modified surfaces inhibit non-specific protein adsorption, the mechanisms involved remain largely undefined. Furthermore, it should be apparent that there is a lack of studies in which polymer film properties (chain density, thickness, volume fraction) have been determined and correlated with protein adsorption data.

Therefore, the overall objective of this work was to determine the properties of tethered PEO layers (chain density, chain length, volume fraction and terminal functional group) for correlation to protein adsorption behaviour. This necessitated the preparation of PEO layers of variable and reproducible chain density, and the precise determination of chain density. Complementary high quality data on protein adsorbed amount were also required, including data on proteins of varying size (as a probe of the mechanism of protein resistance). A model system based on the chemisorption of chain-end thiolated PEO to gold substrates was chosen for these studies. PEO solubility (proximity to cloud point conditions) and time of chemisorption were manipulated to generate variable, controlled surface density of PEO chains.

Fundamental layer properties were determined using water contact angles, x-ray photoelectron spectroscopy (XPS), ellipsometry and specular neutron reflectometry (NR). Ellipsometry and neutron reflectometry were employed with the goal of determining layer properties in the z-direction on the nm scale. Given some *a priori* knowledge of the layer, as discussed previously, ellipsometry and NR can be used to determine accurately

both the amount and volume fraction of any adsorbed species. It was hoped that these techniques would yield accurate PEO layer properties and that, combined with detailed knowledge of protein interactions, a better understanding of the mechanisms by which PEO reduces the adsorption of proteins would be achieved.

Protein adsorption was determined using various techniques including ^{125}I radiolabeling (buffer and plasma), ellipsometry (buffer), and Western Blot analysis of proteins adsorbed after contact with human plasma.

As well as providing insights into the mechanism of protein resistance of tethered PEO, this research may also provide guidance on more practical matters such as the layer properties (chain density, chain length and end-group chemistry) required for maximum inhibition of protein adsorption; information that ultimately affects the design rationale of 'non-fouling' surfaces.

4.0 METHODS

4.1 SESSILE DROP CONTACT ANGLES

Measurement of sessile drop water contact angles allows for rapid assessment of global interfacial characteristics such as relative hydrophilicity. However, interpretation of contact angle data is complicated and depends not only on surface chemistry, but also topography, chemical heterogeneity, contamination and measurement protocol [Dettre and Johnson, 1964-1967; Chibowski, 2003]. The use of water contact angles on polymeric substrates introduces another complication, namely that the interface may rearrange due to water-polymer interactions [Miyama, 1997]. For hydrophilic surfaces such as those under study, the hydrated form of the interface is of greater interest and therefore the receding contact angles may be more relevant. In this work, sessile drop water contact angles were determined using water drops of volume no greater than 3 μL. Advancing and receding angles were obtained using a Ramé-Hart NRL 100-00 goniometer (Mountain Lakes, NJ).

4.2 X-RAY PHOTOELECTRON SPECTROSCOPY

X-ray photoelectron spectroscopy (XPS) was used to determine the surface chemical composition of both the unmodified gold and PEO modified surfaces. Photoelectron emission from the core atomic levels of the elements present in the sample is achieved through exposure to X-rays. The surface sensitivity of this technique arises from the inability of photoelectrons to escape from anywhere but the outermost atomic layers of the surface. The actual range is dependent on the photoelectron attenuation

length which is specific to the substrate atomic composition, but at most a depth of about ~100 Å is sampled [Lamont, 1999; Bain, 1989]. The energy associated with the emitted photoelectrons is indicative of the chemical elements and their bonding environment, while the intensity is related to the species abundance. Furthermore, through variation in the take off angle, it is possible to investigate the chemistry of the surface layers as a function of depth into the material (depth profiling).

XPS spectra were obtained using a Leybold (Specs, Berlin) MAX 200 XPS system employing an unmonochromated Al Kα source operating at 15 kV and 20 mA. Low-resolution spectra (pass energy = 192 eV) were used to determine atomic compositions; high resolution C1s spectra (pass energy = 48 eV) provided additional surface structural information. Specslab (Specs, Berlin) software was used for spectral fitting. Spectra were taken at two takeoff angles: 90° and 20° relative to the surface. The respective spot sizes were 2 x 4 mm and 1 x 1 mm; the smaller area at 20° was used to ensure that the beam footprint remained on the samples.

4.3 ELLIPSOMETRY

4.3.1 SETUP

The null-ellipsometry setup is illustrated in Figure 4-1. Quasi-monochromatic light, produced by a He-Ne laser, passes through a polarizer prism, faraday rod and quarter wave plate (compensator). These optical components produce an elliptically polarized incident beam. Reflection from the sample changes the state of polarization. This change is determined from the position of the polarizer and analyzer prisms required

to fully cross polarize the reflected beam. The photodetector is used in a feedback loop configuration and controls the prism angles so as to achieve the null position.

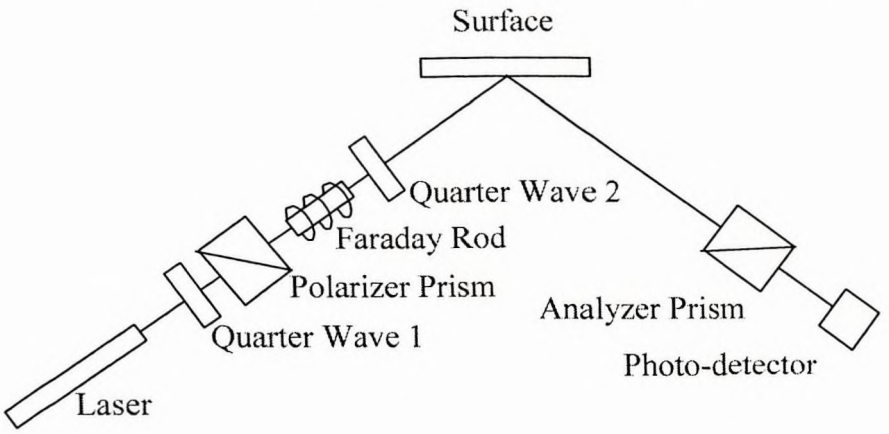

Figure 4-1. General ellipsometric layout. The light from the monochromatic source passes through the Polarizer Prism (generating elliptical polarization) to the surface. Reflection from the surface changes the polarization. The reflected beam passes through the Analyzer Prism (which detects the change in polarization) and finally through the detector which senses the presence of the electromagnetic wave and its intensity.

In practical terms, the most important ellipsometric parameter is the ratio of the amplitude of the outgoing reflected wave to that of the incoming beam, defined as the total reflection coefficient [Azzam, 1977; Heavens, 1965]. Mathematical models have been developed that allow estimation of the average film thickness (d), the complex refractive index (N) and the quantity of material in adsorbed layers at the surface [Azzam, 1977]. These values are considered average in the sense that they are taken over large footprint areas; also adsorbed polymer studies have shown that macromolecular density normal to the interface decreases with increasing distance [Hoeve, 1970; Hoeve, 1971]. Nevertheless, the polarizer (P) and analyzer (A) positions at the null condition are

directly related to the fundamental angle Ψ whose tangent is the ratio of the magnitudes of the total reflection coefficients, and to the change in phase that occurs upon reflection (Δ). From this information the amount adsorbed (Γ, mass per unit area) can also be determined [de Feijter, 1978]. Detailed ellipsometric theory is presented by Azzam and Bashara [1977].

4.3.2 Layer Refractive Index Estimation

Although ellipsometric data for thick films can theoretically be used to calculate both the film thickness and the complex refractive index simultaneously, this convenience does not apply to thin films (d < 50Å). This limitation arises from the lack of significant change in the analyzer readings for thin films. As illustrated in Figure 4-2, differences of only ~0.005° in the analyzer readings (compared to differences of ~ 0.2° in polarizer readings) differentiate between refractive index values of 1.37, 1.40, 1.43, 1.46 for a common film of 50Å thickness; capturing analyzer data to this degree of accuracy is difficult and the resulting refined model is greatly influenced by even small uncertainties. Therefore, when analyzing these thin films the complex refractive index, including both the film refractive index (n_f) and the film extinction coefficient (k_f), must be estimated to determine the average film thickness (d).

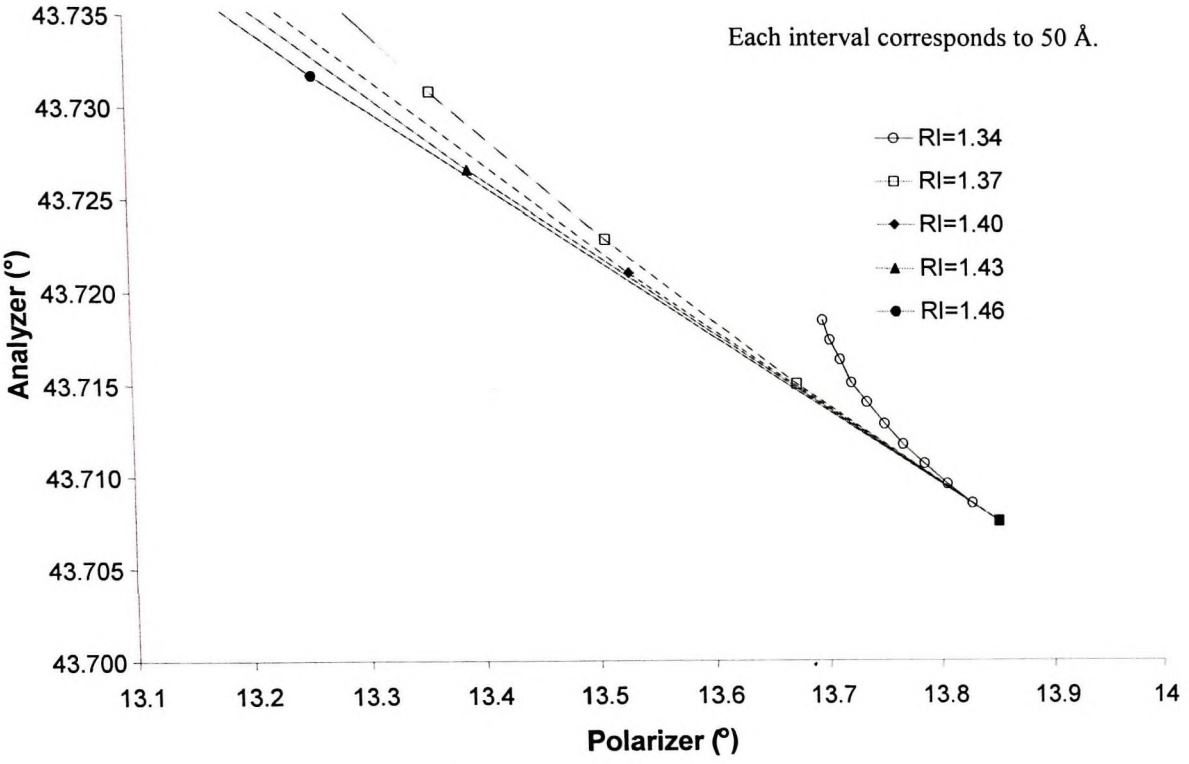

Figure 4-2. Illustration of lack of significant changes in analyzer readings among various models (refractive index values) used to describe thin layers. For layers < 50 Å thick it is impossible to differentiate models using these refractive index values. (Parameters for models shown: solution refractive index of 1.3355 ± i0.00; N_{Si} = 0.18 ± i3.1; wavelength, 6328 Å; 60.0° incident angle.)

Estimation of n_f and k_f values is dependent on the nature of the layer and its environment; the refractive index will be different for the dry and solvent-saturated layers. Furthermore, both n and k are dependent on the wavelength of the incident radiation and the temperature as shown in Eqns. 4-1 to 4-3 [Martensson, 1995]. Usually n_f must be estimated. According to Allara [1985], a value of n_f of 1.5 can be used for any solid, organic layer. This value is based on polyethylene which has a refractive index in the range of 1.49-1.55 [Brandrup, 1975]. Generalized Cauchy equations (Eqns 4-2 and 4-

3) have been developed whereby it is possible to estimate the bulk PEO refractive index as 1.476 for $\lambda = 620.0$ nm [Porter, 1987; Tompkins, 1999].

$$\left(\frac{\partial n}{\partial T}\right)_{P,C} = 5\times10^{-4} \qquad \textbf{Eqn. 4-1}$$

$$n(\lambda) = n_a + \frac{n_b}{\lambda^2} + \frac{n_c}{\lambda^4} \qquad \textbf{Eqn. 4-2}$$

$$k(\lambda) = k_a + \frac{k_b}{\lambda^2} + \frac{k_c}{\lambda^4} \qquad \textbf{Eqn. 4-3}$$

where P, C and T are pressure, concentration and temperature (Kelvin), respectively; n_a, n_b, n_c, k_a, k_b and k_c are the Cauchy coefficients for refractive index (n) and extinction coefficient (k). Tillman [1998] estimated that an increase in n_f of 0.05 resulted in a decrease in thickness of ~1 Å. A similar estimate by Porter [1987] indicated a thickness change of 1.4 Å. Based on the work of Rabe [1988], the inherent error of an ellipsometer is approximately 2 Å, so that n_f values within 0.15 of the true value would be sufficiently accurate not to affect significantly the thickness measurement.

For *in situ* measurements of polymer adsorption from solution, the interaction of the polymer with the surrounding fluid greatly affects the film thickness, refractive index and density profile normal to the interface. For example, layers of poly(ethylene imine)-poly(ethylene glycol) copolymers in water have been shown to have a refractive index of 1.352 [Malmsten, 1988]. This is quite different from the refractive index of solid PEO (1.475). In the present work, a refractive index of 1.37 was used to analyze *in situ* ellipsometry data for PEO chemisorbed on gold [Huang, 2001].

For dry polymer films k_f is generally considered to be zero since these films are usually considered non-absorbing. However, a spectroscopic ellipsometry investigation of thiol-gold surfaces has shown that when k_f is set to zero the model fit does not accurately describe the results obtained for select photon wavelengths [Shi, 1995]. It is suggested that this is due to a strong interaction between the near interface electrons and the thiol group that causes a unique optical transition, for some photon wavelengths, which is localized in the near (1.2 Å) interface layer [Shi, 1995; Martensson, 1995]. This means that for certain wavelengths k_f cannot be considered equal to zero for Au-thiol interactions. However, the wavelength used in the present work is far from these values, thus a k_f of zero was used in all calculations.

4.3.3 *Calculation of Mass in Layer*

For dry films, two methods have been proposed to convert the thickness of tethered PEO layers to surface density [Cuypers, 1983; Sofia, 1998]. In the present work dry chain densities were estimated using the method of Sofia [1998] as in Eqn. 4-4:

$$L = \left(\frac{M}{\rho_{dry} d N_A} \right)^{1/2} \qquad \textbf{Eqn. 4-4}$$

where L is the average distance between chain attachment points, M is the PEO molecular weight, ρ_{dry} is the density of the dry PEO layer (initially assumed to be 1.0 g cm^{-3}), d is the ellipsometrically-determined PEO average layer thickness, and N_A is Avogadro's number. Surface chain density can then be estimated as L^{-2}. A weakness of this method is the requirement that a value for the film mass density must be assumed. Calculations of

adsorbed amount for wet (measured *in situ*) films were carried out using Eqn. 4-5 [de Feijter, 1978],

$$\Gamma = \frac{d(n_2 - n_3)}{dn/dc} \qquad \textbf{Eqn. 4-5}$$

where (d) is the average film thickness, n_2 is the film refractive index, n_3 is the ambient refractive index and *dn/dc* is the specific refractive index increment. This relationship holds only if *dn/dc* is constant and the refractive index of the film is a linear function of the solute concentration. It can be used to determine the adsorbed amount of any macromolecule as long as the appropriate *dn/dc* value is used. The respective *dn/dc* values for PEO, fibrinogen and lysozyme are 0.134, 0.188 and 0.188 cm^3/g [Fu, 1997; Malmsten, 1994]. Furthermore, due to the strong correlation between film refractive index and average thickness, the error in the adsorbed amount is much smaller than in these two parameters individually [Tiberg, 1993]. Also the adsorbed amount, compared to either film refractive index or average thickness, is less sensitive to the optical model used. The adsorbed amount is thus a very robust parameter allowing for the investigation of complex systems [Malmsten, 2003].

4.3.4 ELLIPSOMETRY PROCEDURES

All ellipsometry experiments were conducted using a self-nulling, single wavelength (6328 Å) Exacta 2000™, as purchased from Waterloo Digital Electronics (Waterloo, Canada). All readings were conducted at an incident angle of 70°.

4.3.4.1 *EX SITU* PROCEDURE

Unique substrate optical parameters (A, P) were obtained for the gold – air interface. The gold was cleaned as described in Appendix A, and dried in a stream of ultra-high pure (UHP) N_2 gas (>5 min). Extreme care was taken not to scratch the surface. To ensure that carbonaceous contamination was minimized, the samples were immediately placed in the appropriate chemisorption solution. Chemisorption solutions of 5 mM PEO were prepared using Milli-Q, de-ionized distilled water, and were filtered (< 0.02 μm) prior to contact with the gold. After treatment samples were removed from the chemisorption solution, placed in filtered Milli-Q water and sonicated for 1 min to remove any unbound PEO. The samples were removed from the solution and dried under a nitrogen stream (> 5min). Ellipsometry measurements were then performed and ψ and Δ data were obtained at an incident angle of 70°. The adsorbed layer refractive index was assumed to be 1.475 and the thickness of the PEO film was determined using the Exacta 2000™ variable theta simplex fit program supplied by the ellipsometer manufacturer. *Ex situ* PEO chain densities were determined using Eqn. 4-4.

4.3.4.2 *IN SITU* PROCEDURE

In situ measurements required the design and construction of a "wet" cell capable of maintaining the sample in contact with the solution during the measurement. The wet cell used was constructed entirely of glass (Hellma, Germany) which was carefully annealed so as to reduce residual stresses in the windows which could induce birefringence effects. After cleaning, the substrates were placed in the cell containing

phosphate buffered saline (PBS) and their optical parameters (A, P) were obtained (30 min incubation). Extreme care was taken not to scratch the sample surface. To minimize carbonaceous contamination, the samples were immediately transferred into the appropriate chemisorption solutions, prepared as described above, for times ranging from 10 min to 4 h. The samples were then removed from the chemisorption solution, placed in filtered Milli-Q water and sonicated for 1 min to remove any physisorbed PEO. They were then transferred into the wet cell where A and P data were obtained after 30 min. Adsorbed PEO film refractive index and refractive index increment were assumed to be 1.37 and 0.134 cm^3/g respectively. The PEO film thickness was determined using the Exacta 2000^{TM} Variable theta simplex fit program supplied by the ellipsometer manufacturer. *In situ* PEO chain densities were determined using Eqn. 4-5 as discussed previously.

In situ ellipsometry was also employed to characterize adsorbed protein amounts on both control and PEO modified surfaces. Samples were placed in the wet cell in PBS (19 mL) and the optical parameters (A, P) were obtained every 5 s for 1 h. Protein-PBS solution (10 mg/mL) was then introduced into the cell to give a final protein concentration (after thorough mixing) of 0.5 mg/mL. As protein adsorption proceeded, ellipsometry data (A and P) were collected at an incident angle of 70° every 5 s for more than 3 h. Adsorbed protein layer refractive index and refractive index increment were assumed to be 1.37 and 0.188 cm^3/g, respectively. Protein layer thickness was determined using the Exacta 2000^{TM} Variable theta simplex fit program. Protein adsorbed amounts were determined using Eqn. 4-5. Sample calculations are provided in Appendix A.

4.4 *Neutron reflectometry.*

4.4.1 *Setup and Procedure*

Samples were mounted on the C5 Spectrometer of the Dualspec facility at the NRU reactor, Chalk River, Ontario configured as a reflectometer (Figure 4-3). A pyrolitic graphite monochromator [(002) Bragg reflection] selected neutrons with de Broglie wavelength $\lambda = 2.37$ Å as the incident beam. Beam collimation was controlled by a pair of motorized slits S1 and S2. Reflected intensity was measured as a function of the scattering vector normal to the sample defined by $Q_z = 4\pi \sin\theta/\lambda$, where θ is the incident angle and 2θ the angle between the incident beam and the specularly reflected beam. During the 2θ:θ scans, covering a Q_z range from 0.01 to 0.12 $Å^{-1}$, the incident beam slits were fixed at openings S1 = S2 = 0.4 mm for the low Q_z range (<0.01) and 0.8 mm for the high Q_z range (>0.01). Due to the different S1 and S2 openings for high and low Q_z values the neutron intensities must be scaled prior to analysis. Scaling was achieved by applying the factor $(0.8/0.4)^2 = 4$ (accounting for the different slit openings) to the low-Q_z data. The scattered-side slits, S3 and S4, were also adjusted during the scans, but did not affect the instrument resolution since the opening was kept greater than the width of the specularly reflected beam. No background correction was applied to the data, but a Q_z-independent background was included in the least-squares fitting of the models. The variation of the incident beam slits led to effective wavelength resolution $\Delta\lambda/\lambda = 0.6\%$, and effective $\Delta\theta = 0.5$ milli-radian (FWHM), the values adopted for the analysis.

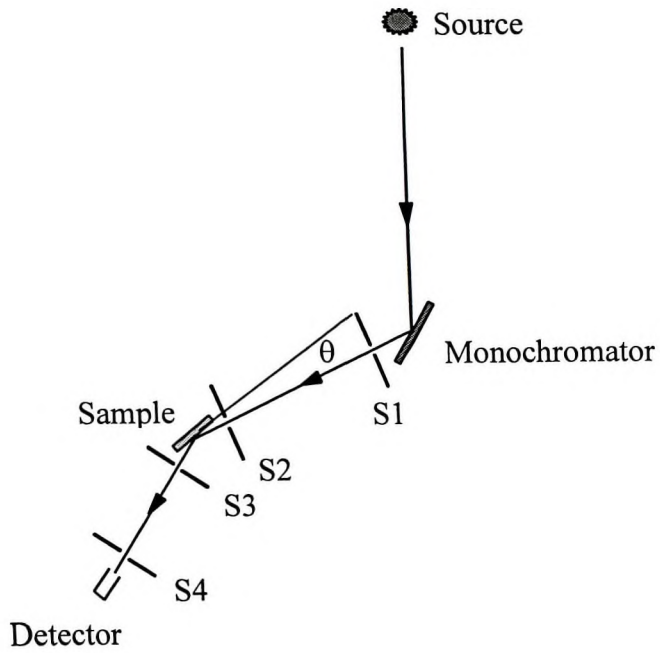

Figure 4-3. Schematic of neutron reflectometer setup.

4.4.2 Neutron Reflectometry Data Analysis

The analysis of reflectometry data involves proposing a layer profile model for the sample and refining its parameters. The least-squares fitting program MLAYER was used for this purpose [Ankner, 1988]. The most general model needed to represent the samples consisted of the following layers: air or contrast matched solution, PEO, gold, chromium, and the silicon substrate. For gold and chromium, the coating thicknesses specified by the supplier and the scattering length densities (SLD) for the bulk metals were adopted as the initial values. For the PEO layer, an initial thickness based on ellipsometry data was used, while the initial SLD was the value corresponding to a bulk density of 1.0 g cm^{-3}. The interfaces between layers were modeled initially as being

sharp, and the roughness parameters were introduced in later iterations provided they led to a significantly better fit.

4.5 *Protein Adsorption using ^{125}I Radiolabeled Proteins*

Radiolabeling of proteins is a standard technique used for determining protein adsorbed amounts and is perhaps the best method for precise quantification of small amounts. Several amino acids in proteins can react with active iodine species, specifically those that contain a sulfur atom or an aromatic structure, *viz.*, cysteine, histidine, methionine, phenylalanine, tryptophan and tyrosine, the latter being the most reactive [Regoeczi, 1984]. The labeled protein can be used as a tracer to measure adsorbed amount.

4.5.1 *Protein Labeling Procedure*

Fibrinogen and lysozyme (Calbiochem, La Jolla, CA) were radiolabeled with $Na^{125}I$ (ICN, Irvine, CA) using the iodine monochloride method, and dialyzed extensively against phosphate buffered saline (PBS, pH 7.4) to remove unbound ^{125}I (held to <1% of total solution radioactivity). Prior to protein adsorption experiments, gold-coated silicon wafers (unmodified or modified with PEO) were equilibrated in PBS-NaI buffer overnight; "cold" NaI was added to the buffer to inhibit the sorption of unbound ^{125}I to the gold surface according to a previously determined protocol [Du, 2000].

4.5.2 *Protein Adsorption from Buffer*

Protein adsorption experiments were performed in PBS-NaI buffer (pH=7.4) at protein concentrations of 1, 0.5, 0.3, 0.1, and 0.001 mg/mL (2% labeled, 98%

unlabelled). The surfaces were placed in the wells of 96-well multiwell plates and incubated for 3 h at room temperature (~22°C). The surfaces were rinsed three times (10 min each) with fresh PBS to remove any loosely bound protein. Surface radioactivity was determined and adsorbed amounts were calculated using background-corrected surface counts relative to the solution count for the highest protein concentration (1 mg/mL). The percent reduction of adsorption on the PEO surfaces relative to the unmodified gold was determined (see Appendix A).

4.5.3 PROTEIN ADSORPTION FROM PLASMA

Human fibrinogen was labeled with ^{125}I as described in Section 4.5.1. Whole human blood was used to prepare platelet poor plasma (PPP). Whole blood from at least ten healthy, drug-free donors was collected and mixed with 3.8% sodium citrate (w/v) solution (blood to citrate solution ratio, 9:1 v/v). The citrated blood was centrifuged at 4°C and 3000 g for 20 min. The PPP supernatant was removed, pooled, aliquoted and stored at -70°C. The PPP fibrinogen concentration was determined by the Clinical Hematology Laboratory at the McMaster University Medical Centre. Labeled fibrinogen was added to the plasma, in amounts corresponding to 2% (w/w) of the fibrinogen already present. Plasma solutions were serially diluted with phosphate buffered saline (PBS). Surfaces were introduced to the diluted plasma solutions, incubated, rinsed and counted as described in Section 4.5.2.

4.6 *Protein Adsorption Using SDS-PAGE and Western Blotting*

The effect of tethered PEO on the adsorption of proteins more generally (not just fibrinogen) from plasma and the identification and quantification of the various adsorbed proteins is of considerable interest. Sodium dodecyl sulfate poly(acrylamide) gel electrophoresis (SDS-PAGE) and immunoblotting, two important methods that are used to identify individual proteins (whole or fragmented) in a complex multi-protein mixture, were employed to identify the proteins eluted from the gold-PEO surfaces after plasma contact.

SDS-PAGE separates the proteins according to size. Colloidal gold staining allowed for observation of the banding patterns in the gels. Immunoblotting, whereby the protein bands in the gel are electrophoretically transferred to a polyvinylidene fluoride (PVDF) membrane and probed immunochemically, was used to identify the proteins. The blot membrane, cut into strips, was probed with various antibodies directed against specific proteins. Alkaline phosphatase conjugated secondary antibody, directed against the primary antibodies was subsequently introduced. Reaction of the alkaline phosphatase component with a chromogenic substrate indicated the presence of the various proteins. Detailed procedures for SDS-PAGE and immunoblotting are given in Appendix A.

4.7 References

Allara, D. L., Nuzzo, R. G., 'Spontaneously organized molecular assemblies. 1. Formation, dynamics, and physical properties of n-alkanoic acids adsorbed from solution on an oxidized aluminum surface.' *Langmuir,* **1**, 45 (1985).

Ankner, J. F., Majkrzak, C. F., *Proceedings of the Society of Photo-Optical Instrumentation Engineers,* **1738**, 260 (1988).

Azzam, R. M. A., Bashara, N. M., *Ellipsometry and Polarized Light,* North-Holland Publishing Company, New York, 1977, pp 2-10.

Bain, C. D., Whitesides, G. M., 'Attenuation lengths of photoelectrons in hydrocarbon films.' *J. Phys. Chem.,* **93**, 1670 (1989).

Brandrup, J., Immergut, E. H., *Polymer Handbook*, John Wiley, NewYork, 1975, pp v13-v22

Chibowski, E., 'Surface free energy of a solid from contact angle hysteresis.' *Adv. Coll. Interf. Sci.*, **103**, 149 (2003).

Cuypers, P.A., Corsel, J.W., Janssen M.P., Kop, J.M.M., Hermens, W.T., Hemker, H.C. 'The adsorption of prothrombin to phosphatidylserine multilayers quantitated by ellipsometry.' *J. Biol. Chem.*, **258**, 2426 (1983).

De Feijter, J. A., Benjamins, J., Veer, F. A., 'Ellipsometry as a tool to study the adsorption behavior of synthetic and biopolymers at the air-water interface.' *Biopolymers,* **17**, 1759 (1978).

Dettre, R.H., Johnson Jr., R.E., 'Contact angle hysteresis. II. Contact angle measurements on rough surfaces.' *Adv. in Chem. Series*, **43**, 136 (1964).

Dettre, R.H., Johnson Jr., R.E., 'Contact angle hysteresis. IV. Contact angle measurements on heterogeneous surfaces.' *J. Phys. Chem.*, **69**, 1507 (1965).

Dettre, R.H., Johnson Jr., R.E., 'Contact angle hysteresis. V. Porous surfaces.' *SCI monograph,* **25**, 144 (1967).

Du, Y.-J., Cornelius, R. M., Brash, J. L., 'Measurement of protein adsorption to gold surface by radioiodination methods: suppression of free iodide sorption.' *Col.and Surf.B: Biointerfaces*, **17**, 59 (2000).

Fu, Z., Santore, M.M., 'Evolution of Layer Density and Thickness during Poly(ethylene oxide) Adsorption onto Silica.' *Langmuir,* **13**, 5779 (1997).

Heavens, O.S., Optical Properties of Thin Solid Films, Dover Publications, New York, 1965, pp 55.

Hoeve, C. A. J., 'General theory of polymer absorption at a surface.' *J. Polym. Sci. C,* **30**, 361 (1970).

Hoeve, C. A. J., 'Theory of polymer adsorption at interfaces.' *J. Polym. Sci. C,* **34**, 1 (1971).

Huang, Y-W., Gupta, V.K., 'Effects of Physical Heterogeneity on the Adsorption of Poly(ethylene oxide) at a Solid-Liquid Interface.' *Macromolecules*, **34**, 3757 (2001).

Lamont, C.A., Wilkes, J., 'Attenuation Length of Electrons in Self-Assembled Monolayers of *n*-Alkanethiols on Gold.' *Langmuir*, **15**, 2037 (1999).

Malmsten, M., 'Competitive adsorption at hydrophobic surfaces from binary protein systems.' *J. Coll. Interfacial Sci.,* **166,** 333 (1994).

Malmsten, M., *"Macromolecular Adsorption: A Brief Introduction,"* in Biopolymers at Interfaces. 2nd Ed., M. Malmsten (ed), Marcel Dekker, Inc., New York, New York, 2003.

Malmsten, M., Emoto, K., van Alstine, J.M., 'Effect of chain density on inhibition of protein adsorption by poly (ethylene glycol) based coatings' *J. Coll. Interfacial Sci.,* **202,** 507 (1998).

Martensson, J., Arwin, H., 'Interpretation of Spectroscopic Ellipsometry Data on Protein Layers on Gold Including Substrate-Layer Interactions.' *Langmuir*, **11**, 963 (1995).

Miyama, M., Yang, Y., Yasuda, T., Okuno, T., Yasuda, H.K., 'Static and Dynamic Contact Angles of Water on Polymeric Surfaces.' *Langmuir,* **13**, 5494 (1997).

Porter, M. D., Bright, T. B., Allara, D. L., Chidsey, C. E. D., 'Spontaneously organized molecular assemblies. 4. Structural characterization of n-alkyl thiol monolayers on gold by optical ellipsometry, infrared spectroscopy, and electrochemistry.' *J.Am.Chem.Soc.,* **109**, 3559 (1987).

Regoeczi, E. Iodine-labeled plasma proteins. Volume 1. CRC Press, Inc. Boca Raton, Florida. Ch. 5,1984.

Shi, J., Hong, B., Parikh, A. N., Collins, R. W., Allara, D. L., 'Optical characterization of electronic transitions arising from the Au/S interface of self-assembled n-alkanethiolate monolayers.' *Chemical Physics Letters,* **246**, 90 (1995).

Sofia, S.J., Premnath, V., Merrill, E.W., 'Poly(ethylene oxide) Grafted to Silicon Surfaces: Grafting Density and Protein Adsorption.' *Macromolecules,* **31**, 5059 (1998).

Tiberg, F., Landgren, M., 'Characterization of thin nonionic surfactant films at the silica/water interface by means of ellipsometry.' *Langmuir,* **9,** 927 (1993).

Tompkins, H.G., McGahan, W.A., Spectroscopic Ellipsometry and Reflectometry, John Wiley and Sons, Inc., New York, New York, 1999, pp 125-131.

5.0 Contributions To Articles.

The following describes my contribution to the articles constituting Chapters 6-10. I was responsible for the refinement of the initial research objective and the conduct of all phases of the project, from the literature search and the planning of experiments through to data analysis. I designed and performed most experiments: Dr. Zin Tun provided guidance on the neutron reflectometry setup and data analysis (Papers I and V) and some data collection was done by various undergraduate summer students (Papers I, II and III). I was also responsible for designing and commissioning new equipment required for various experiments (eg. the wet cell for *in situ* ellipsometry). I generated the first drafts of the papers and worked with my supervisors on subsequent drafts. In the case of papers 1 and 2, I generated initial responses to the comments of the journal reviewers. Paper 3 was accepted without change.

6.0 PAPER ONE: CHEMISORPTION OF THIOLATED POLY(ETHYLENE OXIDE) TO GOLD: SURFACE CHAIN DENSITIES MEASURED BY ELLIPSOMETRY AND NEUTRON REFLECTOMETRY.

Authors: **L.D. Unsworth**, Z. Tun, H. Sheardown and J.L. Brash

Publication Information: Journal of Colloid and Interface Science 2005, 281, 112.

Acceptance Date: August 6, 2004

Working Hypothesis:

PEO layers of controlled chain density can be formed on gold by chemisorption through the regulation of PEO solubility and incubation time.

Main Scientific Contributions:

1. Proposed method of producing variable controlled chain density of PEO proved successful.

2. Ellipsometrically determined chain density ranges for PEO MWs 750, 2000 and 5000 were 0.4-0.7, 0.33-0.58 and 0.12-0.30 chains/nm^2, respectively; among the highest chain densities reported for these systems.

3. Ellipsometry and neutron reflectometry data for the layers in the dry state yielded similar chain density values for systems that were compared.

Copyright information:

ELSEVIER

Available online at www.sciencedirect.com
SCIENCE DIRECT®

Journal of Colloid and Interface Science ••• (••••) •••–•••

JOURNAL OF Colloid and Interface Science

www.elsevier.com/locate/jcis

Chemisorption of thiolated poly(ethylene oxide) to gold: surface chain densities measured by ellipsometry and neutron reflectometry

Larry D. Unsworth [a], Zin Tun [b], Heather Sheardown [a], John L. Brash [a,*]

[a] *Departments of Chemical Engineering and Pathology and Molecular Medicine, McMaster University, Hamilton, ON L8S 4L7, Canada*
[b] *Neutron Program for Materials Research, National Research Council Canada Chalk River Laboratories, Chalk River, ON K0J 1J0, Canada*

Received 19 March 2004; accepted 6 August 2004

Abstract

Physical property studies of surfaces formed by chemisorption of polyethylene oxide (PEO) onto gold are reported. Such surfaces have potential as model materials for elucidation of the mechanism of resistance to protein adsorption by PEO surfaces. Thiolated monomethoxy poly(ethylene oxide) (PEO) was chemisorbed onto gold-coated silicon wafers under various conditions such that different surface chain densities were achieved. Chain density was varied by controlling PEO solubility (proximity to cloud-point conditions) as well as chemisorption time. Films prepared with PEO of molecular weight 750, 2000, and 5000 g/mol were studied. Chain densities determined in the dry state by ellipsometry were found to be in the range of 0.4–0.7, 0.33–0.58, and 0.12–0.30 chains/nm^2 for MW 750, 2000, and 5000 PEO, respectively. Chain density was found to decrease with increasing molecular weight and to increase as cloud-point conditions were approached. PEO-layer mass densities and chain densities were determined independently by neutron reflectometry. Under low-solubility conditions and for a 4-h chemisorption time, film mass and chain density values of 1.0 ± 0.3 g cm^{-3} and 1.8 ± 0.9 chains/nm^2 were found for MW 750 PEO, and 0.82 ± 0.02 g cm^{-3} and 0.23 ± 0.07 chains/nm^2 for MW 5000 PEO. Ellipsometry data for these systems yielded graft densities of 0.63 ± 0.13 and 0.30 ± 0.02 chains/nm^2, respectively. Using the mass densities obtained from the neutron data in the ellipsometry calculations, chain densities of 0.6 ± 0.3 and 0.25 ± 0.02 chains/nm^2, respectively, were obtained for the MW 750 and 5000 films. The ellipsometry and neutron data for the MW 5000 system are thus in agreement within experimental error. In general, the chain-density values are much higher than those corresponding to layers of unperturbed random coil PEO ("mushrooms"), suggesting that the PEO layers are in the brush regime with the chains in an extended conformation.

Keywords: Ellipsometry; XPS; Poly(ethylene oxide); Chemisorption; Conformation; Cloud point; Surface chain density; Neutron reflectometry

1. Introduction

Poly(ethylene oxide) (PEO)-modified surfaces have attracted much attention due to their excellent anti-biofouling properties [1–4]. In particular they have been shown to be resistant to nonspecific protein adsorption. An important class of such materials are formed by grafting, i.e., attachment of PEO to the surface via the polymer chain ends. Although the mechanism of protein resistance on these surfaces is not entirely clear, it is believed that PEO chain length, surface chain density, and chain conformation are important factors [3,5].

Alexander [6] has pointed out that the conformation of end-tethered chains on a surface depends on the chain density (Fig. 1). A random coil conformation (mushroom regime) occurs when the graft spacing (S) is greater than $2R_F$ (R_F is the Flory radius), and a more extended conformation (brush regime) occurs when $S < 2R_F$. It is also well understood that stretching-entropy and excluded-volume interactions influence the chain density in the brush regime, in both cases as a result of lateral confinement. Thus by varying chain density, chain conformations ranging from unperturbed random coil to fully extended can, in principle, be obtained.

* Corresponding author. Fax: 905-521-1351.
E-mail address: brashjl@mcmaster.ca (J.L. Brash).

0021-9797/$ – see front matter
doi:10.1016/j.jcis.2004.08.022

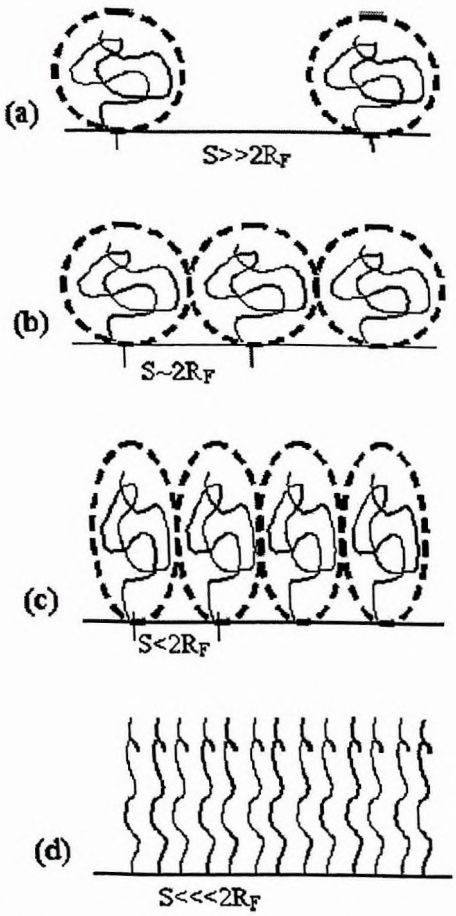

Fig. 1. Illustration of adsorbed PEO conformation and layer structure: (a) dilute nonoverlapping "mushrooms;" (b) semidilute weakly overlapping "mushrooms;" (c) "extended mushrooms," dilute brush regime; (d) highly extended chains, dense brush regime. S = distance between attachment points. R_F = Flory radius.

The focus of the present work is to produce well-characterized PEO-grafted surfaces of variable chain density and chain length to allow a detailed study of the influence of these parameters on protein resistance. In this article the preparation and characterization of a series of surfaces prepared by chemisorption of chain-end thiolated PEO (molecular weight range 750–5000) to gold is reported. Such a system should in principle allow variation of chain density up to high values, with an absolute upper limit corresponding to the density of thiol binding sites on gold.

The coupling of polymers and other molecules to gold by reaction with thiol groups has been widely reported [7–10]. A system that has been investigated extensively consists of intermediate-length alkanes (e.g., C-11), thiol-terminated at one end and "tipped" or not with an oligoethylene oxide (OEO) moiety at the other end. In these systems the ratio of OEO-terminated to non-OEO-terminated chains was used to control the effective PEO chain density on the surface [8–10]. The PEO chain length was in the range of three to six ethylene oxide units.

The approach taken in the present work is to vary surface chain density by varying the temperature and buffer ionic strength of the PEO solutions used for chemisorption [1,2]. Solution conditions can be used to modulate the polymer radius of gyration. Solutions of PEO in water exhibit a reverse dependence of solubility on temperature and begin to precipitate as the temperature is increased toward the cloud point. In addition, the cloud point temperature decreases with increasing ionic strength. As discussed by Kingshott et al. [2], grafting near cloud point conditions, where the polymer coils are relatively small, results in a relatively high surface chain density even though still in the mushroom regime; i.e., the chains are in the unperturbed random coil state. When the temperature is subsequently lowered and/or the ionic strength decreased, the tethered chains tend to expand, and constraints imposed by chain–chain proximity on the surface lead to extended chains and a brush-type layer (see Fig. 1), depending on the chain density and the unperturbed dimensions at the off-cloud-point conditions.

Characterization of the surfaces was carried out by four techniques, water contact angle, X-ray photoelectron spectroscopy (XPS), ellipsometry, and neutron reflectometry, where the latter two methods allow estimates of PEO chain density. Ellipsometry allows determination of the average thickness, the complex refractive index, and the quantity of material in adsorbed layers [11,12]. In the case of layers formed in solution, these quantities can be determined in situ [13] or in air after drying (ex situ) [14]. In the present work ex situ measurements in air are reported.

In neutron reflectometry (NR) [15,16], thin films are investigated by measuring the intensity of specularly reflected neutrons over a range of incident angles. The analysis involves defining a multilayer model of the surface (number and nature of components, thickness of each) whose calculated reflectivity is as close as possible to the experimentally determined value. Information on the layer profile normal to the interface is obtained. An advantage of NR over ellipsometry is that knowledge of the refractive index of the layer is not required to determine the thickness of ultrathin (<20 Å) films.

The objective of the present work was to determine accurate values of PEO chain density for correlation to protein interactions in subsequent studies. The use of ellipsometry and neutron reflectometry as two independent methods giving reasonably concordant values, as found here, represents significant progress toward this objective.

2. Materials and methods

α,ω-Methoxyhydroxypoly(ethylene oxides) (MW 750, 2000, 5000) were purchased from Shearwater Polymers,

Inc. (Huntsville, AL) and used without further purification. Dimethyl formamide (DMF), mercaptoacetic acid, isopropyl ether, dichloromethane, deuterated chloroform (99.9% grade), hydrogen peroxide, ammonium hydroxide, and toluene were purchased from Sigma–Aldrich (Oakville, ON). Silicon(111) wafers (2-in. diameter, 1000-μm thickness) were polished on both sides, treated to remove natural oxide, and sputter-coated with chromium (adhesion layer, nominally 400 Å), followed by gold (nominally 1000 Å), and cut into (0.5 × 0.5)-cm pieces (Thin Film Technology, Buellton, CA).

2.1. *Thiolation of PEO*

PEO was chain-end thiolated by reaction with mercaptoacetic acid as described in detail elsewhere [17,18]. Briefly, a drop of sulfuric acid, 5 g of PEO, and a stoichiometric amount of mercaptoacetic acid (1:1, OH:COOH) were added to 25 ml of toluene preheated to 80 °C. The reaction proceeded for 3 h and was driven forward by the continuous removal of the water produced. The modified polymer was purified by precipitation in isopropyl ether (300 ml) and subsequent dissolution in dichloromethane. This sequence was repeated three times. The reaction product was then dried under vacuum at room temperature for 2 days. Verification of the esterfication reaction was obtained from proton NMR spectra of the products, taken in deuterated chloroform. The products were also characterized by gel permeation chromatography (GPC) using dimethyl formamide as the carrier solvent at 80 °C and 0.25% w/w polymer solutions. Data were analyzed using software provided by the manufacturer and a calibration curve constructed with narrowly distributed PEO standards.

2.2. *Chemisorption procedure*

Conditions for the chemisorption of thiolated PEO onto gold (Table 1) were varied as a means of manipulating PEO chain density on the surface. This strategy is based on the premise that higher chain densities should be obtained as cloud point conditions are approached [2]. Chemisorption time was also varied over the range from 10 min to 4 h.

Table 1
Chemisorption solution conditions

PEO molecular weight (g/mol)	Temperature (°C)	Ionic strength (M)	Solubility
750	25	Low	High
	25	2.9	Intermediate
	35	2.9	Low
2000	25	Low	High
	25	2.8	Intermediate
	35	2.8	Low
5000	25	Low	High
	25	1.9	Intermediate
	30	1.9	Low

Note. All polymer concentrations were 5 mM and solution pH was 7.4 ± 0.1.

Prior to chemisorption, the gold-coated silicon wafers were immersed in a solution consisting of one part by volume hydrogen peroxide (30%), one part by volume ammonium hydroxide (30%), and five parts by volume water at 80 °C for 5 min, sonicated for 1 min, and rinsed with Millipore Milli-Q water to remove carbonaceous contamination. The wafers were immediately placed in the wells of a 96-well plate containing Milli-Q water. Other wells contained the chemisorption solutions. The plate was then placed in a temperature-controlled bath (25 or 35 °C). Once thermal equilibrium was achieved, the wafers were transferred into the wells containing the chemisorption solutions for various times. Following chemisorption, the wafers were placed in wells containing Milli-Q water, sonicated for 4 min, and rinsed extensively with water. They were then dried in a stream of ultra-high-purity nitrogen (UHP-N_2) prior to contact angle, XPS, ellipsometry, and neutron reflectivity measurements.

2.3. *Water contact angles*

Sessile-drop water contact angles were determined using water drops with a volume no greater than 3 μl. Advancing and receding angles were obtained using a Ramé–Hart NRL 100-00 goniometer (Mountain Lakes, NJ).

2.4. *X-ray photoelectron spectroscopy (XPS)*

XPS spectra were obtained using a Leybold (Specs, Berlin) MAX 200 XPS system employing an unmonochromated Al$K\alpha$ source operating at 15 kV and 20 mA. Low-resolution spectra (pass energy = 192 eV) were used to determine atomic compositions; high-resolution C1*s* spectra (pass energy = 48 eV) provided additional surface structural information. Specslab (Specs, Berlin) software was used for spectral fitting. Spectra were taken at two takeoff angles: 90° and 20° relative to the surface. The respective spot sizes were 2 × 4 and 1 × 1 mm; the smaller area at 20° was used to ensure that the beam footprint remained on the samples.

2.5. *Ex situ ellipsometry*

A self-nulling, single-wavelength (6328 Å) ellipsometer (Exacta 2000, Waterloo Digital Electronics, Waterloo, Ontario, Canada), with an incident angle of 70°, was used to determine the properties of the chemisorbed PEO layers. Gold-coated wafers, cleaned and dried as described above, were considered as the substrate. The refractive index (n_s) and extinction coefficient (k_s) were determined to be 0.33 ± 0.01 and 3.3 ± 0.01, respectively. For the PEO-modified surfaces, the polarizer (P) and analyzer (A) angles for the null condition were measured and thickness values were determined using a three-layer air–PEO–gold model. Complex refractive-index values ($n_i + \imath k_i$) of $0 + \imath 0$ and ($n_f + \imath k_f$) of $1.47 + \imath 0$ were used for air and PEO film, respectively. The PEO film refractive index (n_f) was estimated

from the lowest Cauchy parameters, namely $A_n = 1.45$ and $B_n = 0.01$, corresponding to a refractive index of 1.47 at a wavelength of 620.0 nm [19]. Final thickness values were obtained by fitting the experimental data to the model using the Exacta 2000 Variable Theta Simplex Fitting Program (Waterloo Digital Electronics). The relative humidity was not controlled but in all experiments was at a level of 50% or less. Matsuguchi et al. [20] have shown that under these conditions the water content in the PEO layer is less than 1 wt% and thus should make a negligible contribution to the optical properties.

Different methods have been used to convert data on the thickness of PEO layers to surface chain density [4,14]. In this work chain densities were estimated using an equation proposed by Sofia et al. [4],

$$L = \left(\frac{M}{\rho_{dry}\, d\, N_A}\right)^{1/2}, \quad (1)$$

where L is the average distance between chain attachment points, M is the PEO molecular weight, ρ_{dry} is the density of the dry PEO layer (assumed initially to be 1.0 g cm^{-3}), d is the ellipsometrically determined PEO average layer thickness, and N_A is Avogadro's number. Surface chain density can then be estimated as L^{-2}. A weakness of this method is the requirement that a value for the film mass density must be assumed. In the present work this assumption was tested for several systems by determining the layer density using neutron reflectometry.

2.6. Neutron reflectometry

Samples were mounted (in air) on the C5 Spectrometer of the Dualspec facility at the NRU reactor, Chalk River, Ontario, configured as a reflectometer. A pyrolitic graphite monochromator [(002) Bragg reflection] selected neutrons with de Broglie wavelength $\lambda = 2.37$ Å as the incident beam. Beam collimation was controlled by a pair of motorized slits, S1 and S2. Reflected intensity was measured as a function of the scattering vector normal to the sample, as defined by the equation

$$Q_z = 4\pi \sin(\theta)/\lambda, \quad (2)$$

where θ is the incident angle and 2θ the angle between the incident beam and the specularly reflected beam. During the $2\theta{:}\theta$ scans, covering a Q_z range from 0.01 to 0.1 Å^{-1}, the incident-beam slits were fixed at openings S1 = S2 = 0.4 mm for low Q_z range and 0.8 mm for high Q_z range. Scaling between these two ranges was achieved by applying the factor $(0.8/0.4)^2 = 4$ to the low-Q_z-range data. No background correction was applied to the data, but a Q_z-independent background was included in the least-squares fitting of the model. The variation of the incident slits led to effective wavelength resolution $\Delta\lambda/\lambda = 0.6\%$ and effective $\Delta\theta = 0.5$ milliradian (FWHM), the values adopted for the analysis.

As discussed above, the analysis of reflectometry data involves proposing a layer profile model for the sample and refining its parameters. The least-squares fitting program MLAYER was used for this purpose [21]. The most general model needed to represent the samples consisted of the following layers: air (incident medium), PEO, gold, chromium, and the silicon substrate (final medium). For gold and chromium, the coating thicknesses specified by the supplier and the scattering length density (SLD) for the bulk metals were adopted as the initial values. For the PEO layer, the initial thickness was from the ellipsometry data while the initial SLD was the value corresponding to a bulk density of 1.0 g cm^{-3}. The interfaces between layers were modeled initially as being sharp, and the roughness parameters were introduced in later iterations provided they led to a significantly better fit.

3. Results and discussion

3.1. Water contact angles

Experiments in which gold surfaces were exposed to unmodified PEO under various conditions were carried out to verify that the thiol group was necessary both for permanent PEO attachment to the gold surface and for obtaining high PEO densities. Exposure and washing procedures were the same as when the thiolated PEOs were used. Water contact angles were measured before and after exposure to unmodified PEO. It is apparent from the data (Table 2) that the water contact angles of the surfaces incubated with solutions of unmodified PEO (possibly leading to physisorption) and then washed do not differ from those of the unmodified gold surface.

In contrast, surfaces incubated with thiolated PEO show significant decreases in contact angle (Table 3). The advancing and receding angles on unmodified gold were 62° ± 6° and 34° ± 11°, respectively. Following chemisorption, the

Table 2
Water contact angles (°) of surfaces prepared with non-thiolated PEO

	MW 750		MW 2000		MW 5000	
	Advancing	Receding	Advancing	Receding	Advancing	Receding
High solubility, 4 h[a]	62 ± 4	43 ± 4	56 ± 4	41 ± 4	59 ± 3	44 ± 2
Low solubility, 30 min[a]	67 ± 4	46 ± 7	65 ± 2	44 ± 4	60 ± 2	42 ± 6

Note. Unmodified gold advancing and receding contact angles were 62° ± 6° and 34° ± 11°, respectively. Data are mean ±SD ($n \geq 8$).
[a] See Table 1.

Table 3
Water contact angles (°) of surfaces prepared by chemisorption of PEO to Au

	MW 750		MW 2000		MW 5000	
	Advancing	Receding	Advancing	Receding	Advancing	Receding
Unmodified gold	62±6	34±11	62±6	34±11	62±6	34±11
High solubility, 4 h[a]	36±11	23±6	40±4	18±4	47±8	25±10
Intermediate solubility, 4 h[a]	30±5	25±3	30±4	16±5	27±5	12±5
Low solubility, 10 min[a]	46±1	24±2	53±9	25±3	37±10	19±7
Low solubility, 30 min[a]	39±1	16±1	38±5	18±4	41±8	19±4
Low solubility, 2 h[a]	42±4	20±2	40±4	22±6	39±6	18±3
Low solubility, 4 h[a]	35±1	17±1	37±4	20±4	38±4	17±3

Note. Data are mean ±SD ($n \geq 8$).
[a] See Table 1.

Table 4
Atomic compositions (%) from low-resolution XPS data for high- and low-solubility systems

Surface	Takeoff angle (°)	Au4*f* (84 eV)	C1*s* (285 eV)	O1*s* (532 eV)	S2*p* (162 eV)	C:O
Gold	90	37.4	47.8	14.7		3.25
Pure PEO	90		71.8	25.8		2.78
MW 750, high sol, 4 h	90	45.9±10.5	43.5±11.8	14.9±7.6	2.2±1.0	2.92
	20	19.3	62.1	17.8	0.8	3.49
MW 750, low sol, 0.5 h	90	59.5±2.3	31.6±1.3	6.4±0.6	2.6±0.1	4.94
	20	34.4	42.9	17.3	5.3	2.48
MW 750, low sol, 4 h	90	58.0±1.9	32.3±2.2	7.3±0.1	2.5±0.4	4.42
	20	31.4±0.7	48.5±1.8	16.8±0.1	3.4±1.0	2.88
MW 2000, high sol, 4 h	90	53.4±6.1	34.2±4.7	10.9±1.7	1.4±0.4	3.14
	20	25.6±4.7	53.5±5.7	18.5±1.6	2.5±0.7	2.89
MW 2000, low sol, 4 h	90	56.8±7.4	34.5±5.9	6.8±1.1	2.1±0.4	5.07
	20	21.7±2.8	56.2±0.3	20.3±3.0	1.9±0.6	2.76
MW 5000, high sol, 4 h	90	60.6±0.1	31.9±1.3	7.3±0.6	0.8±0.6	4.37
	20	22.4±0.3	53.6±1.2	19.6±4.9	0.1±0.1	2.73
MW 5000, low sol, 4 h	90	51.6±5.5	35.5±5.5	10.3±0.6	2.6±0.6	3.45
	20	23.4±1.6	55.0±4.1	19.6±6.9	2.1±1.2	2.81

Note. Where no error limits are given, $n = 1$. For entries with error limits, data are mean ±SD, $n = 3$.

angles decreased significantly ($\alpha < 0.05$, Student *t*-test) for all exposure conditions and PEO MWs, suggesting the presence of strongly attached PEO. It can also be seen that the receding angle for the MW 750 PEO surface decreased from 23°±6° at high solubility to 17°±1° nearer the cloud point. A similar trend was seen for the MW 5000 systems. Also, for low-solubility conditions, the receding angle reached a constant value after 30 min of chemisorption for MW 750 and 2000, and after 10 min for MW 5000 PEO, suggesting that saturation is achieved more rapidly for the higher molecular weights.

3.2. *X-ray photoelectron spectroscopy (XPS)*

XPS data were obtained at takeoff angles of 90° and 20° for selected surfaces. Atomic compositions derived from low-resolution data are summarized in Table 4. High-resolution C1*s* data are summarized in Table 5. PEO was melted and cast as a 5-mm-thick film for XPS analysis. Data on this "pure" PEO surface and a bare, clean gold surface were obtained for comparison with the PEO-modified surfaces. Reference to the bare gold surface as "clean" is only nominal, as contamination on this surface by carbon- and oxygen-containing material, probably deposited from the atmosphere [22], is evident (C and O contents at 47.8 and 14.7%). For the pure PEO, however, the measured C:O ratio was 2.78, compared to an expected value of 2.0. The discrepancy is again probably due to instrument resolution and atmospheric contaminants. For the PEO-modified surfaces, less gold and more C and O are seen when the takeoff angle is changed from 90° to 20°. This is as expected, as XPS becomes more surface-sensitive at lower takeoff angles. Furthermore, the C and O contents for the modified surfaces, when viewed at a 90° takeoff angle, were consistently less than for the bare gold. This observation may suggest displacement of the contaminants by the thiolated PEO (of lower O and C content), as it is well known that

Table 5
Chain density estimates based on close packed layers of unperturbed PEO (Eq. (3))

System	High solubility (chains/nm^2)	Low solubility (chains/nm^2)
MW 750	0.14	0.24
MW 2000	0.04	0.09
MW 5000	0.01	0.04

gold interacts strongly with thiols [22]. On the other hand, at a 20° takeoff angle, the C:O ratios were close to 2.78 for all modified systems (an exception is the MW 750, high-sol, 4-h, surface with a C:O ratio of 3.49). This trend suggests that the outermost surface formed under low solubility conditions consists of PEO and little else. It is also evident that the surface concentration of PEO is greater when chemisorption occurs under low-solubility, compared to high-solubility conditions.

An indication of how the surface chain density varies with the solubility of PEO is given by the sulfur content data. First, it should be noted that S is not a constituent of the contaminants on bare gold, making it a unique marker of the presence of adsorbed PEO. For the MW 5000 surfaces, it is seen that the S content increases by at least a factor of 2 upon changing from high to low solubility. Thus it appears that as the cloud point is approached the dehydration and collapse of the chains is relatively greater for the MW 5000 than for either the MW 750 or 2000 PEO. Similar trends were seen in the ellipsometry data on chain density, as discussed below.

3.3. PEO chain density in chemisorbed layers

To provide context for the data from ellipsometry and neutron reflectivity measurements, an approximate upper limit to chain density and the chain density corresponding to close-packed layers of unperturbed random coils (mushroom regime) are of interest. An upper limit of 5.8 chains/nm^2 may be estimated based on a layer of close-packed, extended PEO chains of cross section 17.1 Å^2 [23]. The chain density of layers of "equivalent" PEO spheres with radius equal to the Flory radius (R_F) can be estimated using the equation

$$R_F = aN^{\nu}, \tag{3}$$

where a is the characteristic monomer dimension (taken as 2.78 Å for the ethylene oxide repeat [3]), N is the degree of polymerization and ν may be taken as 0.6 for high-solubility conditions, 0.5 for the θ condition. Chain densities estimated for the unperturbed chains at high- and low-solubility conditions for MW 750, 2000, and 5000 PEO are summarized in Table 5.

3.4. Ellipsometry

Chain densities determined by ellipsometry (Table 6) ranged from about 0.1 to 0.7 chains/nm^2, and for each molecular weight were significantly greater than the values for monolayers of unperturbed random coils (Table 5). It is concluded that for all conditions used the PEO layers were in the brush regime, implying that the driving force for chemisorption was sufficient for coverage to proceed beyond the close-packed mushroom regime ($S \sim 2R_F$), thus forcing the chains to adopt an extended conformation [24]. However, it appears that coverage corresponding to a close-packed layer of fully extended chains (i.e., ~5.8 chains/nm^2) did not occur in these systems, presumably due to limitations imposed by steric hindrance at higher coverage. It is also seen that the chain densities decreased significantly with increasing PEO molecular weight, possibly due to the greater steric hindrance associated with insertion of longer chains into the developing layer. For all three molecular weights the chain density increased significantly ($\alpha < 0.05$) with increasing proximity to cloud-point conditions (high to low solubility).

Table 6
Ellipsometrically determined chain densities (chains/nm^2)

	MW 750	MW 2000	MW 5000
High solubility, 4 h[a]	0.4 ± 0.1	0.33 ± 0.08	0.12 ± 0.02
Intermediate solubility, 4 h[a]	0.68 ± 0.16	0.56 ± 0.09	0.22 ± 0.03
Low solubility, 10 min[a]	0.44 ± 0.12	0.33 ± 0.04	0.25 ± 0.01
Low solubility, 30 min[a]	0.47 ± 0.11	0.33 ± 0.10	0.24 ± 0.02
Low solubility, 2 h[a]	0.70 ± 0.16	0.51 ± 0.09	0.27 ± 0.02
Low solubility, 4 h[a]	0.63 ± 0.13	0.58 ± 0.13	0.30 ± 0.02

Note. Estimates from thickness as determined by ellipsometry and the use of Eq. (1). Values are mean ±SD ($n \geq 7$).
[a] See Table 1.

Table 7
Model parameter estimates for gold-coated silicon wafers

Medium	Thickness (Å)	Interface width (Å)	SLD × 10^6 (Å^{-2})
Air	∞		0 (fixed)
		17.3	
Au	826		4.5
		Sharp	
Cr	100		3.0
		Sharp	
Si	∞		2.069 (fixed)

Note. All entries had SD values of 0.1 or less.

Data on the time dependence of chemisorption from 10 min to 4 h were obtained for low-solubility conditions, and for all three molecular weights chain density increased over this interval. The rate of chemisorption decreased with time, presumably since at higher coverage the layer must "re-arrange" to allow access of additional chains to the gold.

3.5. Neutron reflectometry

Neutron reflectometry measurements were first done on a bare gold surface (no PEO) and the SLD profile was least-squares fitted for the model layer structure air/Au/Cr/Si. This surface served as a "control" and allowed validation of the data-acquisition and least-squares refinement procedures. The least-squares fitted model parameters are listed in Table 7. The refined SLD values are slightly lower than the values expected for crystalline gold and chromium, probably indicating that the metal layers are somewhat amorphous. The agreement between observed and calculated intensities (not shown) is excellent over the entire Q_z range, providing strong evidence that the model used to analyze the NR data is appropriate.

The value of the parameter describing the width of the air/gold interface is of interest, since it provides a measure of the roughness of the surface onto which PEO layers were

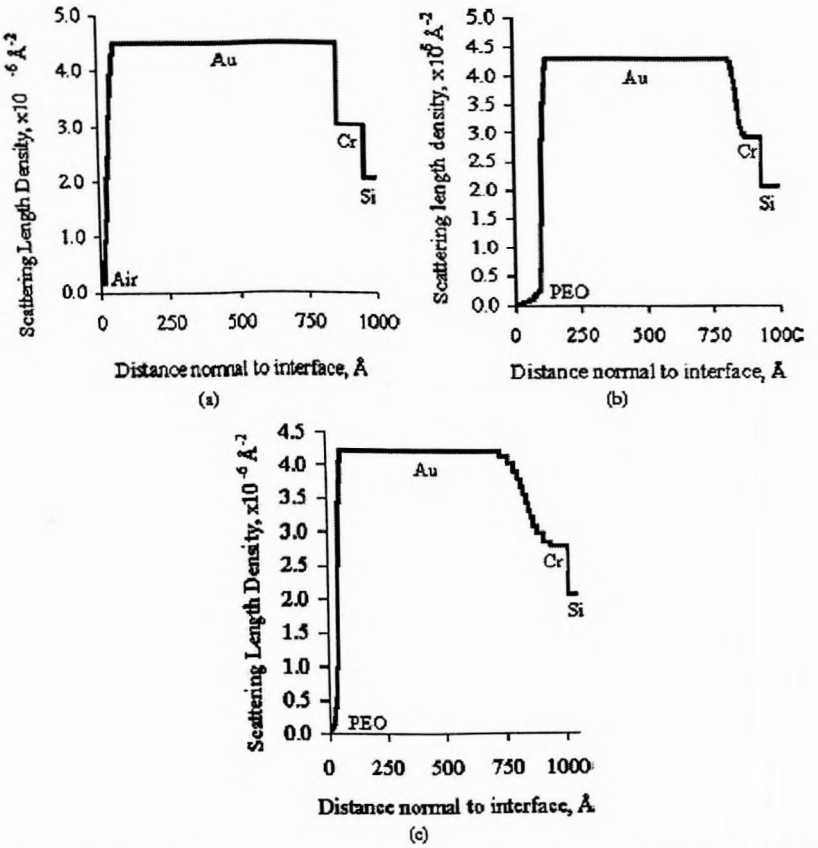

Fig. 2. SLD profiles for PEO-modified gold-coated Si substrate. (a) Control, bare gold surface. (b) MW 750 PEO. Layer formed at 35 °C, 2.9 M ionic strength over 4 h. The layer order of the model is air–PEO–Au–Cr–Si from zero to high z values. (c) MW 5000 PEO. Layer formed at 30 °C, 1.9 M ionic strength over 4 h.

adsorbed. This width, specified by the MLAYER roughness parameter [21], was estimated as 17.31 ± 0.07 Å. We note that the width of the gold/air interface is significant compared to the Flory radii of 11.5 and 29.7 Å for the MW 750 and 5000 PEO, respectively. Consequently the PEO layers are not expected to appear as plateaus in the model profiles (SLD vs z distance curves) since the composition will be changing continuously over the interfacial region. This effect will be especially important for the MW 750 system.

Least-squares fitted SLD profiles obtained for the surfaces chemisorbed for 4 h under low-solubility conditions with PEO of MW 750 and 5000 are shown in Fig. 2, where the assumed layer structure is air/PEO/Au/Cr/Si. The agreement between observed and calculated reflectivity from the models (circles and solid curve) is depicted in Fig. 3, for the MW 5000 system as an example. The agreement obtained for the MW 750 is at the same level and hence is not shown. Fig. 3 also includes the calculated reflectivity from least-squares fitting of a model without a PEO layer (dashed curve). For this test all parameters were allowed to vary except the Q_z-independent background and those rep-

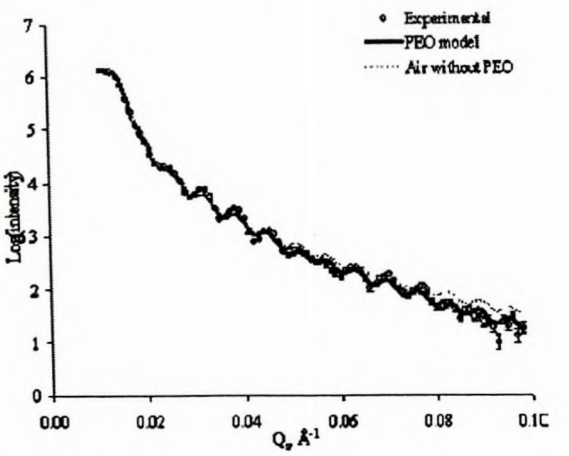

Fig. 3. Reflected neutron intensities for gold-coated Si substrate modified with MW 5000 PEO under low-solubility conditions after 4 h. Observed (circles) and calculated (solid curve) reflected neutron intensities for PEO present ($\chi^2 = 7.03$) and not present ($\chi^2 = 19.40$) at the surface.

Table 8
Least-squares fitted model parameters (±SD) for chemisorbed PEO layers formed under low-solubility conditions. Where two entries are shown, the upper number is for MW 750 PEO and the lower number for MW 5000 PEO

	Thickness (Å)	Interface width (Å)	SLD × 10^6 (Å^{-2})
Air	∞		0 (fixed)
		57.8 ± 4.7	
		16.0 ± 2.4	
PEO	9.8±8.0		0.54 ± 0.12
	19.4±0.5		0.46 ± 0.01
		12.4 ± 0.9	
		12.4 ± 0.6	
Au	735		4.3
	792		4.2
		19.1 ± 0.6	
		65.7	
Cr	92		2.9
	174		2.8
		Sharp	
		Sharp	
Si	∞		2.069 (fixed)

Note. All entries had SD values of 0.1 or less, unless presented.

resenting the instrument resolution. Clearly the "PEO-less" model does not yield satisfactory agreement for the entire Q_z range, indicating that this extra layer *is* essential. Yet, the layers representing the PEO are not seen as well-defined plateaus in Fig. 2, presumably due to the roughness of the underlying gold surface.

The refined parameters for the PEO-containing models are listed in Table 8. The main interest is in the parameters for the PEO layer since changes in the gold and chromium parameters, unless they deviate substantially from expected values, simply reflect sample-to-sample variations in metal deposition. The parameters for the PEO films are reasonable for both MW 750 and 5000 systems. Indeed, the thicknesses of 9.8 ± 8.0 and 19.4 ± 0.5 Å obtained for the MW 750 and 5000 low-solubility systems (4 h incubation) compare well with the values determined by ellipsometry, viz., 7.2 ± 1.4 and 21.0±2.9 Å, assuming a PEO refractive index of 1.475. Furthermore, the calculated dry PEO film densities for the MW 750 and 5000 low-solubility systems (4 h incubation) were 1.0 ± 0.3 and 0.82 ± 0.02 g cm^{-3}. The estimated error in the NR-determined thickness and film density for the MW 750 system is especially large as a result of a low intensity-to-background ratio at very high Q_z values (an inherent instrument problem for very thin layers). In this regard it must be pointed out that although greater layer contrast could have been obtained using deuterated PEO for the NR measurements, natural isotopic PEO was used because direct comparison with ellipsometry data and future solution-contrast matched in situ studies, an important goal of the work, would then be possible.

As stated above, an ultimate goal of this work is to determine the density of PEO chains based on NR without any prior assumptions. If layers with well-defined SLD plateaus were observed this would be straightforward. Since SLD, by definition, is volume density (ρ) times scattering length (b) of constituent molecules, surface density Γ_{poly} is given by

$$\Gamma_{poly} = \frac{(SLD)_{poly} \times t}{b_{poly}}, \tag{4a}$$

where t is the thickness of the PEO layer. To apply this equation, one would identify the SLD value of the plateau as $(SLD)_{poly}$ and the distance between the midpoints of the interfaces on either side of the plateau as the thickness, t. In the absence of a plateau a different method has been devised as follows.

One could calculate the SLD corresponding exclusively to PEO from the model parameters (Table 8). The calculation using the MLAYER program is straightforward—the SLD values for all materials except PEO are set to zero and the calculation that produces the curves in Fig. 2 is repeated. This curve essentially shows how the SLD of PEO varies as a function of depth z, and the numerical integral under the curve is the generalization of the numerator in Eq. (4a). Γ_{poly} is given by

$$\Gamma_{poly} = \frac{\int SLD'_{poly}\, dz}{b_{poly}}, \tag{4b}$$

where SLD'_{poly} is a function of z as described above. Also, b_{poly} is the total scattering length of the PEO molecule which, in our case, is 17 b_{mono} for MW 750 and 114 b_{mono} for MW 5000, where b_{mono} for an H_4C_2O unit is 4.15×10^{-5} Å.

The chain densities obtained by this procedure were 1.8 ± 0.9 chains/nm^2 for MW 750 PEO, and 0.23 ± 0.07 chains/nm^2 for MW 5000 PEO. Ellipsometry measurements on these systems (chemisorption done under low-solubility conditions) yielded chain densities of 0.63 ± 0.13 and 0.30 ± 0.02 chains/nm^2 for MW 750 and 5000 PEO, respectively, assuming a film density of 1 g cm^{-3}. Using the film densities determined by NR in the ellipsometry calculations, chain densities of 0.6 ± 0.3 and 0.25 ± 0.02 chains/nm^2 were obtained for the MW 750 and MW 5000 systems, respectively. Again, for the thicker MW 5000 films the ellipsometry and NR values are very similar. For the MW 750 layers the chain densities are not statistically different, viz., 1.8 ± 0.9 and 0.63 ± 0.13 chains/nm^2 for NR and ellipsometry, respectively.

The chain densities obtained in this work are larger than most previously reported values for end-tethered PEO. Malmsten et al. [3] reported a maximum density, as determined by ellipsometry, of 0.12 chains/nm^2 for MW 5000 PEO grafted to silica or quartz. This value, though lower than those found in the present study, also indicates an extended chain conformation. Efremova et al. [25] found chain densities of 1.16, 0.20, and 0.23 chains/nm^2 for PEO of MW 120, 2000, and 5000 at the air–water interface. In these systems the PEO was conjugated to a phospholipid (1,2-distearoyl-*sn*-glycero-3-phosphoethanolamine, DSPE) adsorbed to the air–water interface and the chain densities

determined using a Langmuir trough. The maximum chain density for the MW 5000 PEO was similar to the value found in the present work and is also in the range expected for an extended chain conformation. Recently, Tokumitsu et al. [19] reported a maximum dry thickness, as determined by ellipsometry, of 120 Å for a layer, formed by chemisorption to gold, of MW 2000 PEO conjugated to C_{11} alkanethiols. This corresponds to a chain density of ~3.6 chains/nm^2, assuming a film mass density of 1 and application of Eq. (1). In the latter system the PEO appears to adopt an extended chain conformation with graft densities much higher than in the simpler HS–PEO chemisorbed layers reported here. Hydrophobic interactions among the alkane components near the gold surface in the systems studied by Tokumitsu et al. may account for this difference. Previous neutron reflectivity measurements conducted by Kuhl et al. [26] may be compared with our data. Their experiments were conducted with a $Q_{z,max}$ in the range of 0.05 to 0.15, compared to our chosen $Q_{z,max}$ of 0.1 (Fig. 3). Kuhl's work showed that going to values of Q_z greater than 0.1 did not yield additional information, nor did it increase the data resolution. Our choice of $Q_{z,max} = 0.1$ thus seems reasonable. It should also be noted that the work of Kuhl et al. employed a strategy for fitting similar to that used in this study; i.e., the dry state layers were analyzed with box models, including interfacial roughness zones.

It is apparent from the results of this study that by varying both PEO solubility and chemisorption time, it is possible to generate surfaces with varying chain densities. Furthermore, it is apparent that ellipsometry and neutron reflectometry measurements returned similar values of chain density for the MW 5000, low-solubility system. For the thinner layers formed in the low-solubility MW 750 PEO system, for which agreement between the two methods is not as good, it is likely that the accuracy of the data is reduced for both methods.

As indicated, these surfaces are of interest for the study of the mechanisms involved in the resistance of PEO-modified surfaces to protein adsorption. Such studies will be reported in future communications.

4. Summary

Thiolated PEO (MW 750, 2000, and 5000) was chemisorbed to gold under various solubility conditions and for various times as a means of varying the surface chain density. The dry layers were characterized using ellipsometry and neutron reflectometry as independent methods for determining chain density.

It was shown that a terminal thiol group on the PEO was required for "permanent" attachment of PEO (resistant to washing with buffer). Following chemisorption, the water contact angles decreased significantly for all MWs, indicating increased hydrophilicity associated with the presence of PEO. The angles were found to level off for the low-solubility MW 750, 2000, and 5000 systems after 30, 30, and 10 min chemisorption, respectively. XPS data showed significantly higher sulfur content for the low- versus high-solubility MW 5000 systems. Similar C:O ratios were observed for pure PEO and the different modified surfaces. These data suggest that the surface density of chemisorbed PEO increases with decreasing solubility (approach to cloud point conditions).

Chain densities were estimated from ellipsometry data assuming a layer density of 1.0 g cm^{-3}, and were found to be in the range of 0.4–0.7, 0.33–0.58, and 0.12–0.30 chains/nm^2 for MW 750, 2000, and 5000 PEO, respectively. Layer densities and surface chain densities determined by neutron reflectometry for layers formed under low-solubility conditions (4 h incubation) were 1.0 ± 0.3 g cm^{-3} and 1.8 ± 0.9 chains/nm^2 for MW 750 PEO and 0.82 ± 0.02 g cm^{-3} and 0.23 ± 0.07 chains/nm^2 for MW 5000 PEO. The large scatter in the neutron reflectometry data for the low-solubility MW 750 PEO system is believed to be due to the fact that the PEO layer is too thin to be resolved accurately with the captured Q_z range.

In general, the chain density values are higher than those expected for layers of unperturbed random-coil PEO (the "mushroom" regime), suggesting that the layers are in the brush regime. Maximum possible coverage, estimated at 5.8 chains/nm^2 based on the cross section of fully extended PEO, did not occur, suggesting that beyond a given (limiting) coverage steric hindrance prevented further chemisorption.

Acknowledgments

Financial support by the Natural Sciences and Engineering Research Council of Canada (NSERC) and the Canadian Institutes of Health Research (CIHR) is gratefully acknowledged.

References

[1] P. Kingshott, H.J. Griesser, Curr. Opin. Solid. State Mater. Sci. 4 (1999) 403.
[2] P. Kingshott, H. Thissen, H.J. Griesser, Biomaterials 23 (2002) 2043.
[3] M. Malmsten, K. Emoto, J.M. Van Alstine, J. Colloid Interface Sci. 202 (1998) 507.
[4] S.J. Sofia, V. Premnath, E.W. Merrill, Macromolecules 31 (1998) 5059.
[5] M. Morra, J. Biomater. Sci. Polym. Edn. 11 (2000) 547.
[6] S.J. Alexander, Physique 38 (1977) 983.
[7] R.G. Nuzzo, D.L. Allara, J. Am. Chem. Soc. 105 (1983) 4481.
[8] F. Zhang, E.T. Kang, K.G. Neoh, W. Huang, J. Biomater. Sci. Polym. Edn. 12 (2001) 515.
[9] K.L. Prime, G.M. Whitesides, J. Am. Chem. Soc. 115 (1993) 10,714.
[10] B. Zhu, T. Eurell, R. Gunawan, D. Leckland, J. Biomed. Mater. Res. 56 (2001) 406.
[11] P. Drude, Annu. Phys. 36 (1889) 865.
[12] R.M.A. Azzam, N.M. Bashara, Ellipsometry and Polarized Light, North-Holland, New York, 1977.

[13] J.A. De Feijter, J. Benjamins, F.A. Veer, Biopolymers 17 (1978) 1759.
[14] P.A. Cuypers, J.W. Corsel, M.P. Janssen, J.M.M. Kop, W.T. Hermens, H.C. Hemker, J. Biol. Chem. 258 (1983) 2426.
[15] J. Penfold, R.K.J. Thomas, Phys. Condensed Matter 2 (1990) 1369.
[16] T.P. Russell, Mater. Sci. Rep. 5 (1990) 171.
[17] Y.J. Du, J.L. Brash, J. Appl. Polymer Sci. 90 (2003) 594.
[18] R.V. Barbosa, M.A.R. Moraes, A.S. Gomes, B.G. Soares, Macromol. Rep. A 32 (1995) 663.
[19] S. Tokumitsu, A. Liebich, S. Herrwerth, W. Eck, M. Himmelhaus, M. Grunze, Langmuir 18 (2002) 8862.
[20] M. Matsuguchi, S. Umeda, Y. Sadoaka, Y. Sakai, Sens. Actuat. B 49 (1998) 179.
[21] J.F. Ankner, C.F. Majkrzak, Proc. Soc. Photo-opt. Instrum. Eng. 1738 (1988) 260.
[22] E.B. Troughton, C.D. Bain, G.M. Whitesides, R.G. Nuzzo, D.L. Allara, M.D. Porter, Langmuir 4 (1988) 365.
[23] P. Harder, M. Grunze, R. Dahint, G.M. Whitesides, P.E. Laibinis, J. Phys. Chem. B 102 (1998) 426.
[24] G.J. Fleer, M.A. Cohen Stuart, J.M.H.M. Scheutjens, T. Cosgrove, B. Vincent, Polymers at Interfaces, first ed., Chapman & Hall, New York, 1993, ch. 4.1.4.
[25] N.V. Efremova, S.R. Sheth, D.E. Leckband, Langmuir 17 (2001) 7628.
[26] T.L. Kuhl, J. Majewski, J.Y. Wong, S. Steinberg, D.E. Leckband, J.N. Israelachvili, G.S. Smith, Biophys. J. 75 (1998) 2352.

7.0 PAPER TWO: PROTEIN RESISTANCE OF SURFACES PREPARED BY SORPTION OF END-THIOLATED POLY(ETHYLENE GLYCOL) TO GOLD: EFFECT OF SURFACE CHAIN DENSITY.

Authors: **L.D. Unsworth**, H. Sheardown, and J.L. Brash

Publication Information: Langmuir 2005, 21, 1036.

Accepted Date: November 15th, 2004.

Working Hypothesis:

Protein adsorption to chemisorbed thin films of PEO with MWs 750, 2000 and 5000 may be greatly affected by film chain density.

Main Contributions:

1. It was found that for 750 and 2000 MW PEO layers, resistance to fibrinogen adsorption increased with chain density and was maximal at a density of ~0.5 chains/nm^2 (80% decrease in adsorption compared to unmodified gold). For PEO of 5000 MW the optimal chain density was 0.27 per nm^2 and gave only a 60% reduction in fibrinogen adsorption. The PEO-modified surfaces were found also to be resistant to lysozyme adsorption with reductions similar to, if somewhat less than, those for fibrinogen.

2. As PEO chain density increased beyond the 'optimum' chain density protein adsorption increased.

3. It is suggested that at high chain density, the chemisorbed PEO becomes dehydrated giving a surface that is no longer protein resistant.

Copyright information:

Protein Resistance of Surfaces Prepared by Sorption of End-Thiolated Poly(ethylene glycol) to Gold: Effect of Surface Chain Density

Larry D. Unsworth, Heather Sheardown, and John L. Brash*

Department of Chemical Engineering and Department of Pathology and Molecular Medicine, McMaster University, Hamilton, Ontario Canada, L8S 4L7

Received September 17, 2004. In Final Form: November 15, 2004

Nonspecific protein adsorption generally occurs at the biomaterial–tissue interface and usually has adverse consequences. Thus, surfaces that are protein-resistant are eagerly sought with the expectation that these materials will exhibit improved biocompatibility. Surfaces modified with end-tethered poly(ethylene oxide) (PEO) have been shown to be protein-resistant to some degree. Although the mechanisms are unclear, it has been suggested that chain length, chain density, and chain conformation are important factors. To investigate the effects of PEO chain density, we selected a model system based on the chemisorption of chain-end thiolated PEO to a gold substrate. Chain density was varied by varying PEO solubility (proximity to cloud point) and incubation time in the chemisorption solution. The adsorption of fibrinogen and lysozyme to these surfaces was investigated. It was found that for 750 and 2000 MW PEO layers, resistance to fibrinogen increased with chain density and was maximal at a density of ~0.5 chains/nm^2 (80% decrease in adsorption compared to unmodified gold). As PEO chain density increased beyond 0.5/nm^2 adsorption increased. For PEO of 5000 MW the optimal chain density was 0.27/nm^2 and gave only a 60% reduction in fibrinogen adsorption. It is suggested that, at high chain density, the chemisorbed PEO is dehydrated giving a surface that is no longer protein resistant. The PEO-modified surfaces were found also to be resistant to lysozyme adsorption with reductions similar to, if somewhat less than, those for fibrinogen. The fibrinogen to lysozyme molar ratios were within the expected range for close-packed layers of these proteins in their native conformation and were relatively insensitive to PEO chain density and MW. This may suggest that such adsorption as did occur, even at chain densities giving minimum adsorption, may have been on patches of unmodified gold.

Introduction

Protein adsorption at the biomaterial–tissue interface is the first and fate-determining event that orchestrates subsequent host responses, including blood coagulation, platelet activation, and complement activation.[1] Poly(ethylene oxide) (PEO) has attracted much attention as a biomaterial coating due to the fact that it inhibits nonspecific protein adsorption.[2] Although the exact mechanism of PEO-mediated protein resistance is still a matter of debate, it is thought that PEO density, chain length, conformation, and charge neutrality are important factors.[3-6] The possible effect of PEO–water binding on protein adsorption has also been discussed, and it has been proposed that the interactions between PEO and water exert a strong influence on protein resistance.[3,7]

Although chain density is believed to be important, there is very little work where this quantity has been varied systematically and where it has been measured with any degree of precision. In recent work from the authors' laboratory, ellipsometry and neutron reflectometry were employed to measure the density of PEO on surfaces prepared by chemisorption of chain-end thiolated PEO to gold.[8] In this paper we present data on the adsorption of proteins to similar surfaces.

A common approach to achieving variable surface density in gold–thiol systems is the use of an "inert" thiol as a diluent in the chemisorption solution.[9-11] In this work we have varied PEO density via solution conditions (proximity to cloud point) and incubation time.[12,13] The relevant solution variables are ionic strength and temperature: PEO solubility decreases as both of these variables increase, ultimately reaching a cloud point where the polymer becomes insoluble. As discussed by Kingshott et al.,[12,13] grafting near cloud point conditions, where the polymer coils are relatively small, results in a relatively high surface chain density. Conversely at conditions away from the cloud point, the coils are more expanded and lower densities are achieved. Of course changing conditions after chemisorption will alter the size and conformation of the PEO chains. We have shown previously that chemisorption under varying solution conditions produces reproducible chain densities over a broad range for the PEOs used here.[8]

* To whom correspondence should be addressed at the Department of Chemical Engineering. Telephone: (905) 525-9140, ext.24946. E-mail: brashjl@mcmaster.ca.

(1) Brash, J. L. *J. Biomater. Sci., Polym. Ed.* **2000**, *11*, 1135.
(2) Harris, J. M. Introduction to Biotechnical and Biomedical Applications of Poly(ethylene glycol). In *Poly(ethylene glycol) Chemistry: Biotechnical and Biomedical Applications*; Harris, J. M., Ed.; Plenum Press: New York, 1992; pp 1–14.
(3) Morra, M. *J. Biomater. Sci., Polym. Ed.* **2000**, *11*, 547.
(4) Malmsten, M.; Emoto, K.; Van Alstine, J. M. *J. Colloid Interface Sci.* **1998**, *202*, 507.
(5) Szleifer, I. *Biophys. J.* **1997**, *72*, 595.
(6) Tosatti, S.; De Paul, S. M.; Askendal, A.; Vandevondele, S.; Hubbell, J. A.; Tengvall, P.; Textor, M. *Biomaterials* **2003**, *24*, 4949.
(7) Vogler, E. A. *J. Biomater. Sci., Polym. Ed.* **1999**, *10*, 1015.
(8) Unsworth, L. D.; Tun, Z.; Sheardown, H.; Brash, J. L. *J. Colloid Interface Sci.* **2005**, *281*, 112.
(9) Nuzzo, R. G.; Allara, D. L. *J. Am. Chem. Soc.* **1983**, *105*, 4481.
(10) Prime, K. L.; Whitesides, G. M. *J. Am. Chem. Soc.* **1993**, *115*, 10714.
(11) Zhu, B.; Eurell, T.; Gunawan, R.; Leckband, D. *J. Biomed. Mater. Res.* **2001**, *56*, 406.
(12) Kingshott, P.; Griesser, H. J. *Curr. Opin. Solid State Mater. Sci.* **1999**, *4*, 403.
(13) Kingshott, P.; Thissen, H.; Griesser, H. J. *Biomaterials* **2002**, *23*, 2043.

Alexander[14] has pointed out that the conformation of end-tethered chains depends on spacing. The so-called mushroom conformation (unperturbed random coils) occurs when the spacing (L) is greater than $2R_F$ (R_F = Flory radius), whereas a brush or extended conformation occurs when $L < 2R_F$. It is also well-understood that stretching entropy and excluded volume interactions influence the brush density, in both cases as a result of chain–chain imposed lateral confinement. By varying brush density, conformations ranging from slightly perturbed (extended mushroom conformation) to fully stretched would be obtained. Furthermore, it is apparent that an increase in chain density implies an increase in PEO volume fraction.

In the present work, the protein resistance of PEO–gold surfaces has been evaluated by measuring the adsorption of fibrinogen and lysozyme as single proteins in buffer. These proteins were selected for various reasons. Fibrinogen is a large protein (340 kDa, 450 × 90 × 90 Å)[15] that plays a crucial role in wound healing, clot formation,[16] and platelet adhesion and activation,[17] the latter associated with catalytic effects in the coagulation cascade.[18,19] Fibrinogen is also known to facilitate macrophage and leukocyte attachment, leading to inflammation, degradation, and fibrous encapsulation.[20,21] In contrast to fibrinogen, lysozyme is a small protein (14.6 kDa, 46 × 30 × 30 Å)[22,23] and it was of interest to investigate whether the PEO surfaces would be less resistant to lysozyme than to fibrinogen as might be expected if adsorption is facilitated by easier access to the underlying gold substrate. It was also of interest that the isoelectric points of fibrinogen and lysozyme are 5.5 and 11.4, respectively, so that at physiologic pH, the net charge on these proteins will be negative and positive, respectively.

We report here on the effect of surface chain density of PEO (MW 750, 2000, and 5000) on fibrinogen and lysozyme adsorption from buffer. Chain density data determined previously by ellipsometry were used for this purpose.[8]

Materials and Methods

Surfaces. Gold-coated silicon wafers were cleaned and exposed to solutions of 5 mM end-thiolated, methoxy-terminated PEO[24,25] as discussed elsewhere.[8] Briefly, silicon wafers (2 in. diameter; 1000 μm thickness; Institute of Electronic Materials Technology, Warsaw, Poland) were polished on both sides to $\lambda/10$ (EL CAT, Warsaw, Poland), treated to remove any natural oxide layer, coated with a 400 Å chromium adhesion layer followed by a 1000 Å layer of gold, and diced into 0.5 cm × 0.5 cm pieces (Thin Film Technology, Inc., Buellton, CA). The gold-coated wafers were cleaned in a solution of 1 part hydrogen peroxide, 1 part ammonium hydroxide, and 5 parts water at 80 °C, for 5 min to remove any carbonaceous contamination, sonicated for 1 min, rinsed in Millipore Milli-Q water, and placed in Milli-Q water-filled wells of a 96-well microtiter plate. The surfaces were equilibrated in a water bath at different temperatures and were then placed in the appropriate chemisorption solutions.

Table 1. Chemisorption Solution Conditions[a]

PEO MW	temp (°C)	ionic strength (M)	PEO solubility
750	25	0.05	high
	25	1.5, 2.5	intermediate
	35	2.9	low
2000	25	0.05	high
	25	1.5, 2.5	intermediate
	35	2.8	low
5000	25	0.05	high
	25	1.9	intermediate
	30	1.9	low

[a] Solution PEO concentration was fixed at 5 mM and pH 7.4 ± 0.1.

Chemisorption solution conditions (Table 1) were varied as a means of varying PEO chain density based on the idea, as explained above, that higher densities should be obtained as proximity to the cloud point increases. The conditions indicated as low solubility are essentially θ conditions. The surfaces were immersed in the chemisorption solutions for the appropriate time (10 min to 4 h), then placed in microtiter plate wells containing Milli-Q water, sonicated for 4 min, and rinsed extensively with Milli-Q water. As discussed elsewhere,[8] this procedure generates PEO layers of reproducible chain density and water contact angle. Static water contact angle data showed that PEO was present and that as chemisorption time increased, the receding contact angles decreased with values in the range 17–20°.

Protein Adsorption. Fibrinogen and lysozyme (Calbiochem, La Jolla, CA) were radiolabeled with Na^{125}I (ICN, Irvine, CA) using the iodine monochloride method and dialyzed extensively against phosphate-buffered saline (PBS, pH 7.4) to remove unbound ^{125}I (held to < 1% of total solution radioactivity). Prior to protein adsorption experiments, gold-coated silicon wafers were equilibrated in PBS–NaI buffer overnight; "cold" NaI was added to the buffer to inhibit the sorption of unbound ^{125}I to the gold surface according to a previously determined protocol.[26] Protein adsorption experiments were performed in PBS–NaI buffer (pH = 7.4) at protein concentrations of 1, 0.5, 0.3, 0.1, and 0.001 mg/mL (2% labeled, 98% "cold"). The surfaces were placed in the wells of 96-well multiwell plates and incubated for 3 h at room temperature (~22 °C). It was determined that no further adsorption occurred at times longer than 3 h. The surfaces were rinsed three times (10 min each) with fresh PBS–NaI to remove any loosely bound protein. Surface radioactivity was determined and adsorbed amounts were calculated using background-corrected surface counts relative to the solution count for the highest protein concentration (0.5 mg/mL). The percent reduction of adsorption on the PEO surfaces relative to the unmodified gold was determined.

PEO Surface Density from Ellipsometry Measurements. As discussed in detail elsewhere,[8] a self-nulling, single-wavelength (6328 Å) ellipsometer, with an incident angle of 70°, was used to determine the properties of the chemisorbed PEO layers. Thickness values were determined using a three-layer air–PEO–gold model. Chain densities were estimated from the thickness data using eq 1.

$$L = \left(\frac{M}{\rho_{dry} d N_A}\right)^{1/2} \quad (1)$$

where L is the average distance between chain attachment points, M is the PEO molecular weight, ρ_{dry} is the density of the dry PEO layer (assumed initially to be 1.0 g cm^{-3}), d is the ellipsometrically determined PEO average layer thickness, and N_A is Avogadro's number.[8,27] Surface chain densities were estimated as L^{-2}.

(14) Alexander, S. *J. Phys. (Paris)* **1977**, *38*, 983.
(15) Herde, H.; Haupt, H.; Schwick, H. B. In *Plasma Protein Fractionation*: Academic Press: New York, 1977.
(16) Shen, M.; Horbett, T. A. *J. Biomed. Mater. Res.* **2001**, *57*, 336.
(17) Brash, J. L.; Horbett, T. A. Proteins at Interfaces. In *Proteins at Interfaces II: Fundamentals and Applications*; Horbett, T. A., Brash, J. L., Eds.; American Chemical Society: Washington, DC, 1995; p 18.
(18) Adams, G. A.; Feuerstein, I. A. *Trans.–Am. Soc. Artif. Intern. Organs* **1981**, *27*, 219.
(19) Tsai, W.-B.; Grunkmeier, J. M.; McFarland, C. D.; Horbett, T. A. *J. Biomed. Mater. Res.* **2002**, *60*, 348.
(20) Tang, L.; Ugarova, T. P.; Plow, E. F.; Eaton, J. W. *J. Clin. Invest.* **1996**, *97*, 1329.
(21) Anderson, J. M. *Curr. Opin. Hematol.* **2000**, *7*, 40.
(22) Arai, T.; Norde, W. *Colloids Surf.* **1990**, *51*, 1.
(23) Norde, W.; Haynes, C. A. Reversibility and the Mechanism of Protein Adsorption. In *Proteins at Interfaces II: Fundamentals and Applications*; Horbett, T. A., Brash, J. L., Eds.; American Chemical Society: Washington, DC, 1995; pp 26–40.
(24) Du, Y. J.; Brash, J. L. *J. Appl. Polym. Sci.* **2003**, *90*, 594.
(25) Barbosa, R. V.; Moraes, M. A. R.; Gomes, A. S.; Soares B. G. *Macromol. Rep.* **1995**, *A32*, 663.
(26) Du, Y. J.; Cornelius, R. M.; Brash, J. L. *Colloids Surf., B* **2000**, *17*, 59.
(27) Sofia, S. J.; Premnath, V.; Merrill, E. W. *Macromolecules* **1998**, *31*, 5059.

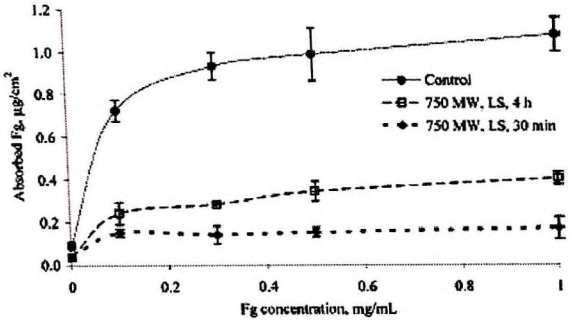

Figure 1. Fibrinogen adsorption to the unmodified gold and two PEO750 surfaces prepared under low solubility conditions and chemisorption times of 4 h and 30 min with respective chain densities of 0.63 ± 0.13 and 0.47 ± 0.11 chain/nm². Fibrinogen adsorption time was held constant at 3 h. Error bars are ±1 SD; $n \geq 18$. The curves are trend lines and are included as a guide to the eye.

The chain density of layers of "equivalent" PEO spheres with radius equal to the Flory radius (R_F) can be estimated using eq 2:

$$R_F = aN^{\nu} \tag{2}$$

where a is the characteristic monomer dimension (taken as 2.78 Å for the ethylene oxide repeat[4]), N is the degree of polymerization, ν may be taken as 0.6 for high-solubility conditions, and 0.5 for the θ condition. R_F values estimated for the unperturbed chains at low- and high-solubility conditions for 750, 2000, and 5000 MW PEO were determined to be 11 and 15; 18 and 27; and 30 and 47 Å, respectively.[5] In discussing PEO packing on the surface it is helpful to consider the ratio $L/2R_F$; values less than unity indicate close packing with molecules occupying space less than would be required for the unperturbed random coils.

Results

Fibrinogen Adsorption. Representative fibrinogen adsorption data for unmodified gold and two 750 MW PEO modified surfaces are shown in Figure 1. The unmodified gold surface adsorbed 0.93 ± 0.09 μg/cm² of fibrinogen (average of data in the plateau region), i.e., in the range expected for close-packed monolayer coverage. For both of the PEO modified surfaces in Figure 1, fibrinogen adsorption was reduced significantly compared to gold. Surprisingly, the PEO film formed after 30 min (0.47 ± 0.11 chain/nm²) incubation adsorbed significantly less protein than after 4 h (0.63 ± 0.13 chain/nm²).

Figure 2 shows the effects of solution conditions on the inhibition of fibrinogen adsorption to the 750 MW PEO surfaces. The data are reported as percent reduction vs bare gold. It should be noted that since the adsorption data for a given surface varied somewhat from experiment to experiment, a bare gold surface was included in every experiment and its adsorption value used in estimating percent reduction. It is clear that it was only when chemisorption was carried out under low solubility conditions, i.e., either at high ionic strength or high temperature and high ionic strength (near the cloud point), that adsorption was inhibited to any significant extent. Similar trends were seen for the 2000 and 5000 MW systems (data not shown).

Figures 3–5 show, for each PEO molecular weight, plots of protein resistance (expressed as percent reduction in adsorption of fibrinogen) versus PEO chain density. The chain density data were obtained from ellipsometric measurements on the dry PEO surfaces as reported previously.[8] The relatively large errors in chain density

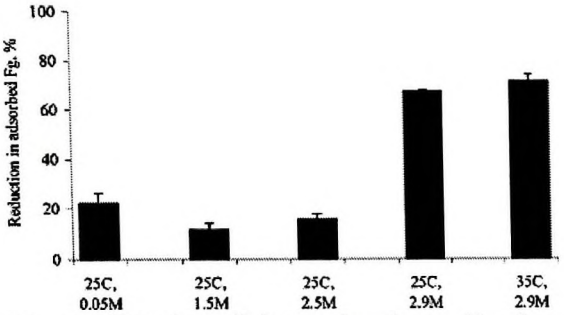

Figure 2. Reduction in fibrinogen adsorption to gold surfaces modified with 750 MW PEO: effect of ionic strength and temperature during chemisorption. The chemisorption time was 4 h. The adsorption data are averages across the isotherm plateau region from 0.1 to 1.0 mg/mL. Error bars are ±1 SD; $n \geq 18$.

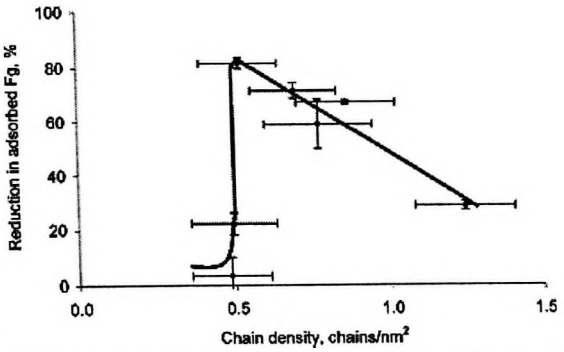

Figure 3. Reduction in fibrinogen adsorption to gold surfaces modified with 750 MW PEO: effect of surface chain density as measured by ellipsometry. The protein adsorption data are averages across the isotherm plateau region from 0.1 to 1.0 mg/mL. Data are mean ± 1 SD with $n = 9$ and $n \geq 18$ for chain density and protein adsorption, respectively. The trend line is provided as a guide for the eye.

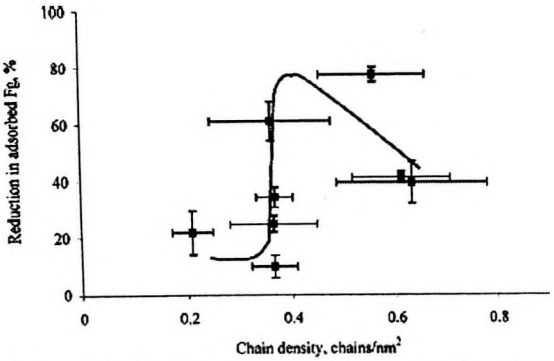

Figure 4. Reduction in fibrinogen adsorption to gold surfaces modified with 2000 MW PEO: effect of surface chain density as measured by ellipsometry. The protein adsorption data are averages across the isotherm plateau region from 0.1 to 1.0 mg/mL. Data are mean ± 1 SD with $n = 9$ and $n \geq 18$ for chain density and protein adsorption, respectively. The trend line is provided as a guide for the eye.

seen in Figures 3–5 are probably due to the low values of film thickness from which the chain densities were derived. It is apparent that for *all* three plots of resistance vs chain density there are multiple points "stacked" at about the same chain density (e.g., Figure 5 at ~0.25 chain/

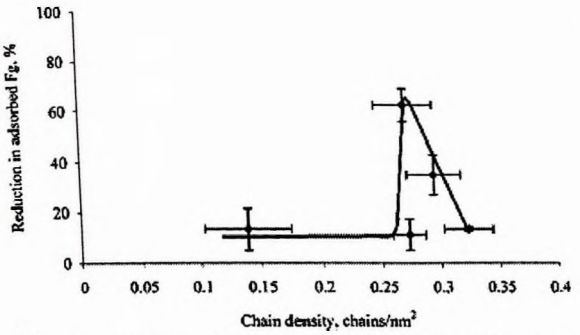

Figure 5. Reduction in fibrinogen adsorption to gold surfaces modified with 5000 MW PEO: effect of surface chain density as measured by ellipsometry. The protein adsorption data are averages across the isotherm plateau region from 0.1 to 1.0 mg/mL. Data are mean ± 1 SD with $n = 9$ and $n \geq 18$ for chain density and protein adsorption, respectively. The trend line is provided as a guide for the eye.

nm²). The chain densities for these points were not statistically different, but the adsorption data were. It appears that the transition from modestly protein resistant to strongly resistant as PEO chain density increases is sharp. The data suggest that even a slight change in chain density, not discernible using our measurement technique, causes a large change in protein adsorption. The fact that all three molecular weights showed the same behavior reinforces this viewpoint.

It is seen that in each case there was a maximum in resistance at an intermediate density, leading to the conclusion that there is an optimum chain density for protein resistance. For 750 MW PEO (Figure 3), there appears to be a threshold chain density of ~0.5 chain/nm² ($L/2R_F \sim 0.5$) above which protein resistance increased sharply. At higher chain densities, resistance decreased. The same trends were seen for 2000 and 5000 MW PEO, with resistance maxima occurring at ~0.5 ($L/2R_F \sim 0.3$) and 0.28 ($L/2R_F \sim 0.2$) chain/nm², respectively (Figures 4 and 5). (It should be noted that these $L/2R_F$ values are based on the R_F for the chain as found in the protein buffer.) These results are in large measure counterintuitive: it might be expected, rather, that resistance would increase continuously with increasing chain density to a constant limiting value.

Chain densities and fibrinogen adsorption values, including data for the surfaces formed under low solubility conditions that showed the greatest fibrinogen resistance, are listed in Table 2. It is apparent that the optimum 750 and 2000 MW surfaces had similar chain densities (~0.5 chain/nm²) and adsorbed similar amounts of fibrinogen (~0.14 μg/cm²) despite the fact that the chemisorption conditions were very different, as indicated in Table 1. It is also apparent that the 5000 MW surface was a less effective inhibitor of fibrinogen adsorption, possibly due to the fact that the maximum chain density is relatively low for this surface at 0.33 chain/nm². Again these data indicate that chain density is a key variable in the inhibition of protein adsorption. Moreover, as chain conformation and hydration are related to chain density, these properties may also play a role in repelling proteins that has yet to be defined.

Lysozyme Adsorption. The adsorption of lysozyme was also investigated, the objective being to ascertain whether the protein resistance of these PEO surfaces is affected by protein size and, in particular, to determine whether a small protein is resisted to the same extent as a large one. Table 2 shows lysozyme data for surfaces prepared under conditions that gave the highest and lowest adsorption for each PEO molecular weight. Both plateau adsorption and reduction of adsorption compared to the unmodified gold are shown. Adsorbed amounts range from 0.06 to 0.30 μg/cm² and reductions from about 3 to 80%. A close-packed monolayer of lysozyme should have a surface concentration between 0.2 and 0.3 μg/cm². The layers adsorbed on the "high solubility" surfaces are in this vicinity. It is clear again, as for the fibrinogen data, that chemisorption of PEO near the cloud point gives surfaces that are significantly lysozyme resistant, whereas formation under high solubility conditions gives surfaces that are only weakly resistant. Also, as observed for fibrinogen, similar adsorbed amounts (0.11 ± 0.04 and 0.06 ± 0.03 μg/cm²) were seen on the 750 and 2000 MW surfaces of similar chain density (~0.5 chain/nm²) and the 5000 MW PEO surfaces were not as effective at inhibiting adsorption, probably due to the fact that chain densities on these surfaces were lower.

The molar ratios of lysozyme to fibrinogen adsorbed to these surfaces are also presented in Table 2. For most of the surfaces, this ratio is of the order of 8–9. It is somewhat higher for the 5000 MW PEO surfaces at about 12. The low-solubility 750 PEO surface is higher yet at about 18. For a given area of surface on which adsorption is unimpeded (and thus on which close-packed layers could potentially form), these ratios are approximately as would be expected on the basis of the dimensions and thus the "footprints" of the intact, native molecules. The footprint ratio fib:lys may be estimated to be in the range ~30:1 to 9:1 depending on molecular orientation.

Discussion

Although investigations of fibrinogen and lysozyme adsorption to PEO modified surfaces have been reported by others, studies in which chain densities as well as adsorbed amounts are measured are rare. Malmsten et al.[4] found that adsorption of fibrinogen decreased significantly with increasing PEO chain density (determined by ellipsometry). Thus, at densities of 0.004 and 0.12 chain/nm², fibrinogen adsorption was 0.28 and 0.02 μg/cm², respectively. Sofia et al.[27] showed that at a chain density of 0.17 chain/nm² (end-tethered, MW 3400) the adsorption of several proteins was completely inhibited as judged by the absence of nitrogen in X-ray photoelectron spectroscopy (XPS; a less sensitive method than radiolabeling). Tosatti et al.[6] also used *in situ* ellipsometry to quantify protein adsorption from heparinized human plasma to titanium surfaces modified with poly(L-lysine)-*graft*-poly(ethylene oxide) (PLL-*g*-PEO) polymers (2000 MW PEO segments). These surfaces gained very little mass upon exposure to plasma. This nonfouling behavior was attributed to suppression of protein adsorption through steric stabilization and the reduction of electrostatic interactions between the surface and the proteins. Similar PLL-*g*-PEO surfaces with grafted PEO chains of 2000 and 5000 MW were also studied by Kenausis et al.[28] It was observed that the lowest fibrinogen adsorbed amount, as determined using the OWLS technique, was ~2 ng/cm² and occurred at an $L/2R_F$ ratio of ~0.47. Similar calculations using our data show that the lowest fibrinogen adsorption, as determined by radiolabeling, was 140 ng/cm² and occurred at an $L/2R_F$ ratio of ~0.4. $L/2R_F = 0.47$ was the lowest value observed by Kenausis et al., whereas in the present

(28) Kenausis, G. L.; Voros, J.; Elbert, D. L.; Huang, N.; Hofer, R.; Ruiz-Taylor, L.; Textor, M.; Hubbell, J. A.; Spencer, N. D. *J. Phys. Chem. B* **2000**, *104*, 3298.

Table 2. Comparison of Fibrinogen and Lysozyme Adsorption (Isotherm Plateau)[a]

system	chain density (chain/nm²)	fibrinogen (μg/cm²)	reduction vs control (%)	lysozyme (μg/cm²)	reduction vs control (%)	mol ratio lysozyme:fibrinogen
control		0.93 ± 0.09		0.31 ± 0.02		7.9
750 MW, high solubility, 4 h	0.4 ± 0.1	0.71 ± 0.1	24	0.23 ± 0.01	25	7.5
750 MW, low solubility, 30 min	0.47 ± 0.11	0.14 ± 0.04	85	0.11 ± 0.04	65	18.3
2000 MW, high solubility, 4 h	0.33 ± 0.08	0.71 ± 0.09	24	0.27 ± 0.02	13	8.8
2000 MW, low solubility, 2 h	0.51 ± 0.09	0.15 ± 0.03	84	0.06 ± 0.03	81	9.5
5000 MW, high solubility, 4 h	0.12 ± 0.02	0.52 ± 0.15	44	0.30 ± 0.02	3	12.8
5000 MW, low solubility, 30 min	0.24 ± 0.02	0.31 ± 0.03	66	0.21 ± 0.02	33	15.9

[a] Data are mean ± 1 SD, with $n = 9$ and $n \geq 18$ for chain density and protein adsorption values, respectively.

work lowest values of 0.39, 0.24, and 0.2, respectively, were observed for the 750, 2000, and 5000 MW PEO layers. This tight packing implies that the PEO chains are in an entropically unfavorable state.[29]

Several studies of the adsorption of fibrinogen and lysozyme to self-assembled monolayers (SAMs) of oligo(ethylene oxide) (EO) "tipped" alkane-thiols have been reported. Prime and Whitesides[10] showed that EO-6 (PEO 260) tipped SAMs adsorbed very low amounts of fibrinogen. Block copolymers of structure PEO–PPO–PEO (Pluronics) adsorbed to glass at respective densities of 0.08 and 0.19 chain/nm² showed fibrinogen adsorption of 0.1 and 0.05 μg/cm² and lysozyme adsorption of 0.02 and 0.06 μg/cm² for 3300 and 5500 MW PEO blocks, respectively.[30] Again these may be considered surfaces of significant protein resistance.

In the present work, the surfaces of greatest resistance gave reductions of the order of 80% compared to the controls, with adsorbed amounts of about 0.14 μg/cm² for fibrinogen (750 MW, low solubility, 30 min) and 0.06 μg/cm² for lysozyme (2000 MW, low solubility, 2 h). In both cases the chain density was ~0.5 chain/nm². These adsorbed quantities are of the same order of magnitude as those reported by others, although generally speaking the chain densities are higher. However, it should be noted that comparisons between results from different laboratories are difficult due to the different methods used to determine adsorption and chain density.

The experiments comparing lysozyme and fibrinogen show that for most of the surfaces the percent reduction in adsorption vs the unmodified gold is similar for both proteins, suggesting that resistance is about the same whether the protein is big or small. Moreover for a given PEO molecular weight, the molar ratio of the two proteins is similar for the low and high chain densities and similar to that on the bare gold. As mentioned, the molar ratios are also similar to the "footprint" ratio of the two proteins. Taken as a whole, these data may indicate that such adsorption as does occur, even at chain densities giving minimum adsorption, is on patches of unmodified gold. Since we do not have data for lysozyme at densities where adsorption has increased beyond the minimum, we do not know if the same ratios would be seen for these densities. At these higher chain densities it is less likely that any bare gold would be accessible to the proteins. However if the PEO is dehydrated (see below for further discussion of this possibility) giving hydrophobic patches that are strongly adsorbent, one might expect close-packed layers of protein such that the molar ratio lys:fib would be similar to that on gold. In support of this proposition, it is noted that the fibrinogen adsorption levels at the highest chain densities return more or less to those on the bare gold (Figures 3–5).

The most interesting finding in this work is the occurrence of an adsorption minimum as a function of PEO surface density, suggesting that there is an optimal surface density for protein resistance. Minima were found for fibrinogen adsorption to surfaces modified with PEO of different MW (750 and 2000) at approximately the same chain density (~0.5 chain/nm²). Furthermore, similar lysozyme adsorption levels were observed for surfaces having the same PEO chain density (~0.5/nm²) but different MW. This suggests that chain density plays a role of major importance in protein resistance mediated by end-tethered PEO. While it is obvious that at very low chain density protein resistance should be negligible, it is less obvious why at higher chain density resistance should decrease. It might rather be expected that resistance would increase with density, reaching a plateau value once density (and thus coverage) had reached a sufficient level.

A possible explanation might be that a hydrophobic contaminant is introduced in the surface preparation process and that contamination increases with increasing PEO density. Water contact angle data[6] showing receding angles in the range of 17–20° argue against this possibility. Another possibility is that the terminal methoxy groups begin to dominate the surface at the higher densities. That this is probably not the case is indicated by recent work in our laboratory (unpublished) showing that the same trends are seen with hydroxyl-terminated PEO.

It is possible that it is the decrease in chain mobility[3,6] and hydration[6,31] associated with increased chain density that is the root cause of the loss of resistance at higher density (though water contact angles do not indicate any global increase in hydrophilicity). As chain density increases, the effective "solubility" limit of tethered PEO chains will be reached with a corresponding decrease in hydration and mobility, both of which are components crucial to effective protein resistance. Work by Tiberg et al.[32] bears on the question of hydrophilic–hydrophobic transitions in PEO surfaces. For surfaces consisting of immobilized PEO–PPO block copolymers it was found that the thickness of a polymer layer of fixed chain density decreased as the temperature increased through the cloud point. This was attributed to loss of hydration at the higher temperatures. The adsorption of IgG increased through this same temperature interval as would be expected if the surface were becoming more hydrophobic.

Minima in protein adsorption as chain density varies have been reported by Vanderah et al.[33] They showed that on oligo(ethylene oxide)–SAM–gold surfaces, the adsorption of both fibrinogen and albumin decreased as coverage increased. At an OEO coverage of 80%,

(29) Benesch, J.; Svedhem, S.; Svensson, S. C. T.; Valiokas, R.; Liedberg, B.; Tengvall, P. *J. Biomater. Sci., Polym. Ed.* **2001**, *12*, 581.
(30) McPherson, T.; Kidane, A.; Szleifer, I.; Park, K. *Langmuir* **1998**, *14*, 176.
(31) Harder, P.; Grunze, M.; Dahint, R.; Whitesides, G. M.; Laibinis, P. E. *J. Phys. Chem. B* **1998**, *102*, 426.
(32) Tiberg, F.; Brink, C.; Hellsten, M.; Holmberg, K. *Colloid Polym Sci.* **1992**, *270*, 1188.
(33) Vanderah, D. J.; La, H.; Naff, J.; Silin, V.; Rubinson, K. A. *J. Am. Chem. Soc.* **2004**, *126*, 13639.

however, adsorption increased sharply. This sharp reversal was attributed to the reduction of chain mobility in the OEO domains accompanying the transition to the highly ordered 7/2 helical conformation, implying that protein resistance is due mainly to the excluded volume effect since, as lateral packing density increases, chain mobility and hydration most likely decrease. Herrwerth et al.,[34] working with gold- and silver-alkanethiol-OEO surfaces where the methoxy-terminated OEO was of chain length 1 to 6, showed that protein adsorption was low at intermediate chain density up to about 4/nm^2, and increased sharply at higher chain density.

It seems likely that the lack of observation by others of the adsorptive nature of dense higher molecular weight PEO layers is due to the fact that the layers were not of sufficiently high density. The chain densities achieved in this work ranged from about 0.4 to 1.3 per nm^2 for 750 PEO, from 0.2 to 0.7 per nm^2 for 2000 PEO, and from 0.14 to 0.32 per nm^2 for 5000 PEO; i.e., chain density decreased with increasing chain length. The limitations on achievable density for this type of surface have been discussed elsewhere and involve steric restrictions on the addition of chains to partially covered surfaces.[4] Thus our surfaces have densities well below the theoretical maximum of about 5/nm^2 for a close-packed layer of helical PEO. Anne et al.[35] found a maximum density of 0.1/nm^2 for surface-grafted PEO 3400 chains.

The results of the present work, along with those from other laboratories,[3,4,13,34] may indicate that it is the hydration state of particular conformations (as determined by chain density) of end-tethered PEO that is largely responsible for inhibiting protein adsorption to these surfaces. Our data suggest that an optimal hydration state exists at a chain density of 0.4–0.5 chain/nm^2. Additional support for this mechanism could come from knowledge of the hydration of PEO attached to surfaces. It is possible that DSC measurements on finely dispersed systems of high surface-to-volume ratio could provide such information.[36]

Acknowledgment. Financial support of this work by the Natural Sciences and Engineering Research Council of Canada (NSERC) and the Canadian Institutes of Health Research (CIHR) is gratefully acknowledged.

LA047672D

(34) Herrwerth, S.; Eck, W.; Reinhardt, S.; Grunze, M. *J. Am. Chem. Soc.* **2003**, *125*, 9359.

(35) Anne, A.; Demaille, C.; Moiroux, J. *Macromolecules* **2002**, *35*, 5578.

(36) Yan, G.; Li, J.-T.; Huang, S.-C.; Caldwell, K. D. Calorimetric Observations of Protein Conformation at Solid–Liquid Interfaces. In *Proteins at Interfaces II: Fundamentals and Applications*; Horbett, T. A., Brash, J. L., Eds.; American Chemical Society: Washington, DC, 1995; pp 256–268.

8.0 PAPER THREE: POLYETHYLENE OXIDE SURFACES OF VARIABLE CHAIN DENSITY BY CHEMISORPTION OF PEO-THIOL ON GOLD: ADSORPTION OF PROTEINS FROM PLASMA STUDIED BY RADIOLABELLING AND IMMUNOBLOTTING.

Authors: **L.D. Unsworth**, H. Sheardown, and J.L. Brash

Publication Information: Biomaterials 2005, in press.

Acceptance Date: March 10, 2005

Working Hypothesis:

Protein resistant surfaces formed under optimal chemisorption conditions should show decreased transient fibrinogen adsorbed from plasma and decreased overall adsorption of plasma proteins compared to both the unmodified control and surfaces formed under high solubility conditions. Also PEO layers where the distal chain ends are methoxy and hydroxyl groups, should show different protein resistance.

Main Contributions:

1. PEO layers formed from solutions near the cloud point adsorbed the lowest amount of fibrinogen from plasma. Layers of OH-terminated PEO of MW 600 showed almost complete suppression (versus controls) of the Vroman effect.

2. Respective Vroman peak amounts of adsorbed fibrinogen for 600-OH, 750-OCH_3 and 2000-OCH_3 were 20 ± 1, 70 ± 20, and 50 ± 3 ng/cm^2 compared to 400 ng/cm^2 for unmodified gold; adsorption levels at higher plasma concentration were 6.7 ± 0.6, 16 ± 9 and 12 ± 3 ng/cm^2 respectively compared to 150 ng/cm^2 for gold. Fibrinogen adsorption from plasma was not significantly different for surfaces prepared with PEO of molecular weight 750 and 2000 when the chain density was the same (~0.5 chains/nm^2) supporting the conclusion that chain density may be the key property for suppression of protein adsorption.

3. The data suggested a distal chain end group effect such that fibrinogen adsorption was reduced and/or displacement from the surface facilitated on hydroxyl-terminated compared to methoxy-terminated PEO layers.

4. SDS-PAGE gels and immunoblots of the proteins eluted from these surfaces after plasma contact showed that a number of proteins were adsorbed, including fibrinogen, albumin, C3 and apolipoprotein A-I. However, the blot responses were weak for all four proteins of the contact system; some complement activation was observed on all of the surfaces studied.

Abstract

The mechanisms involved in the inhibition of protein adsorption by polyethylene oxide (PEO) are not completely understood, but it is believed that PEO chain length, chain density and chain conformation all play a role. In this work, surfaces formed by chemisorption of PEO-thiol to gold were investigated: the effects of PEO chain density, chain length (600, 750, 2000 and 5000 MW) and end-group (-OH, -OCH_3) on protein adsorption from plasma are reported. Similar to previous single protein adsorption studies it was found that, of the different surfaces investigated, PEO layers formed from solutions near the cloud point adsorbed the lowest amount of fibrinogen from plasma. Layers of hydroxyl-terminated PEO of MW 600 formed under these low solubility conditions showed almost complete suppression (versus controls) of the Vroman effect, with 20 ± 1 ng/cm^2 adsorbed fibrinogen at the Vroman peak and 6.7 ± 0.6 ng/cm^2 at higher plasma concentration. By comparison, Vroman peak adsorption was 70 ± 20 and 50 ± 3 ng/cm^2 respectively for 750-OCH_3 and 2000-OCH_3 layers formed under low solubility conditions; adsorption on these surfaces at higher plasma concentration was 16 ± 9 and 12 ± 3 ng/cm^2. Thus in addition to the effect of solution conditions noted previously, the results of this study also suggest a chain end group effect which inhibits fibrinogen adsorption to and/or facilitates displacement from hydroxyl terminated PEO layers. Fibrinogen adsorption from plasma was not significantly different for surfaces prepared with PEO of molecular weight 750 and 2000 when the chain density was the same (~0.5 chains/nm^2) supporting the conclusion that chain density may be the key

property for suppression of protein adsorption. The proteins eluted from the surfaces after contact with plasma were investigated by SDS-PAGE and immunoblotting. A number of proteins were detected on the various surfaces including fibrinogen, albumin, C3 and apolipoprotein A-I. The blot responses were zero or weak for all four proteins of the contact system; some complement activation was observed on all of the surfaces studied.

Introduction

Protein adsorption is believed to occur to some extent on all implanted biomaterials [1]. It is the initiating event that determines subsequent host responses including blood coagulation, platelet activation and complement activation. Surface modification of biomaterials with polyethylene oxide (PEO) has been shown to inhibit non-specific protein adsorption [2]. Although the exact mechanism of PEO mediated protein resistance is still a matter of debate, it is thought that chain density, chain length, chain conformation and charge neutrality are important factors [3-5]. It has also been proposed that the interactions of PEO with water exert a strong influence on protein resistance [6].

The attachment of polymers and other molecules to gold via a thiol end group has been studied extensively [7-12]. In the case of polymers, solution conditions can be used to modulate the polymer dimensions thus allowing variation of the surface density of PEO [13,14]. Also, it has been shown that end-tethered chain conformation depends on chain density (spacing), with chain conformations ranging from unperturbed (mushroom) to slightly perturbed (extended mushroom) to fully extended (brush layer) [15].

A model PEO surface system based on the chemisorption of chain-end thiolated PEO to gold has been under investigation in our laboratory [7,8,16]. In this system the PEO is attached to the surface via the chain ends (end tethered). Convenient manipulation of surface properties, including PEO chain density, molecular weight and distal chain end chemistry is possible. Chain density can be varied by varying PEO solubility (proximity to cloud point) and chemisorption time.

Fibrinogen adsorption from blood and plasma and its subsequent displacement from the surface (Vroman effect) has been discussed extensively [17,18]. More generally it has been shown that abundant plasma proteins, such as fibrinogen, adsorbed initially from blood or plasma, may be replaced by other proteins of lower concentration and higher binding affinity [19]. *In vitro* plasma adsorption experiments using ^{125}I labeled fibrinogen can be used to determine both the transient (i.e. Vroman peak) and kinetically stable adsorbed amounts of fibrinogen. These data may be diagnostic of the overall effectiveness of a surface in inhibiting platelet adhesion, platelet activation and thrombus formation. It has been suggested, for example, that fibrinogen adsorption must be less than 5 ng/cm^2 to prevent significant platelet adhesion [20].

In this communication the effects of PEO chain density, chain length (600, 750, 2000 and 5000 MW) and end-group (-OH, -OCH_3) on protein adsorption from plasma are reported. Protein adsorption was studied by Vroman effect experiments using radioiodinated fibrinogen [21] and by analysis of the proteins eluted following plasma contact using SDS-PAGE and immunoblotting. The physical properties of the surfaces studied have been described elsewhere [7,8]; these surfaces were selected for study here

since in previous work they were shown to be effective in suppressing adsorption of fibrinogen from buffer [16].

Materials and Methods

Surfaces

Chain end thiolated PEOs were prepared as described elsewhere [7,8,16,22]. Gold coated silicon wafers were cleaned and exposed to solutions of 5 mM end-thiolated methoxy terminated PEO [7,8]. Silicon wafers treated to remove the native oxide layer, and coated with a chromium (400 Å) adhesion layer followed by layer of gold (1000 Å) were obtained from Thin Film Technology, Buellton, CA, and diced into 0.5 cm x 0.5 cm pieces. They were cleaned in a solution consisting of 1 part hydrogen peroxide, 1 part ammonium hydroxide, and 5 parts water at 80°C for 5 min to remove any carbonaceous contamination, sonicated for 1 min, rinsed in Millipore™-Milli Q water, and placed in Milli-Q water-filled wells of a 96-well microtitre plate. The plates were immersed in a water bath at the desired temperature. Once equilibrated, the samples were placed in the appropriate PEO-thiol solution at the same temperature.

Chemisorption solution conditions (Table 1) were varied as a means of manipulating PEO chain density; for example it has been shown that higher densities can be obtained as proximity to the cloud point increases [13,14]. The conditions indicated as low solubility (LS) are essentially theta conditions. Following chemisorption, wafers were placed in microtitre wells containing Milli-Q water, sonicated for 4 min and rinsed with copious amounts of Milli-Q water to remove loosely adsorbed polymer.

Table 1. Chemisorption solution conditions[A].

Molecular Weight (g/mol)	Solution Temperature (°C)	Ionic Strength (M)	Chemisorption Time (h)	PEO Solubility	Surface chain density (chn/nm^2)[b]
600	25	Low	4	High	0.9 ± 0.2
	25	4.4	2	Low	1.1 ± 0.2
750	25	Low	4	High	0.4 ± 0.1
	35	2.9	0.5	Low	0.47 ± 0.11
2000	25	Low	4	High	0.33 ± 0.08
	35	2.8	2	Low	0.51 ± 0.09
5000	25	Low	4	High	0.12 ± 0.02
	30	1.9	0.5	Low	0.24 ± 0.02

[A] ALL POLYMER CONCENTRATIONS 5 MM; PH, 7.4 ± 0.1.
[B] DETERMINED BY ELLIPSOMETRY AS REPORTED IN REFERENCES 7, 8.

Protein labelling

Fibrinogen (Calbiochem, La Jolla, CA) was radiolabeled with ^{125}I ($Na^{125}I$, ICN, Irvine, CA), using the iodine monochloride method, and dialyzed extensively against phosphate buffered saline (PBS, pH 7.4) to remove unbound radioactive iodide (held to <1% of total solution radioactivity) as discussed elsewhere [23].

Adsorption from plasma

Blood was taken from normal human donors into 3.8% sodium citrate (blood: citrate, 9:1, v/v), centrifuged at 4°C and 3000 x g for 20 min, and the supernatant plasma collected. The plasma samples from multiple donors were pooled, aliquoted, and stored at –70°C prior to use.

For fibrinogen adsorption experiments radioiodinated fibrinogen was added to the plasma in amounts equivalent to about 10% of the endogenous fibrinogen level. Prior to plasma exposure the gold surfaces were incubated overnight in PBS containing "cold" NaI. This step is required to prevent uptake of free radioactive iodide by the gold [23]. The surfaces were incubated in the radiolabeled plasma for 3 h under static conditions at room temperature as described previously [21]. Adsorption was measured as a function of plasma "concentration" by exposing the surfaces to a series of plasmas diluted to varying extents (from undiluted to 10,000:1) with PBS. This allows observation of any Vroman effect that may be occurring since adsorption goes through a maximum in the low plasma concentration range due to competitive adsorption effects [17,24].Following plasma exposure surfaces were washed three times (10 min each) with fresh PBS-NaI prior to gamma counting.

In other experiments proteins eluted after plasma contact were investigated by SDS-PAGE and immunoblotting. Surfaces were exposed to undiluted pooled human plasma for 3h at room temperature and washed extensively to remove loosely bound proteins (as well as residual plasma) as described above. Adsorbed proteins were eluted from the surfaces by incubating for 24 h in 2% aqueous sodium dodecyl sulfate (SDS) [25].

SDS-PAGE and immunoblotting

Eluted proteins were analyzed using reduced SDS-PAGE (12% gels) and immunoblotting analysis as described elsewhere [25,26]. Proteins were transferred from the gels to Immobilon PVDF membranes (Millipore, Bedford, MA) and exposed to

primary antibodies (dilution 1:1000). Affinity-purified secondary antibodies conjugated to alkaline phosphatase (dilution 1:1000) were used to detect specific proteins. To allow comparisons among the different surfaces, the surface area for adsorption, the volume of eluent buffer used to elute the proteins, and the volume of eluate loaded onto the gels were the same for each surface.

Results and Discussion

Fibrinogen adsorption from plasma

Vroman effects were evident for all surfaces studied with peak adsorption occurring at about 0.1 plasma (Figures 1 – 4) as has been observed for other surfaces [17,18]. At higher plasma concentration, adsorption tended to level off although a slight increase was observed at the highest concentration. As shown in Table 2, the adsorption at the Vroman peak and at higher plasma concentration appear to be sensitive to both PEO MW and chemisorption conditions. Surfaces formed under low solubility conditions showed significant reduction in adsorption compared to the unmodified gold for all MWs [16]. The 600-OH "low solubility" surface showed the lowest Vroman peak of 20 ± 1 ng/cm^2. While higher than the 5 ng/cm^2 criterion suggested for prevention of significant platelet adhesion [20], this value is significantly lower (α<0.05) than those for the other surfaces. The 750-OCH_3 and 2000-OCH_3 low solubility surfaces showed peak adsorbed amounts of 70 ± 20 and 50 ± 3 ng/cm^2, respectively, while the 5000-OCH_3 surface adsorbed 140 ± 20 ng/cm^2 at the peak. Adsorption levels at higher plasma concentration

for the low solubility 600-OH, 750-OCH_3, 2000-OCH_3 and 5000-OCH_3 surfaces were 6.7 ± 0.6, 16 ± 9, 12 ± 3 and 50 ± 20 ng/cm^2, respectively.

We showed previously that in buffer, fibrinogen adsorption to the 750-OCH_3 and 2000-OCH_3 systems was at a minimum at a chain density of ~0.5 chains/nm^2 [16]. Similarly, the Vroman-type plasma experiments reported here indicate that at this chain density (low solubility conditions, Table 1) these surfaces adsorbed similar quantities of fibrinogen at the peak (70 ± 20 and 50 ± 3 ng/cm^2 respectively) and at higher plasma concentration (16 ± 9, 12 ± 3 ng/cm^2). This result strongly supports our previous conclusion [16] that PEO chain density perhaps plays the key role in determining the extent of protein resistance.

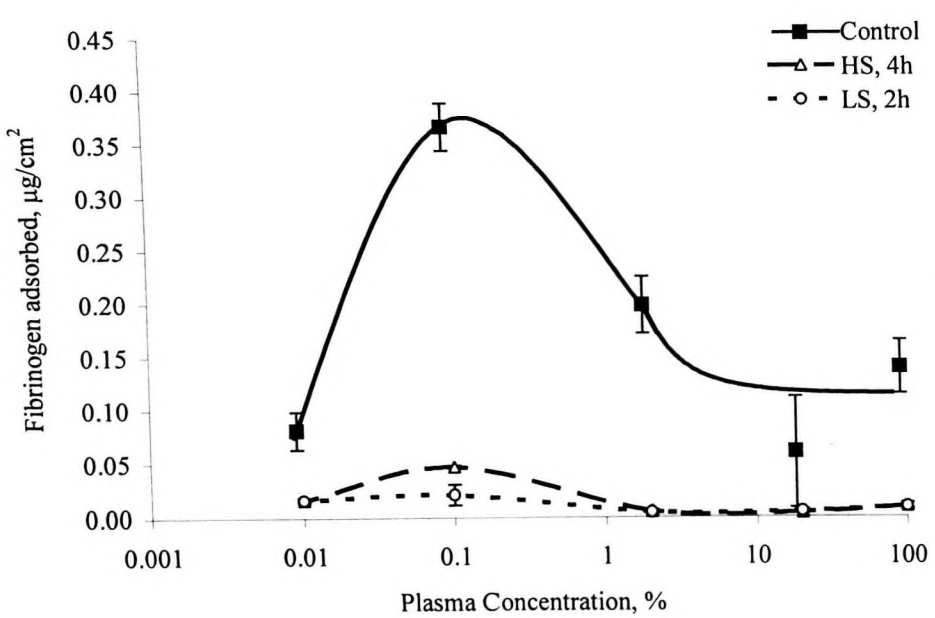

Figure 1. Fibrinogen adsorption from plasma to OH-terminated PEO, MW 600. Effect of chemisorption conditions. Data are mean ± SD, n=6.

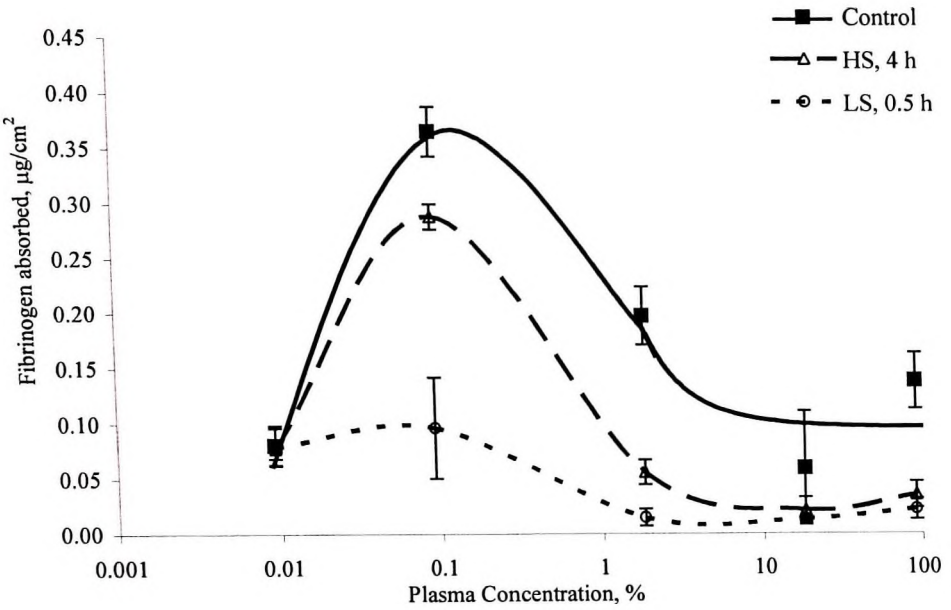

Figure 2. Fibrinogen adsorption from plasma to CH_3O-terminated PEO, MW 750. Effect of chemisorption conditions. Data are mean ± SD, n=3.

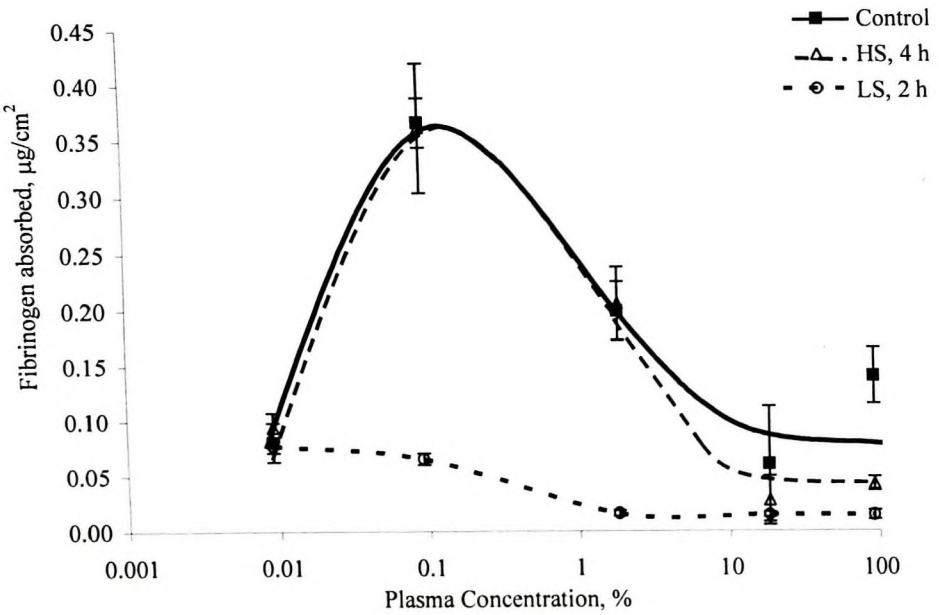

Figure 3. Fibrinogen adsorption from plasma to CH_3O-terminated PEO, MW 2000. Effect of chemisorption conditions. Data are mean ± SD, n=3.

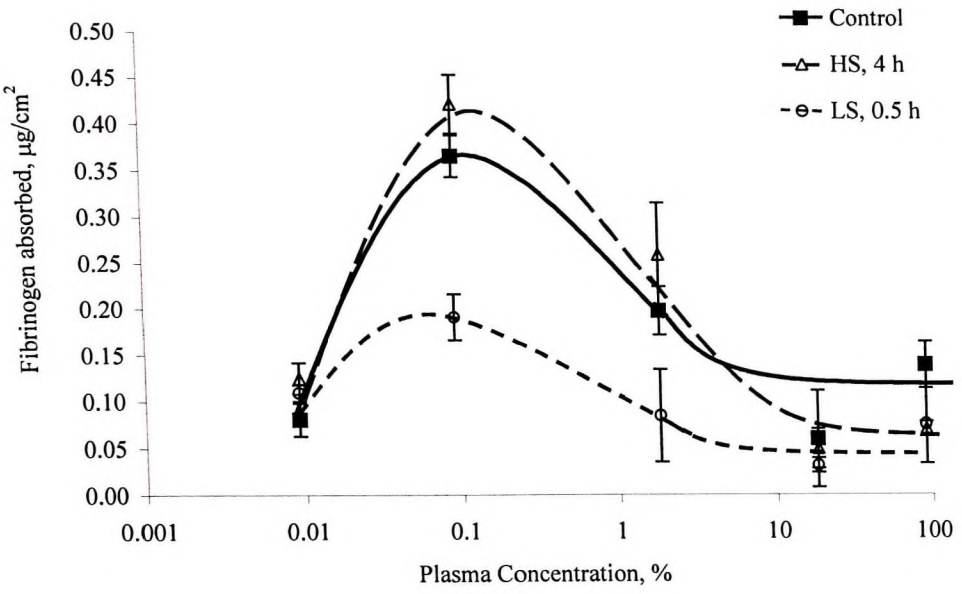

Figure 4. Fibrinogen adsorption from plasma to CH_3O-terminated PEO, MW 5000. Effect of chemisorption conditions. Data are mean ± SD, n=3.

Table 2. Vroman peak and plateau percent reductions and adsorbed amounts for fibrinogen adsorption from plasma.

Surface	Vroman peak adsorption (% reduction, ng/cm^2) (mean ±SD, n=6)	Plateau adsorption (% reduction, ng/cm^2) (mean ±SD, n≥11
600 MW, high solubility, 4 h	75 ± 2, 50 ± 10	65 ± 3, 6 ± 1
600 MW, low solubility, 2 h	90 ± 1, 20 ± 1	60 ± 1, 6.7 ± 0.6
750 MW, high solubility, 4 h	20 ± 1, 230 ± 20	76 ± 10, 35± 16
750 MW, low solubility, 30 min	76 ± 3, 70 ± 20	91 ± 5, 16 ± 9
2000 MW, high solubility, 4 h	6 ± 6, 280 ± 30	76 ± 14, 25 ± 7
2000 MW, low solubility, 2 h	85 ± 4, 50 ± 3	92 ± 3, 12 ± 3
5000 MW, high solubility, 4 h	-11 ± 5, 330 ± 20	54 ± 24, 80 ± 20
5000 MW, low solubility, 30 min	54 ± 9, 140 ± 20	67 ± 19, 50 ± 20

Of the various surfaces studied, those prepared with 5000 MW PEO clearly show the lowest protein resistance. We have no definitive explanation for this observation; it may be due to the inability of the system to optimize chain density, hydration state and chain mobility. In previous work we found that for materials prepared by blending PEO copolymers with a polyurethane matrix, those based on higher MW PEO were less protein resistant [27].

The present results support previous conclusions that PEO layers formed from solutions of PEO near the cloud point [13,14] are of relatively high chain density and high protein resistance. In general these results also suggest that with appropriate chain density, chain length, and end group chemistry, PEO modified surfaces may reduce fibrinogen adsorption to levels that should be non-reactive to platelets. The adsorption level at high plasma concentration (ie. normal plasma) on the 600-OH low solubility surface, viz. 6.7 ± 0.6 ng/cm^2, is close to the threshold of 5 ng/cm^2 below which significant platelet adhesion and activation are expected to be negligible. However, the Vroman peak adsorption, about 20 ng/cm^2, is significantly above this threshold.

Analysis of eluted proteins by SDS-PAGE and immunoblotting

SDS-PAGE and immunoblot analysis of the proteins eluted after plasma contact was conducted to provide a broader assessment of the effect of PEO modification on protein adsorption from plasma. The blots (not shown) were similar in general appearance to those shown in previous publications [25,26]. It should be noted that for the different surfaces, equal surface areas and equal volumes of SDS eluent were used in

these experiments. In addition, equal volumes of eluate were loaded on the gels. The relative intensities of the lanes for a given protein should therefore give an indication of the relative amounts of that protein for the different surfaces. The major proteins detected were fibrinogen, albumin, IgG, complement C3, apolipoprotein A-I and high molecular weight kininogen. Band intensity data are summarized in Tables 3, 4 and 5. It should be emphasized that while these proteins were detectable, the adsorbed amounts (not available from the blot data) were undoubtedly low. Detection limits, of the order of 0.1 ng, are inherently low. Moreover the intensities of the bands for the different proteins were similar to or less than those for fibrinogen, which as we have shown was adsorbed in very low amounts from undiluted plasma.

TABLE 3. RELATIVE BAND INTENSITIES IN IMMUNOBLOTS FOR FIBRINOGEN AND ALBUMIN.*

		Fibrinogen				Albumin
		α, 68 kDa	β, 56 kDa	γ, 48 kDa	Fragments	66 kDa
Control		***-	***+	*	*	**+
600 MW	HS	*+	***-	****-	*	***-
	LS	*	**-	***-	*	***+
750 MW	HS	*	**-	***-	*	***+
	LS	**+	**-	***-	*	****-
2000 MW	HS	***	***+	*	*	***+
	LS	*	***-	***-	*	****-
5000 MW	HS	*	**+	***-	*	***+
	LS	*	*	*+	*+	***+

*FIVE STARS INDICATES A HIGH INTENSITY BAND. ONE STAR INDICATES ZERO INTENSITY. + AND – INDICATE, RESPECTIVELY, SLIGHTLY GREATER OR LESS THAN THE INDICATED INTENSITY LEVEL. (LOWEST TO HIGHEST INTENSITY: *, *+, **-, **, **+, ***-, ***, ***+ ....)

TABLE 4. RELATIVE BAND INTENSITIES IN IMMUNOBLOTS FOR COMPLEMENT C3, IGG AND APOLIPOPROTEIN A-I.*

		C3		IgG		Apo A-I
		70 kDa	42 kDa	55 kDa	27 kDa	27 kDa
Control		****-	***-	****-	*	***+
600 MW	HS	*+	****-	*	*	*+
	LS	***+	****	*	*	**+
750 MW	HS	*	**+	**-	*	****+
	LS	****-	***	**	*	**-
2000 MW	HS	****-	**+	****-	*	*****
	LS	**+	**-	*	*	****+
5000 MW	HS	****+	****-	**-	*	***+
	LS	***+	**-	*+	*	***+

*FIVE STARS INDICATES A HIGH INTENSITY BAND. ONE STAR INDICATES ZERO INTENSITY. + AND – INDICATE, RESPECTIVELY, SLIGHTLY GREATER OR LESS THAN THE INDICATED INTENSITY LEVEL. (LOWEST TO HIGHEST INTENSITY: *, *+, **-, **, **+, ***-, ***, ***+ ....)

TABLE 5. RELATIVE BAND INTENSITIES IN IMMUNOBLOTS FOR CONTACT PHASE COAGULATION PROTEINS.*

		HK	FXI		FXII	Prekallikrein
		Fragments	83 kDa	50, 33 kDa	80 kDa	85 kDa
Control		***-	**+	*	*	*
600 MW	HS	**+	*	*	*	*
	LS	**-	*	*	*+	*+
750 MW	HS	*	*	*	*	*
	LS	**+	*	*	*	*
2000 MW	HS	*+	*	*	*	*
	LS	*	*	*	*	*
5000 MW	HS	*+	*	*	*+	*+
	LS	*+	*	*	*	*

*Five stars indicates a high intensity band. One star indicates zero intensity. + and – indicate, respectively, slightly greater or less than the indicated intensity level. (Lowest to highest intensity: *, *+, **-, **, **+, ***-, ***, ***+ ....)

Fibrinogen normally runs in reduced SDS-PAGE as three bands at 68, 56, and 48 kDa, corresponding to the α, β and γ chains respectively. Bands of lower molecular weight are generally indicative of fibrinogen cleavage resulting from activation of the fibrinolytic system. The 750 PEO surfaces showed the highest intensity fibrinogen bands, possibly indicating that fibrinogen was adsorbed to and/or eluted more readily from these surfaces than from the others. The 5000 PEO low solubility surface showed a weak band at ~ 35 kDa, indicating cleavage of the molecule on this surface.

Albumin runs as a single band at ~66 kDa. Significant responses on all surfaces were observed for this protein (Table 3). The control surface showed the lowest band intensity and the 750 and 2000 MW low solubility systems showed the highest intensities. In general, the low solubility surfaces showed higher intensity for albumin than the high solubility surfaces, except for the 5000 MW systems where both the high solubility and low solubility surfaces showed similar intensities. Both the increased presence of albumin on the PEO modified surfaces, compared to the control, and the high band intensity for surfaces with higher PEO chain density (600, 750 and 2000 MW systems) may be related to albumin–PEO affinity as reported by Vert et al. [28].

IgG runs as two bands at ~55 and ~27 kDa corresponding to the heavy and light chains respectively. The IgG blots showed significant responses for the control, and for the 2000 PEO high solubility surfaces (Table 4). Only weak responses were seen for the 600 surfaces and all of the other low solubility surfaces.

Complement C3 usually runs as two bands at 115 and 72 kDa corresponding to the α and β chains respectively. In the process of complement activation the α chain is

cleaved while the β chain remains intact [29]. All of the C3 blots showed bands at ~110 (weak), ~70, and ~42 kDa (activation fragment), the latter suggesting that all of the surfaces are complement-activating to some extent. The control, 750 low solubility, 600 (both high and low solubility) and 5000 (both high solubility and low solubility) surfaces appeared to be the most active.

Apolipoprotein A-I is the major apolipoprotein of high density lipoprotein [30]. It has a molecular weight of ~27 kDa and a concentration in plasma of 1.1 to 1.4 mg/mL (40-50 μM). We have found previously that apolipoprotein A-I is a major component of the protein layer adsorbed from plasma to many biomaterials [31]. In this study, the immunoblots for apo A-I indicate significant adsorption to the control and to all of the PEO-modified surfaces, thus confirming the high surface activity of this protein.

The four contact phase coagulation proteins, factor XI factor XII, prekallikrein (PK) and high molecular weight kininogen (HK) are of interest because of their role in initiating coagulation on surfaces. These four proteins interact on blood contacting surfaces through a complex series of reactions to produce activated factor XI, which then continues the clotting cascade leading ultimately to fibrin formation [32]. Their concentrations in plasma are ~5, ~30, ~50 and ~70 μg/mL, respectively and adsorbed amounts are expected to reflect these relatively low concentrations. HK is known as a strongly surface active protein and is believed to play an important role in displacing initially adsorbed fibrinogen via the Vroman effect [19,21]. The molecular weight of intact HK is 120 kDa. It is normally present in plasma as a binary complex with prekallikrein and is cleaved by kallikrein yielding a two chain disulfide linked protein

which runs at 56 and 46 kDa in reduced gels. The intensities for the HK response were in the order: Control > 600 PEO HS and 750 PEO LS > 600 PEO LS > 2000 PEO HS and both 5000 PEO systems > 750 PEO HS and 2000 PEO LS surfaces (Table 5). The other contact phase proteins showed very weak or zero responses, indicating low adsorption and/or low elutability. In general the immunoblot data on the contact phase proteins suggest that activation of coagulation via the contact phase would be low on these surfaces.

Conclusions

In agreement with previously reported single protein adsorption studies, PEO layers formed by chemisorption to gold under low solubility conditions adsorbed the lowest amounts of fibrinogen from plasma. The 600-OH "low solubility" surface showed the lowest Vroman peak (20 ± 1 ng/cm^2) at 0.1 % plasma and adsorption of only 6.7 ± 0.6 ng/cm^2 at normal plasma concentration. The latter is similar to the value of 5 ng/cm^2 suggested as the threshold below which significant platelet adhesion does not occur [20]. A low Vroman peak is significant because even transient adsorption of fibrinogen could result in platelet adhesion and activation. Adsorption to the 750-OCH_3 and 2000-OCH_3 surfaces with Vroman peaks of 70 and 50 ng/cm^2, respectively, was significantly higher, suggesting that chain end chemistry affects the adsorption and/or displacement of fibrinogen on these PEO surfaces. The 750-OCH_3 and 2000-OCH_3 "low solubility" surfaces with similar chain densities (~0.5 chains/nm^2) showed similar overall fibrinogen adsorption behavior, suggesting the importance of chain density for protein interactions.

Immunoblots of eluted proteins confirmed adsorption of fibrinogen, and showed that some albumin, IgG, complement C3, apolipoprotein A-I, and HK were also adsorbed on most of the surfaces. Adsorbed complement C3 (all surfaces) was degraded in a manner suggesting the occurrence of complement activation.

Acknowledgements

Financial support by the Natural Sciences and Engineering Research Council of Canada (NSERC), and the Canadian Institutes of Health Research (CIHR) is gratefully acknowledged.

References

1. Andrade JD. In: Andrade JD, editor. Surface and Interfacial aspects of Biomedical Polymers. New York: Plenum Press, 1985. p. 1-80.

2. Harris JM. In: Harris JM, editor. Poly(ethylene glycol) Chemistry: Biotechnical and Biomedical Applications. New York: Plenum Press, 1992. p. 1-14.

3. Morra M. On the molecular basis of fouling resistance. J Biomater Sci, Polym Edn 2000;11:547-69.

4. Malmsten M, Emoto K, Van Alstine JM. Effect of chain density on inhibition of protein adsorption by poly(ethylene glycol) based coatings. J Colloid Interface Sci 1998;202:507-17.

5. Szleifer I. Protein adsorption on surfaces with grafted polymers: a theoretical approach. Biophysical J 1997;72:595-612.

6. Vogler EA. Water and the acute biological responses to surfaces. J Biomater Sci, Polym Edn 1999;10:1015-45.

7. Unsworth LD, Tun Z, Sheardown H, Brash JL. Chemisorption of thiolated poly(ethylene oxide) to gold: surface chain densities measured by ellipsometry and neutron reflectometry. J Colloid Interface Sci 2005;281:112-21.

8. Unsworth LD, Sheardown H, Brash JL. Effect of chain density on protein adsorption to 600 molecular weight hydroxyl-poly(ethylene glycol)-thiol thin films as measured by ellipsometry and radiolabeling techniques. In preparation.

9. Nuzzo RG, Allara DL. Adsorption of biofunctional organic disulphides on gold surfaces. J Am Chem Soc 1983;105:4481-3.

10. Zhang F, Kang ET, Neoh KG, Huang W. Modification of gold surface by grafting of poly(ethylene glycol) for reduction in protein adsorption and platelet adhesion. J Biomater Sci Polym Edn 2001;12:515-31.

11. Prime KL, Whitesides GM. Adsorption of proteins onto surfaces containing end-attached oligo(ethylene oxide): a model system using self assembled monolayers. J Am Chem Soc 1993;115:10714-21.

12. Zhu B, Eurell T, Gunawan R, Leckband D. Chain length dependence of the protein and cell resistance of oligo(ethylene glycol)-terminated self-assembled monolayers on gold. J Biomed Mater Res 2001;56:406-16.

13. Kingshott P, Griesser HJ. Surfaces that resist bioadhesion. Curr Opinion Solid State Mater Sci 1999;4:403-12.

14. Kingshott P, Thissen H, Griesser HJ. Effects of cloud point grafting, chain length, and density of PEG layers on competitive adsorption of ocular proteins. Biomaterials 2002;23:2043-56.

15. Alexander S. Adsorption of chain molecules with a polar head a scaling description. J Physique 1977 38:983-7.

16. Unsworth LD, Sheardown H, Brash JL. Protein resistance of surfaces prepared by sorption of end-thiolated poly(ethylene glycol) to gold: effect of surface chain density. Langmuir, in press, 2004.

17. Brash JL. The fate of fibrinogen following adsorption at the blood-biomaterial interface. Ann NY Acad Sci 1987;516:206-22.

18. Slack SM, Horbett TA. The Vroman Effect: A Critical Review. In: Horbett TA, Brash JL, editors. Proteins at Interfaces II: Fundamentals and Applications. Washington, DC: American Chemical Society, 1995. p. 112-8.

19. Vroman L, Adams AL. Identification of adsorbed proteins by exposure to antisera and water vapor. J Biomed Mater Res 1969;3:669-71.

20. Tsai WB, Grunkemeier JM, McFarland CD, Horbett TA. Platelet adhesion to polystyrene-based surfaces preadsorbed with plasmas selectively depleted in fibrinogen, fibronectin, vitronectin, or von Willebrand's factor. J Biomed Mater Res 2002;60:348-59.

21. Wojciechowski P, ten Hove P, Brash JL. Phenomenology and mechanism of the transient adsorption of fibrinogen from plasma (Vroman Effect). J Colloid Interface Sci 1986; 111: 455-65.

22. Du YJ, Brash JL. Synthesis and characterization of thiol-terminated poly(ethylene oxides) for chemisorption to gold surface. J Appl. Polymer Sci 2003;90:594-607.

23. Du YJ, Cornelius RM, Brash JL. Measurement of protein adsorption to gold surface by radioiodination methods: suppression of free iodide sorption. Coll and Surf B: Biointerfaces 2000;17:59-67.

24. Brash JL, ten Hove P. Effect of plasma dilution on adsorption of fibrinogen to solid surfaces. Thromb. Haemostas 1984;51:326-30.

25. Cornelius RM, Archambault JG, Berry L, Chan AKC, Brash JL. Adsorption of proteins from infant and adult plasma to biomaterial surfaces. J Biomed Mater Res 2002;60:622-32.

26. Cornelius RM, Brash JL. Identification of proteins adsorbed to hemodialyser membranes from heparinized plasma. J Biomater Sci Polym Edn 1993;4:291-304.

27. Tan J, Brash JL. Novel PEO-containing copolymers as protein repellent additives in polyurethanes. Trans Soc Biomat 2001;24:499.

28. Vert M, Domurado D. Poly(ethylene oxide): Protein-repulsive or albumin-compatible? J Biomater Sci Polymer Edn 2000;11:1307-11.

29. Jahns G, Haeffner-Cavaillon N, Nydegger UE, Kazatchkine MD. Complement activation and cytokine production as consequences of immunological bioincompatibility of extracorporeal circuits. Clinical Materials 1993;14:303-36.

30. McIntyre N, Harry DS In: McIntyre N, Harry DS, editors. Lipids and Lipoproteins in Clinical Practice. New York: Wolfe Publishing Ltd., 1991.

31. Cornelius RM, Archambault JG, Brash JL. Identification of apolipoprotein A-I as a major adsorbate on biomaterial surfaces after blood or plasma contact. Biomaterials 2002;23:3583-7.

32. Davie EW, Fujikawa K, Kisiel W. The coagulation cascade: initiation, maintenance, and regulation. Biochemistry 1991;30:10363-70.

9.0 PAPER FOUR: PEO-GRAFTED SURFACES FOR SUPPRESSION OF PROTEIN ADSORPTION: EFFECT OF CHAIN DENSITY DETERMINED BY *IN SITU* ELLIPSOMETRY.

Authors: **L.D. Unsworth**, H. Sheardown, and J.L. Brash

Working Hypothesis:

Determination of the chemisorbed amount of PEO and the corresponding protein adsorbed amounts using *in situ* ellipsometry may provide useful insights on protein adsorption mechanisms to PEO-modified surfaces.

Main Contributions:

1. Hydrated chain densities were found to be in the range of 0.21 to 2.3 and 0.18 to 0.98 chains/nm^2 for 750 and 2000 MW PEO films, respectively; these are among the highest densities observed for these systems.

2. The respective fibrinogen and lysozyme adsorption minima for the 750 and 2000 MW systems were similar and occurred at similar chain densities.

3. The observed fibrinogen and lysozyme adsorption trends suggest that chain density, and not molecular weight, is the major determinant of protein resistance. Furthermore, at chain densities of ~0.5 chains/nm^2, protein resistance seems to be independent of protein size.

4. It may be that as chain density increases to very high values, the chains become dehydrated and lose mobility, thus facilitating increased protein adsorption to these films.

Abstract:

In situ ellipsometry was used to determine both the chain densities of layers formed by chemisorption of polyethylene oxide (PEO) to gold, as well as the corresponding fibrinogen and lysozyme adsorption. Thiolated-monomethoxy PEO was chemisorbed to gold-coated silicon wafers. Surface chain density was varied by controlling PEO solubility (proximity to cloud point conditions) as well as incubation time. Hydrated chain densities were found to be in the range of 0.21 to 2.3 and 0.18 to 0.98 chains/nm^2 for 750 and 2000 MW PEO layers, respectively. These chain densities are much higher than those corresponding to layers of PEO chains with an unperturbed random coil ("mushroom") conformation, suggesting that the layers are in the brush regime. For both fibrinogen and lysozyme it was observed that adsorption decreases and then increases as chain density increases. The respective fibrinogen minima for the 750 and 2000 PEO surfaces were 11.6 ± 0.5 and 20 ± 1 ng/cm^2 and occurred at similar chain densities of 0.5 ± 0.1 and 0.4 ± 0.1 chains/nm^2. Fibrinogen adsorption of 61 ± 3 and 62 ± 2 ng/cm^2 for the 750 and 2000 PEO surfaces were observed at similar chain densities of 1.2 ± 0.2 and 1.0 ± 0.5 chains/nm^2, respectively. For lysozyme adsorption, minima for the 750 and 2000 PEO surfaces were 22 ± 2 and 15 ± 4 ng/cm^2, respectively, and also occurred at similar chain densities (0.5 ± 0.1 and 0.4 ± 0.1 chains/nm^2). At very high chain density (~2.3 chains/nm^2) lysozyme adsorption on the 750 PEO surface was similar to that on the unmodified gold. It may be that as chain density increases to high values, the chains become dehydrated and lose mobility, thus facilitating increased protein adsorption. The

results of this study suggest that chain density, not chain length, is the main determinant of protein resistance on PEO-tethered surfaces.

Introduction

It is well known that, when present at the material-tissue interface, poly(ethylene oxide) (PEO) impedes nonspecific protein adsorption [1-4]. Surfaces where the PEO is tethered at one end have been found to be particularly effective in this regard. Despite extensive study, the mechanisms responsible for the protein resistant nature of these surfaces are not entirely clear. However, it is believed that PEO chain length, surface chain density, and chain conformation are some of the factors involved [3,5]. In general it has been found that protein resistance increases with chain length to an upper limit of about 100 ethylene oxide (EO) units, beyond which there is no additional benefit, although some investigators have shown that chain lengths of just a few ethylene oxide units can be sufficient to provide significant effects [6]. One difficulty in determining the effects of PEO chain density and chain conformation derives from the fact that these two factors are interdependent. As pointed out by Alexander [7], the conformation of end-tethered chains on a surface depends directly on the chain density. General conformations have been described for various chain density 'regimes': a random coil conformation (mushroom regime) occurs when the chain density is low and the graft spacing (S) is greater than $2R_F$ (R_F is the Flory radius) and a more extended conformation (brush regime) occurs at higher chain density when $S<2R_F$ [8,9].

The chemisorption of thiolated polymers to gold-coated substrates has been widely employed to prepare well-defined polymer layers in which the chains are end-tethered [10-13]. An example are alkanes (e.g. C-11) thiol-terminated at one end and having an oligoethylene oxide (OEO) moiety at the other. The PEO density in these surfaces can be varied by using mixtures of OEO-terminated and non-OEO-terminated chains [10-12]. It has been shown that protein adsorption to surfaces of this type can be reduced to levels near or below the detection limit of the adsorption measurement.

The approach taken in the present work was to chemisorb thiol-terminated PEO of variable molecular weight (MW) to gold, and to vary chain density by varying incubation time under conditions where PEO is marginally soluble [1,2]. It is well known that aqueous PEO solutions exhibit a reverse dependence of solubility on temperature and the polymer begins to precipitate as the temperature is increased towards the cloud point. In addition, the cloud point temperature decreases with increasing ionic strength. It has been shown that relatively high PEO chain densities can be achieved by grafting near cloud point conditions, even though the tethered polymer chains remain in the unperturbed random coil state [2]. The tethered chains tend to expand when the temperature is lowered and/or the ionic strength decreased, leading to chain extension and the formation of brush-type layers.

The objective of the present work was to prepare and characterize layers of end-tethered PEO of variable MW and chain density by chemisorption to gold and to investigate their ability to suppress protein adsorption. In particular we wanted to perform *in situ* measurements for comparison to previous *ex situ* studies of these surfaces [8,14].

In situ observations may more reflective of the interactions occurring at the interfaces during adsorption, avoiding in particular the necessity of separating the surface from the protein solution. In this article the chain densities of PEO surfaces prepared by chemisorption of chain-end thiolated PEO to gold, and the adsorption of fibrinogen and lysozyme (as single proteins) to these surfaces as measured by *in situ* ellipsometry are reported.

Materials and Methods

Surfaces:

As described elsewhere [15,16], gold-coated silicon wafers, obtained commercially, were carefully cleaned and exposed to solutions of 5 mM chain end-thiolated, monomethoxy poly(ethylene oxide) (PEO) of molecular weight 750 or 2000. Chemisorption solution conditions (Table 1) were chosen to be near the cloud point of the PEO. In previous work [8,14] we found that high chain densities can be achieved under these conditions. Chain density was varied by varying the chemisorption time over the range of 30 min to 4 h. Following chemisorption, wafers were placed in multiwell plates containing Milli-Q water, sonicated for 4 min and rinsed extensively with water.

Table 1. Chemisorption conditions.

PEO Molecular Weight (g/mol)	Temperature (°C)	Ionic Strength (M)
750	35	2.9
2000	35	2.8

PEO concentration, 5 mM; pH, 7.4 ± 0.1.

Ellipsometry:

A self-nulling, single wavelength (6328 Å) ellipsometer (Exacta 2000, Waterloo Digital Electronics, Waterloo ON, Canada), with an incident angle of 70°, was used to determine the properties of both the chemisorbed PEO and adsorbed protein layers. The gold coated wafers were considered as the substrate, with refractive index (n_s) and extinction coefficient (k_s) determined to be 0.33 ± 0.01 and 3.34 ± 0.01, respectively. For the PEO- and protein-modified surfaces, the polarizer (P) and analyzer (A) angles for the null condition were measured *in situ* using a specially designed "wet cell", and thickness values were determined.

In situ measurements of both the PEO and the adsorbed protein layers were conducted using fixed complex refractive index values ($n_i + \imath k_i$) of 1.33 + ι0 for the aqueous medium and 1.37 + ι0 for both the PEO [17] and adsorbed protein layers [12,18]. Fixed values of refractive index were used for these layers since they were too thin, in most cases, to allow determination of both average thickness and refractive index from the ellipsometry data. Final thickness values were obtained by fitting the experimental data to a three-layer model: aqueous medium-PEO-gold or aqueous medium-protein- PEO/gold substrate. Calculations were carried out using the Exacta 2000 Variable Theta Simplex Fitting Program (Waterloo Digital Electronics).

In situ PEO and protein adsorbed amounts were estimated using the de Feijter equation [19], eq. (1).

$$\Gamma = \frac{d\left(n_f - n_a\right)}{dn/dc} \tag{1}$$

The adsorbed amount, Γ, is a function of the average thickness (d) returned by the ellipsometry measurements, the difference in layer (n_f) and aqueous medium(n_a) refractive index and the specific refractive index increment (dn/dc). The latter accounts for the effect of the atomic concentration within the layer on the overall layer refractive index. This quantity is unique for a given macromolecule of interest. Values of 0.134 cm^3/g for PEO [20] and 0.188 cm^3/g for both fibrinogen and lysozyme [18] were used in this work.

Results and Discussion

Chain Density

In situ ellipsometrically determined chain density data are shown in Figure 1. It can be seen that density increased with chemisorption time, with values ranging from 0.21 ± 0.10 to 2.3 ± 0.14 and from 0.18 ± 0.02 to 0.98 ± 0.05 chains/nm^2, for 750 and 2000 MW PEO respectively. These values are similar to, or greater than the densities of 0.24 and 0.09 chains/nm^2 estimated for layers of close packed 750 and 2000 MW PEO where the chains are in the random coil conformation (mushroom regime) [8]. Also, they are significantly lower than the estimated upper limit of 5.8 chains/nm^2 for a layer of close packed, fully extended PEO chains [21]. Thus it appears that in all cases the chemisorbed PEO layers were in the brush regime, implying that the chains adopted an extended conformation [9]. As seen in Figure 1, chain densities under comparable chemisorption conditions were lower for the 2000 than the 750 MW PEO, probably due

to increased steric hindrance associated with the introduction of longer chains into the developing layer.

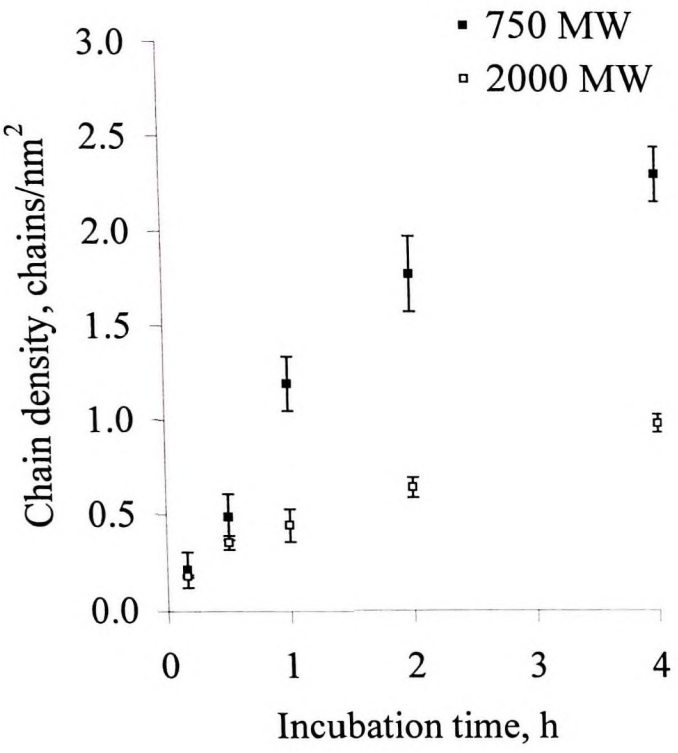

Figure 1. Hydrated chain densities for 750 (■) and 2000 (□) MW PEO layers vs. incubation time under low solubility conditions. Data are mean ± SD, n=4.

Our previous work on similar PEO layers gave chain densities measured in the dry state (*ex situ*) much smaller than those reported here [8]. Values for 750 and 2000 MW PEO layers formed under similar chemisorption conditions ranged from 0.4 to 0.7 and 0.33 to 0.58 chains/nm^2, respectively. The apparent discrepancy between the *in situ* and *ex situ* chain densities most likely arises from the assumption (for the ex situ case) of a constant layer mass density of 1 g/cm^3 regardless of whether the chain density is high or low. Furthermore, even though a refractive index must be assumed for the calculation

(eq. 1) of both the PEO and protein adsorbed amounts *in situ*, the resulting values are relatively insensitive to the value assumed. This is because the average thickness and the refractive index are interdependent: different refractive index estimates, within a reasonable range, while yielding different average thickness values, nonetheless give similar adsorbed amounts. Therefore, the *in situ* chain density values may be considered more accurate than the *ex situ*.

The PEO chain densities reported in this work appear to be significantly greater than those found by others. For surfaces formed by adsorption of PEO-conjugated phospholipid at the air-water interface, Efremova et al. [22] found chain densities of 1.16, 0.20 and 0.23 chains/nm^2 for PEO of MW 120, 2000 and 5000 respectively. Lin, et al. [23] found a maximum chain density of 0.4 chains/nm^2 for 2000 MW PEO grafted surfaces formed through two-phase silanization of flat silica surfaces. Malmsten, et al. [3] reported a maximum density, as determined by ellipsometry, of 0.12 chains/nm^2 for 5000 MW PEO grafted to silica or quartz. The high chain densities achieved in the present work may be attributable to the strategy of "grafting" under low solubility conditions where the chains are contracted.

Protein adsorption:

Data on fibrinogen adsorption to the unmodified gold and to the surfaces modified with 750 and 2000 MW PEO are shown in Figure 2. It is apparent that as chain density increases there is a decrease and then an increase in fibrinogen adsorption, i.e. there is a particular chain density at which adsorption is a minimum. The respective adsorption minima for the 750 and 2000 PEO surfaces were 11.6 ± 0.5 and 20 ± 1 ng/cm^2 and

occurred at similar chain densities (0.5 ± 0.1 chains/nm^2 for 750 PEO; 0.4 ± 0.1 for 2000 PEO). Furthermore, at chain densities around 0.2 and 1.0 chains/nm^2 both surfaces showed similar adsorbed amounts of ~ 120 and ~ 60 ng/cm^2, respectively. The trends in these data thus suggest that protein adsorption is more strongly dependent on chain density than on PEO MW.

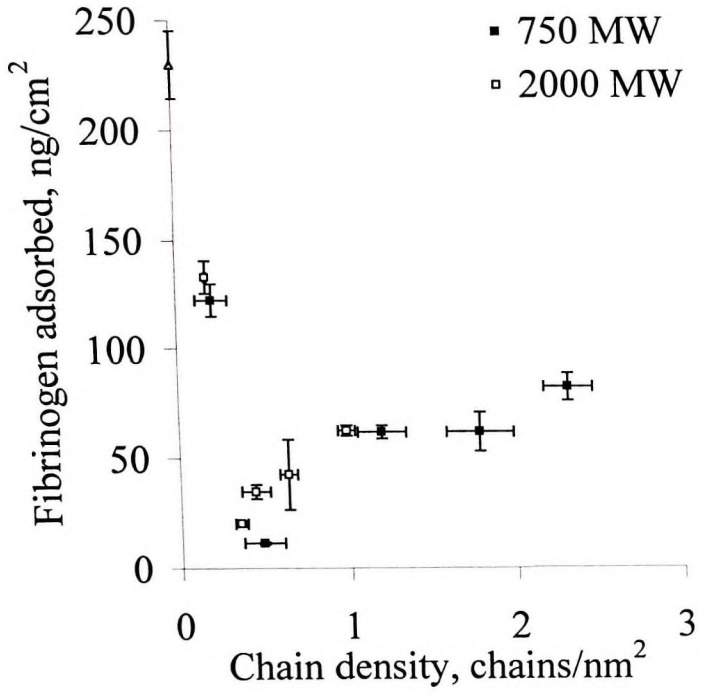

Figure 2. Fibrinogen adsorption as a function of chain density determined by *in situ* ellipsometry. Fibrinogen adsorption to the unmodified control is shown as a filled triangle at the zero chain density position. Data are mean ± SD, n=4.

Data on lysozyme adsorption are shown in Figure 3. Again it is apparent that there is a minimum in adsorption as a function of chain density. The respective adsorption minima for the 750 and 2000 PEO surfaces were 22 ± 2 and 15 ± 4 ng/cm^2 and again they occurred at similar chain densities (0.5 ± 0.1 chains/nm^2 for 750 PEO; 0.4

± 0.1 for 2000 PEO). At the highest high chain density of ~2.3 chains/nm^2, adsorption on the 750 PEO surface was similar to that on the unmodified gold, indicating that the 750 PEO surface at this density is not protein resistant to any significant extent. Adsorption at the lowest chain density was greater on the 750 PEO surface than on the 2000 PEO, possibly because the latter is able to resist adsorption more effectively by "covering" a larger area. However in general, the lysozyme data again point to the conclusion that the protein resistance of PEO-grafted surfaces is strongly dependent on chain density and less so on PEO MW.

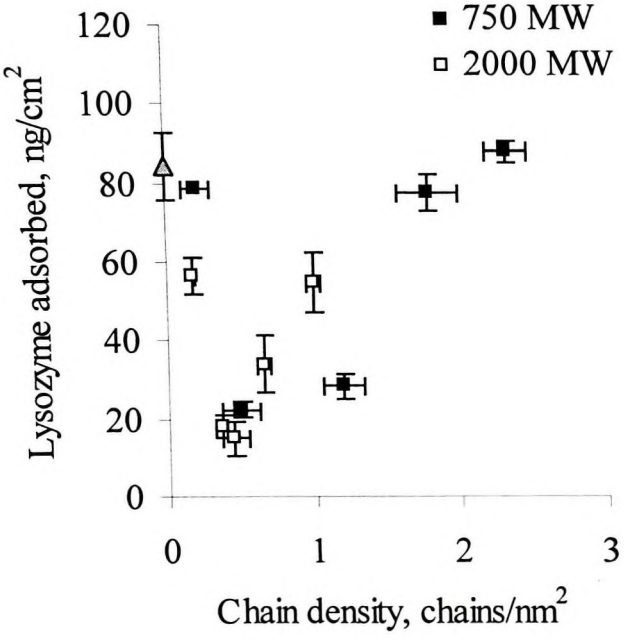

Figure 3. Lysozyme adsorption as a function of chain density determined by *in situ* ellipsometry. Lysozyme adsorption to the unmodified control is shown as a filled triangle at the zero chain density position. Data are mean ± SD, n=4.

The phenomenon of a minimum in adsorption as a function of PEO density was observed previously in our laboratory. In the earlier work adsorption was measured using ^{125}I-labeled proteins [14]. For a similar set of surfaces (PEO molecular weight and chain density) adsorption minima of ~ 40 and 60 ng/cm^2, respectively, were observed for fibrinogen and lysozyme, ie significantly greater than those determined using *in situ* ellipsometry in the present work. The reason for the difference is not clear, but it may be noted that for the ^{125}I measurements the buffer contained cold NaI to suppress the adsorption of free radioactive iodide to the gold [24].

The occurrence of an adsorption minimum suggests that there is an optimal surface chain density for protein resistance. The lysozyme minima on surfaces modified with PEO of different MW (750 and 2000) occurred at approximately the same chain density (~ 0.5 chains/nm^2). Perhaps more striking is the observation that for both MWs the protein adsorption vs chain density data are virtually co-incident. These observations suggest strongly that chain density, and its effect on the polymer layer structure, plays a role of major importance, perhaps the key role, in protein resistance mediated by tethered PEO. The increase in adsorption of protein at higher chain density is counter-intuitve. As discussed elsewhere [14], it may be that decreases in chain mobility and hydration associated with increased chain density are responsible for this observation.

The role of PEO chain density on protein resistance has been investigated by others. Using oligo(ethylene oxide)-SAM-gold surfaces, Vanderah et al.[25] showed that the adsorption of fibrinogen and albumin decreased as coverage increased up to 80%, beyond which adsorption increased sharply. It was suggested that the increase in

adsorption was due to a reduction of chain mobility in the OEO domains, implying that protein resistance is due mainly to the excluded volume effect related to lateral packing density. Similarly, Zheng et al. [26] showed that fibrinogen adsorption to OEO_4-SAMs decreased as the OEO fractional packing density approached 0.6 and then increased at packing density above 0.8. Simulations of OEO layer formation suggested that both OEO flexibility and hydrogen bonding between water and OEO chains are greater when the packing density is in the region of 0.5-0.8. This work is in accord with the present observations on the effects of PEO chain density as well as with those of Prime et al. [12] suggesting that protein adsorption is strongly influenced by chain hydration and flexibility.

In other work Pasche et al. [27] showed, using poly (L-Lysine)-graft-poly(ethylene glycol) (PLL-g-PEG) surfaces, that EO density was the determining factor in reducing protein adsorption, with strong effects on surfaces having densities greater than ~ 15 EO units/nm^2. This agrees with the observations of Malmsten et al. [3] and of Sofia et al. [4] that maximum protein resistance occurred at densities of 15-20 EO units/nm^2 and greater. In the present work the EO densities at the lowest adsorption were in a similar range, *viz.*, 8 and 15 EO units/nm^2 for the 750 and 2000 MW surfaces, respectively. However none of the other investigators reported an increase in adsorption at higher density as seen here. It may well be that the densities in these other studies were not high enough to observe this effect. Thus in the present work EO densities up to 39 and 45 EO units/nm^2 were achieved for the 750 and 2000 systems, respectively, whereas the highest density investigated by Pasche et al. [27] for 5000 MW was 30.

Our results, and those of others [2,3,21,28], may imply that it is the hydration state of particular conformations (as determined by chain density) of end-tethered PEO, regardless of the MW, which determines largely whether the surface will be protein resistant. The data suggest that, at intermediate chain densities, a state may exist where the chain properties (flexibility, conformation, hydration, etc.) are optimal for inhibiting protein adsorption.

Adsorbed lysozyme:fibrinogen ratio

A comparison of lysozyme and fibrinogen adsorption from single protein solutions is shown in Figure 4 as the lysozyme:fibrinogen molar ratio. In most cases this ratio was higher on the PEO-modified surfaces than on the unmodified gold, suggesting that the PEO surfaces are able to resist the bigger protein better than the smaller one. This is expected if the chain density is such that "residual" adsorption to the PEO surfaces is mainly of type 1 [29], ie adsorption to the gold-PEO interface requiring penetration of the PEO layer by the protein.

It is also of note that for the lower density PEO 2000 surfaces the lysozyme:fibrinogen ratio is similar to that for the unmodified gold, again suggesting that at this density the proteins are able to reach the gold and adsorb to it. In general the ratios for the 2000 PEO are lower and closer to the control than the PEO 750 surfaces at a given chain density, indicating that the grafted PEO of lower chain length discriminates more effectively on the basis of size than the higher chain length. This seems intuitively correct, at least for the lower density surfaces where penetration of the PEO is more likely. At the higher densities, in the brush regime, it seems more likely that steric

hindrance would limit access to the gold-PEO interface; thus most of the adsorption would occur at the PEO-water interface. If, for example the layer becomes regionally dehydrated, and forms small hydrophobic patches, these patches may not affect the adsorption of the larger protein, while significantly affecting the adsorption of the smaller one. However, more extensive data on a wider range of proteins and PEO densities will be required to resolve these questions.

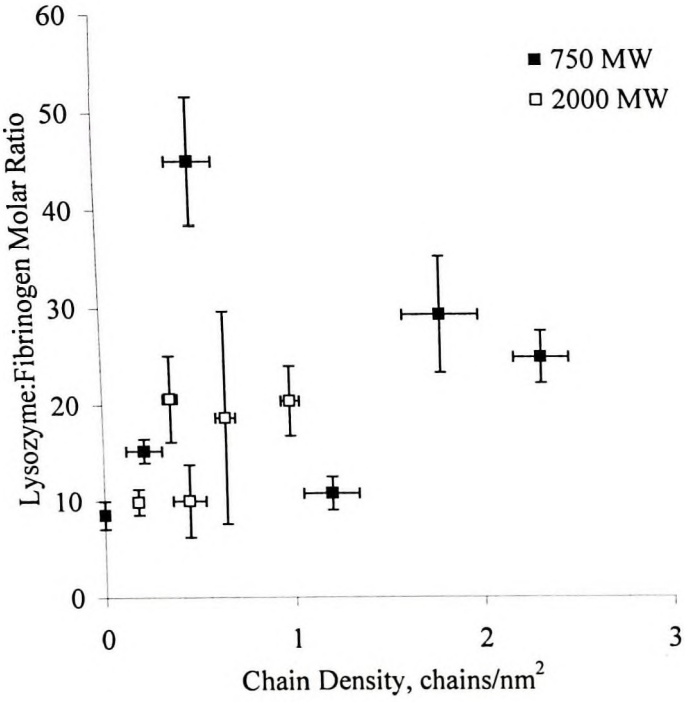

Figure 4. Comparison of lysozyme and fibrinogen (molar ratio lysozyme:fibrinogen) adsorbed from single protein solutions to surfaces modified with PEO of MW 750 and 2000.

Summary

PEO-grafted surfaces were prepared by chemisorption of thiolated-PEO (750 and 2000 MW) to gold. A range of PEO surface chain density was achieved by varying the

chemisorption time. Chain densities were estimated from *in situ* ellipsometry data assuming a PEO layer refractive index of 1.37 and a specific refractive index increment of 0.134 cm^3/g, and were found to be in the range of 0.5 to 2.3 and 0.4 to 1.0 chains/nm^2 for 750 and 2000 MW PEO, respectively. Protein adsorption was also measured *in situ* by ellipsometry. Similar to previous work using radiolabeling techniques, the adsorption of both fibrinogen and lysozyme was found to pass through a minimum as the chain density increased. The chain density at the minimum was similar for both molecular weights. It may be that as chain density increases to higher values, the chains become dehydrated, lose mobility and thus facilitate increased protein adsorption. Comparison of fibrinogen and lysozyme suggests that adsorption on the PEO surfaces is similar for both proteins, although a slight preference for lysozyme, the smaller of the two, was evident. In general the data also suggest that the PEO of lower chain length discriminates between proteins of different size more effectively than the higher chain length PEO.

Acknowledgements

Financial support by the Natural Sciences and Engineering Research Council of Canada (NSERC), and the Canadian Institutes of Health Research (CIHR) is gratefully acknowledged.

References

1 Kingshott P, Griesser HJ. Surfaces that resist bioadhesion. Curr Opinion Solid State Mater. Sci. **4**, 403 (1999).

2 Kingshott, P., Thissen, H., Griesser, H.J., 'Effects of cloud-point grafting, chain length, and density of PEG layers on competitive adsorption of ocular proteins.' *Biomaterials,* **23,** 2043 (2002).

3 Malmsten, M., Emoto, K., van Alstine, J.M., 'Effect of chain density on inhibition of protein adsorption by poly (ethylene glycol) based coatings' *J. Coll. Interfacial Sci.,* **202,** 507 (1998).

4 Sofia, S.J., Premnath, V., Merrill, E.W., 'Poly(ethylene oxide) Grafted to Silicon Surfaces: Grafting Density and Protein Adsorption.' *Macromolecules,* **31**, 5059 (1998).

5 Morra, M., 'On the molecular basis of fouling resistance.' *J.Biomater.Sci.Polymer Edn.* **11**, 547 (2000).

6 Gombotz, W.R., Guanghui, W., Horbett, T.A., Hoffman, A.S., 'Protein adsorption to poly(ethylene oxide) surfaces.' *J. Biomed. Mater. Res.,* **24**, 1547 (1991).

7 Alexander, S., 'Adsorption of chain molecules with a polar head a scaling description.' *J. de Physique*, **38**, 983 (1977).

8 Unsworth, L.D., Tun, Z., Sheardown, H., Brash, J.L., 'Chemisorption of thiolated poly(ethylene oxide) to gold: surface chain densities measured by ellipsometry and neutron reflectometry.' *J. Colloid Interface Sci.,* **281**, 112 (2005).

9 Fleer, G.J., Cohen Stuart, M.A., Scheutjens, J.M.H.M., Cosgrove, T., Vincent, B. In: Polymers at Interfaces, 1st ed., Chapman & Hall: New York, 1993, Chapter 4.1.4.

10 Nuzzo, R.G., Allara, D.L., 'Adsorption of biofunctional organic disulphides on gold surfaces.' *J. Am. Chem. Soc.* **105**, 4481 (1983).

11 Zhang, F., Kang, E.T., Neoh, K.G., Huang, W., 'Modification of gold surface by grafting of poly(ethylene glycol) for reduction in protein adsorption and platelet adhesion.' *J. Biomater. Sci. Polym. Edn.*, **12**, 515 (2001).

12 Prime, K.L., Whitesides, G.M., 'Adsorption of proteins onto surfaces containing end-attached oligo(ethylene oxide): a model system using self assembled monolayers.' *J. Am. Chem. Soc.*, **115**, 10714 (1993).

13 Zhu, B., Eurell, T., Gunawan, R., Leckband, D., 'Chain length dependence of the protein and cell resistance of oligo(ethylene glycol)-terminated self-assembled monolayers on gold.' *J. Biomed. Mater. Res.*, **56**, 406 (2001).

14 Unsworth, L.D., Sheardown, H., Brash, J.L., 'Protein resistance of surfaces prepared by sorption of end-thiolated poly(ethylene glycol) to gold: effect of surface chain density.' *Langmuir*, **3**, 1036 (2005).

15 Du, Y.J., Brash, J.L., 'Synthesis and characterization of thiol-terminated poly(ethylene oxides) for chemisorption to gold surface.' *J. Appl. Polymer Sci.*, **90**, 594 (2003).

16 Barbosa, R.V., Moraes, M.A.R., Gomes, A.S., Soares, B.G., 'VA-based graft copolymers as compatibilizing agents for polymer blends.' *Macromolecular Reports* **A32**, 663 (1995).

17 Huang, Y-W., Gupta, V.K., 'Effects of Physical Heterogeneity on the Adsorption of Poly(ethylene oxide) at a Solid-Liquid Interface.' *Macromolecules,* **34**, 3757 (2001).

18 Malmsten, M., 'Competitive adsorption at hydrophobic surfaces from binary protein systems.' *J. Coll. Inter. Sci.*, **166**, 333 (1994).

19 de Feijter, J.A., Benjamins, J., Veer, F.A., 'Ellipsometry as a tool to study the adsorption behavior of synthetic and biopolymers at the air-water interface.' *Biopolymers,* **17**, 1759 (1978).

20 Kinugasa, S., Nakahara, H., Fudagawa, N., Koga, Y., 'Aggregative Behavior of Poly(ethylene oxide) in Water and Methanol.' *Macromolecules,* **27**, 6889 (1994).

21 Harder, P., Grunze, M., Dahint, R., Whitesides, G.M., Laibinis, P.E., 'Molecular Conformation in Oligo(ethylene glycol)-Terminated Self-Assembled Monolayers on Gold and Silver Surfaces Determines Their Ability To Resist Protein Adsorption.' *J. Phys. Chem. B.,* **102**, 426 (1998).

22 Efremova, N.V., Sheth, S.R., Leckband, D., 'Protein-Induced Changes in Poly(ethylene glycol) Brushes: Molecular Weight and Temperature Dependence.' *Langmuir*, **17**, 7628 (2001).

23 Lin, Y.S., Golander, C.-G., 'The surface density gradient of grafted poly(ethylene glycol): preparation, characterization and protein adsorption.' *Colloids and Surfaces B: Biointerfaces,* **3**, 49 (1994).

24 Du, Y-J., Cornelius, R.M., Brash, J.L., 'Measurement of protein adsorption to gold surface by radioiodination methods: suppression of free iodide sorption.' *Colloids and Surfaces B: Biointerfaces,* **17**, 59 (2000).

25 Vanderah, D.J., La, H., Naff, J., Silin, V., Rubinson, K.A., 'Control of Protein Adsorption: Molecular Level Structural and Spatial Variables.' *J. Am. Chem. Soc.,* **126**, 13639 (2004).

26 Zheng, J., Li, L., Chen, S., Jiang, S., 'Molecular Simulation Study of Water Interactions with Oligo (Ethylene Glycol)-Terminated Alkanethiol Self-Assembled Monolayers.' *Langmuir*, **20**, 8931 (2004).

27 Pasche, S., de Paul, S.M., Voros, J., Spencer, N.D., Textor, M., 'Molecular Simulation Study of Water Interactions with Oligo (Ethylene Glycol)-Terminated Alkanethiol Self-Assembled Monolayers.' *Langmuir,* **19**, 9216 (2003).

28 Herrwerth, S., Eck, W., Reinhardt, S., Grunze, M., 'Factors that Determine the Protein Resistance of Oligoether Self-Assembled Monolayers - Internal Hydrophilicity, Terminal Hydrophilicity, and Lateral Packing Density.' *J. Am. Chem. Soc.,* **125**, 9359 (2003).

29 Halperin, A. 'Polymer Brushes that Resist Adsorption of Model Proteins: Design Parameters.' *Langmuir*, **15**, 2525 (1999).

10.0 PAPER FIVE: *IN SITU* NEUTRON REFLECTOMETRY INVESTIGATION OF CHEMISORBED PEO FILMS OF VARYING CHAIN DENSITY: INSIGHTS INTO PROTEIN ADSORPTION BEHAVIOUR.

Authors: **L.D. Unsworth**, Z. Tun, H. Sheardown, and J.L. Brash

Working Hypothesis:

Investigation of end-tethered 750 MW PEO film evolution using neutron reflectometry may allow for a better understanding of how film characteristics (chain density, PEO volume fraction) affect protein adsorption: in particular addressing the question of the increase in protein adsorption at very high chain density and the layer properties that may account for the 'optimum' chain density for protein resistance.

Main Contributions:

1. Films formed under high solubility conditions had PEO volume fraction, film thickness and chain density of 0.33, 28 Å, and 0.56 chains/nm^2 respectively after 0.5 h of chemisorption and 0.31, 28.5 Å, 0.59 chains/nm^2 respectively after 11 h, suggesting that the layer is fully formed after 0.5 h.

2. For low solubility conditions, the corresponding values were 0.39, 34 Å, 0.99 chains/nm^2 after 0.5 h, 0.57, 37.4 Å, 1.32 chains/nm^2 after 4 h, and 0.57, 35.9 Å, 1.17 chains/nm^2 after 11 h.

3. The data suggest that at high chain densities there may be regions within the PEO film where the effective concentration is above the solubility limit of PEO in aqueous solution. It is hypothesized that in these regions the polymer has been "forced" from solution forming hydrophobic patches that facilitate increased protein adsorption.

Abstract

Chain density, chain length and chain conformation are considered important for the anti-biofouling properties (protein and cell resistance) of end-tethered polyethylene oxide (PEO) layers. Previous experiments (Unsworth et al, Langmuir, 21 (2005) 1036) investigated PEO layers formed by chemisorption of thiol-PEO on gold. It was shown that, as a function of surface chain density, protein adsorption decreased, passed through a minimum, and increased again at higher chain density. In the follow-on work reported here, neutron reflectometry (NR) was used to investigate, *in situ*, the properties of such PEO layers (volume fraction and chain density) for the purpose of gaining further insight into their interactions with proteins. Chain density was varied by varying solubility conditions (far from and near the cloud point) and chemisorption time. Neutron experiments were carried out at the NRU (Chalk River, Ontario) using neutrons of de Broglie wavelength 2.37 Å. Contrast matching techniques were used to improve sensitivity. Layers formed under high solubility conditions were found to have PEO volume fraction, layer thickness and chain density of 0.33, 28 Å, and 0.56 chains/nm^2 respectively after 0.5 h chemisorption; and 0.31, 28.5 Å, and 0.59 chains/nm^2 respectively after 11 h, suggesting that the layer is fully formed within 0.5 h. For low solubility conditions, PEO volume fraction, layer thickness and chain density were 0.39, 34 Å, and 0.99 chains/nm^2 after 0.5 h; 0.57, 37.4 Å, and 1.32 chains/nm^2 after 4 h; and 0.57, 35.9 Å, 1.17 chains/nm^2 after 11 h. Both chain density and PEO volume fraction in the chemisorbed layers were significantly greater when the layers were formed under low

solubility conditions. The PEO layers shown in our previous work (Unsworth et al, Langmuir, 21 (2005) 1036) to have maximum protein resistance were found to have a PEO volume fraction of ~ 40%. Moreover limiting volume fractions in the PEO films formed under low solubility conditions were ~57%, a value similar to the solubility limit of PEO in aqueous solution, suggesting that local regions in the layers may be phase separated. This may result in increased hydrophobicity and may explain why protein adsorption was found to increase on the layers of higher chain density.

Introduction

The use of poly(ethylene oxide) (PEO) to reduce protein interactions at the biomaterial-tissue interface has attracted much attention [1-5]. The mechanism of protein resistance of tethered PEO layers is not well understood but it is thought that chain density, chain length, chain conformation and hydration state are significant factors [5-8]. Thus through systematic investigation of these variables, knowledge of the protein repulsion mechanism of PEO layers should be improved, and the design of non-fouling surfaces should be facilitated. Few studies have been aimed at elucidating the effects of chain density on protein adsorption. Also, while it has been suggested that definition of the layer at the molecular level is crucial to the understanding of protein resistance [9, 10], information of this nature is lacking.

As discussed elsewhere [11, 12], when the tethered polymer chain density is such that neighbouring chains begin to interact (graft spacing less than twice the Flory radius, R_F: i.e. the "brush" regime) the chains are constrained to stretch normal to the interface.

Thus, tethered polymer conformation, layer thickness and solvation state are strongly dependent on chain density. The Flory radius ($R_F = a N^{\nu}$) and the solvated layer thickness model (eq 1)

$$L = N a^{5/3} / s^{2/3} \quad (1)$$

can be used to describe grafted PEO conformation on a surface in contact with a solvent. Here a is the effective monomer length reported to be in the range of 2.78 Å (crystalline) to 4 Å (hydrated) [7, 13], N is the degree of polymerization, ν accounts for the effect of PEO solubility (with values of 1/2 under the theta condition and 3/5 under high solubility conditions), L is the solvated layer thickness in a good solvent and s is chain spacing [14]. A difficulty in using these equations to describe systems of similar PEO MW, but different chain density, is that it is not clear how the effective monomer length changes with chain density. Although one would expect the 'a' value to decrease with increasing chain density due to reduced hydration and excluded volume, the relationship between the two is unknown. In this work an 'a' value of 4 Å was used to describe all layers, whether formed under high or low solubility conditions.

To investigate the effect of tethered PEO chain density on protein resistance we have chosen a model system based on chemisorption of chain-end thiolated PEO (in aqueous solution) to gold [11, 15] Chain density is varied by varying both the solubility of PEO in the contacting aqueous medium, which affects the polymer dimensions, and the chemisorption time. The PEO solubility limit, or cloud point, can be manipulated by varying the solution temperature and ionic strength. In principle, manipulation of these variables should allow for the preparation of surfaces having chain densities over a broad

range. In previous work we measured layer thickness and chain density values for similar PEO layers using ellipsometry and neutron reflectometry [11]. In that work the layers were dried prior to measurement. In the work reported here the neutron measurements have been repeated for gold-PEO layers in the hydrated condition, ie the condition under which proteins would actually encounter the PEO layers.

In the earlier work on PEO of MW 750 we showed that as chain density increases protein adsorption passes through a minimum [15] at ~0.5 chains/nm^2. The "optimal" layer was formed by incubating for 0.5 h under conditions close to the cloud point. Additional motivation for the work reported here was to investigate possible differences in structure, as revealed by neutron reflectometry measurements *in situ*, between this optimal PEO layer and those of higher and lower chain density. The new information generated (hydration and kinetics of formation) provides new insight on the mechanism of the protein resistance of PEO modified surfaces.

Materials and Methods

α,ω methoxy hydroxy poly(ethylene oxide) (PEO) of MW 750 was purchased from Shearwater Polymers (Huntsville, AL) and used without further purification. Dimethyl formamide (DMF), mercaptoacetic acid, isopropyl ether, dichloromethane, deuterated chloroform (99.9% grade), hydrogen peroxide, ammonium hydroxide, toluene and potassium phosphate (mono and di basic) were purchased from Sigma-Aldrich (Oakville, ON) and used without further purification. Silicon wafers (2" diameter, 1 mm thick) treated to remove the native oxide layer, and coated with a chromium (400 Å)

adhesion layer followed by a platinum (200 Å) layer, to prevent chromium-gold mixing, and a gold (1000 Å) layer, were obtained from Thin Film Technology, Buellton, CA, and diced into 0.5 cm x 0.5 cm pieces. D_2O (Chalk River Labs, AECL) was used to prepare contrast matched solutions.

Chemisorption of PEO on Gold

The PEO was chain-end thiolated (replacement of hydroxyl group) by reaction with mercaptoacetic acid as described elsewhere [11]. The reaction was verified by proton NMR spectra taken in d-chloroform. The products were also characterized by gel permeation chromatography (Waters 600 system, DMF mobile phase, 80°C, 0.25% wt polymer solutions).

Gold-coated silicon wafers were immersed in a solution consisting of 1 part hydrogen peroxide, 1 part ammonium hydroxide, and 5 parts water at 80°C for 5 min, sonicated for 1 min and rinsed in Milli-Q water to remove any carbonaceous contamination. After cleaning, the wafer was mounted in a temperature controlled Lucite cell, with the gold coated surface exposed to the solution, as shown in Figure 1.

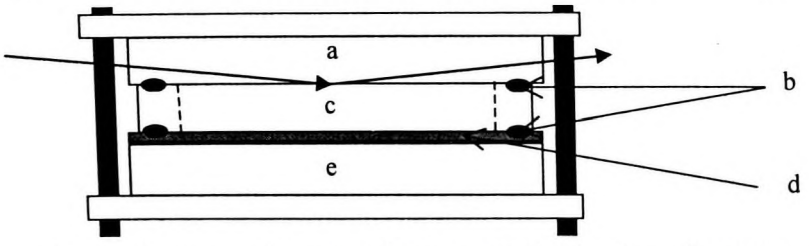

Figure 1. Experimental setup and neutron beam path for *in situ* reflectivity measurements. The assembly is clamped between two outer plates: (a) gold coated silicon wafer; (b) O-rings; (c) cylindrical lucite wet cell containg PEO solution; (d) thin silicon wafer acting as heat conductor ; (e) copper block with embedded heater and thermocouple.

The cell was first filled with contrast matched water (CMW) and a neutron reflectometry scan performed (see below for details) to characterize the unmodified gold surface. The use of CMW increases measurement sensitivity through isotopic matching of the scattering length density (SLD) of the solution to that of the gold substrate using a D_2O:H_2O mixture (CMW) [16]. Under these conditions the presence of small amounts of adsorbate at the interface can more easily be detected. Chemisorption was then carried out by introducing solutions of PEO and incubating for various times (0.5, 4 and 11 h). Solution conditions were varied as a means of manipulating PEO chain density, with higher PEO densities expected as conditions approach the cloud point [1,2]. Two sets of conditions were investigated, *viz*, "high solubility" (0.05 M phosphate buffer prepared with H_2O, 25°C), and "low solubility" near the cloud point (2.9 M phosphate buffer prepared with H_2O, 35°C). After the initial chemisorption period (0.5 h) the cell was flushed extensively with CMW and a neutron scan performed *in situ*, i.e. in the presence of CMW. The CMW was then replaced with PEO solution and chemisorption was continued. CMW flushing and neutron scanning were carried out at the end of each chemisorption period. The chemisorption times indicated represent total exposure time. The temperature in the cell was controlled by a built in heater/controller.

NR Experiment and Layer Profile Model

Neutron reflectometry measurements were performed on the C5 Spectrometer of the Dualspec facility at the NRU reactor (Chalk River), configured as a reflectometer. A pyrolitic graphite monochromator [(002) Bragg reflection] selected neutrons with de

Broglie wavelength λ = 2.37 Å as the incident beam. Collimation was controlled by a pair of motorized slits S1 and S2. Reflected intensity was measured as a function of scattering vector normal to the sample: $Q_z = 4\pi \sin(\theta)/\lambda$, where θ is the grazing incident angle, and 2θ is the angle between the incident beam and the specularly reflected beam. Normally, during a 2θ:θ scan, the incident-side slits S1 and S2 are adjusted in order to maintain a constant footprint of the beam on the sample. It was found, however, that such a strategy led to unacceptably high background scattering from the CMW, especially as the slits were opened wider for the high-Q_z measurements. Consequently, except for the lowest Q_z range ($Q_z < 0.01$), S2 was kept at a fixed width (for $0.011 < Q_z < 0.064$, and for $Q_z > 0.065$) and the width of S1 was varied in such a way as to progressively increase the flux on the sample at high Q_z. The scattered-side slits, S3 and S4, were also adjusted during the scans, but did not affect the instrument resolution since the opening was kept greater than the width of the specularly reflected beam. This method of varying the slits with Q_z gave an effective instrument resolution corresponding to $\Delta\lambda/\lambda$ = 2.5% and $\Delta\theta$ = 0.7 milli-radian (FWHM); these values were adopted for the analysis. No background correction was applied to the data, but a series of θ-rocking scans showed that the background was largely Q_z-independent. Its contribution to the absolute reflectivity, estimated at the level 1.0×10^{-5}, was included as a fixed parameter in the least-squares refinement.

To obtain absolute reflectivity, the incident neutron flux on the sample was measured. Subsequent to measuring reflected intensities, the detector was placed at 2θ = 0 and the sample cell shifted so that the neutron beam traversed the Si slab (see Figure 1).

A "scan" was then performed, varying the slits in exactly in the same manner as in the measurement of the reflected beam except that both θ and 2θ angles were kept at zero. Absolute reflectivity was obtained by dividing the measured intensity by the incident neutron flux.

The reflectivity data were analyzed using a layer profile model that was refined by least-squares fitting. The final result is a model representing the variation of scattering length density (SLD), ρb(z), with depth in the layer (ρ and b are the number density of atoms at depth z and their nuclear scattering-length respectively). Provided that the model is realistic and the neutron wavelength calibration is accurate, layer thicknesses determined by NR are highly reliable and free from *a priori* assumptions. In the present work, the least-squares fitting program MLAYER was used for the analysis [17]. The most general model needed to represent the samples consisted of layers for Si (incident medium), Cr, Pt, Au, PEO and CMW (final medium). For the metallic layers, we adopted the specified thicknesses as given by the manufacturer. The scattering length densities (SLD) for the bulk metals were used as the initial values for subsequent refinement. All interfaces were initially modeled as sharp and the roughnesses, modeled with a hyperbolic tangent function, were introduced gradually provided they led to a significantly better fit (with the understanding that it is better to limit unnecessary parameters in an already large parameter space). Moreover, models with extra layers incorporated to represent roughness of PEO interfacial regions were attempted, but it was found (results not shown) that they produce SLD profiles similar to those generated with the *tanh* function, without greatly reducing χ^2. Determining the best model was based on

a minimization of χ^2. In the case of similar χ^2 values for different models, the simplest model was taken as the final model.

Results and Discussion

Unmodified gold

Prior to chemisorption, several gold-coated wafers prepared in the same batch were characterized by taking neutron data with the cell dry, filled with CMW, or filled with pure D_2O. These measurements served as "controls" for analysis of the data obtained after chemisorption. While sample-to-sample variations were detected, the general trends as described in the following paragraph were clear.

The surface of a "blank" gold-coated wafer is not free of contamination. Evidence that contamination is present is that a significantly better least-squares fit is obtained if a layer with reduced SLD (i.e. lower than the SLD of Au or CMW) is introduced at the gold-CMW interface (Figure 2). This layer appears to be minimal, however, since: (1) it was not required (for the fit) when the samples were in contact with pure D_2O (results not shown), but only when the sensitivity of the measurements was increased using CMW; and (2) the best refinement of this system resulted in a relatively large χ^2 value of ~30, whereas all other models gave $\chi^2 < 10$. It is important to note that the large χ^2 value attests to the difficulty in generating an accurate model for this system using MLAYER. The model parameters (Table 1) used to generate the SLD profile for the gold control show that while the contamination layer thickness, 0.4 ± 0.2 Å, is not different from zero the interface roughness (188.1 ± 0.7 Å) is significant. Although these parameters for the

contamination layer do not seem meaningful, nonetheless they generate a credible SLD profile (Figure 2) for this system. Although the nature of the contaminant is not known it will be treated as carbonaceous (CC).

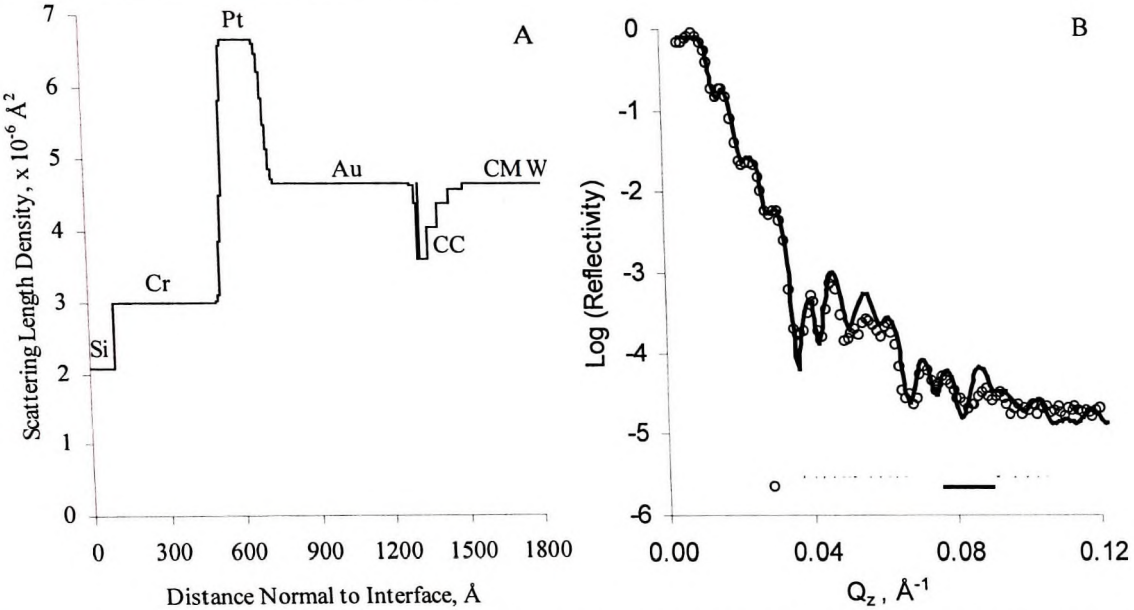

Figure 2. A. The SLD profile model obtained by neutron reflectivity for the unmodified gold substrate. The layer order is Si/Cr/Pt/Au/Carbonaceous Contamination (CC)/CMW from zero to high z values. Zero on the distance axis is 100 Å within the silicon. B. Neutron reflectivity profiles showing agreement between the observed (circles) and calculated (curve) values.

This control sample was used as the substrate for chemisorption of PEO under high solubility conditions and the values in Table 1 were used in the analysis of the PEO surfaces. The gold sample used for chemisorption experiments under low solubility conditions showed a similar contamination layer and SLD profile (data not shown). The rapid surface contamination of gold is a well known phenomenon; Troughton et al. [18] suggested that airborne hydrocarbons are mainly responsible. Based on the general observation that the structure of polymers chemisorbed on such a "not-so-clean" surface does not depend on the history of substrate handling, these authors concluded that the

contaminants are displaced by the thiolated adsorbate if the gold-adsorbate bond is sufficiently strong. There is evidence (see below) that such displacement occurs for the thiolated PEO used in the present work.

Table 1. Model parameters for the control surface and films formed under high solubility conditions after chemisorption times of 0.5 and 11 h, as illustrated in Figures 2 and 3. Errors given in parentheses are ± 1 s.d. (last digit of parameter value), and the parameters held constant during refinement are listed without errors.

Layer	Thickness (Å)			SLD × 10^{-6} (Å^{-2})			Interface width (Å)		
	Control	0.5 h	11 h	Control	0.5 h	11 h	Control	0.5 h	11 h
Si	∞	∞	∞	2.07	2.07	2.07			
							Sharp	Sharp	Sharp
Cr	431.9(2)	431.9	431.9	3.064(4)	3.064	3.064			
							21.9	21.9	21.9
Pt	174.9(2)	174.9	174.9	6.704(3)	6.704	6.704			
							33.4(3)	33.4	33.4
Au	608.8(2)	608.8	608.8	4.526(2)	4.526	4.526			
							18.0(5)	18.0(2)	18.0(2)
PEO/ CC	0.4(2)	28.7(3)	29.2(3)	2.032(8)	3.20(1)	3.26(1)			
							188.1(7)	0.7(4)	0.2(4)
CMW	∞	∞	∞	4.526(8)	4.526	4.526			

The thicknesses of the metallic layers of the substrate (Cr, Pt and Au) were found to be close to but not exactly as specified by the sample manufacturer. The discrepancies are most likely the result of differences in precision of the measurements. The refined SLD values for the metal layers differ by up to 5% compared to the values estimated using the densities of the crystalline materials, thus suggesting that the crystallinity of the metal films is not perfect. Given that these parameters were found to be relatively insensitive to conditions in the contacting fluid (e.g. CMW or D_2O) they were held constant in refinements of the data for the PEO layers.

PEO-modified surfaces

Representative least-squares fitted SLD profiles for the PEO-modified surfaces are shown in Figures 3 and 4 for PEO formed after 0.5 h incubation under high and low solubility solutions, respectively. However, model pararmeters for all systems studied are summarized in Tables 1 and 2. Figures 3B and 4B illustrates that the agreement between observed and calculated reflected intensities is excellent over the entire Q_z range (0.005 to 0.128 $Å^{-1}$), thus providing strong support for the refined NR models of the PEO modified surfaces.

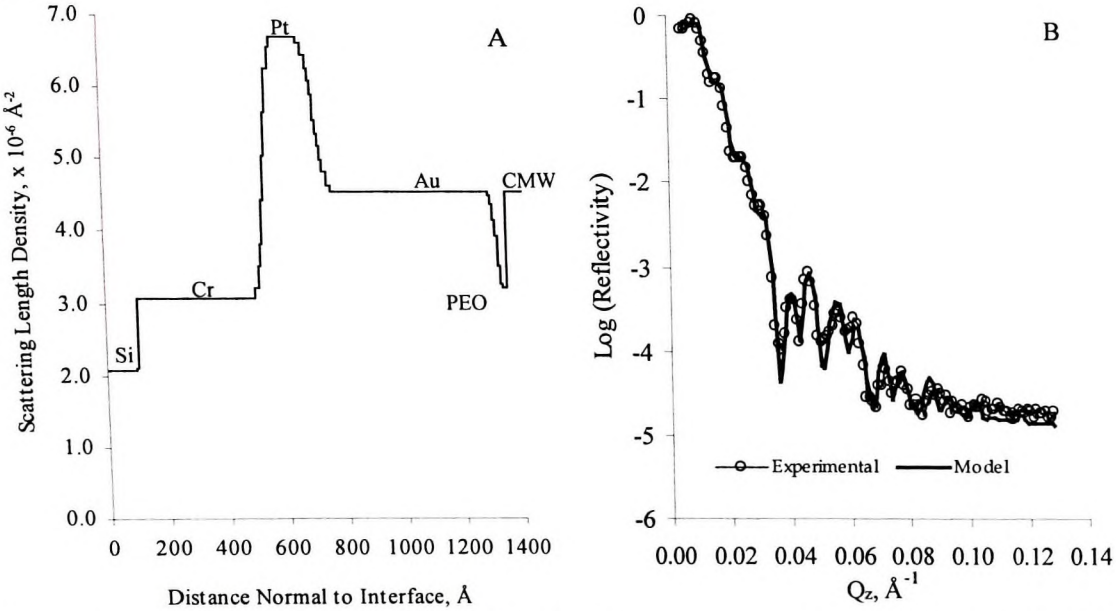

Figure 3. A. The SLD profile model obtained by neutron reflectivity for the 750 MW PEO layers formed under high solubility conditions for 0.5 h. The layer order is Si/Cr/Pt/Au/Carbonaceous Contamination (CC)/CMW from zero to high z values. Zero on the distance axis is 100 Å within the silicon. B. Neutron reflectivity profiles showing agreement between the observed (circles) and calculated (curve) values (χ^2=7.1).

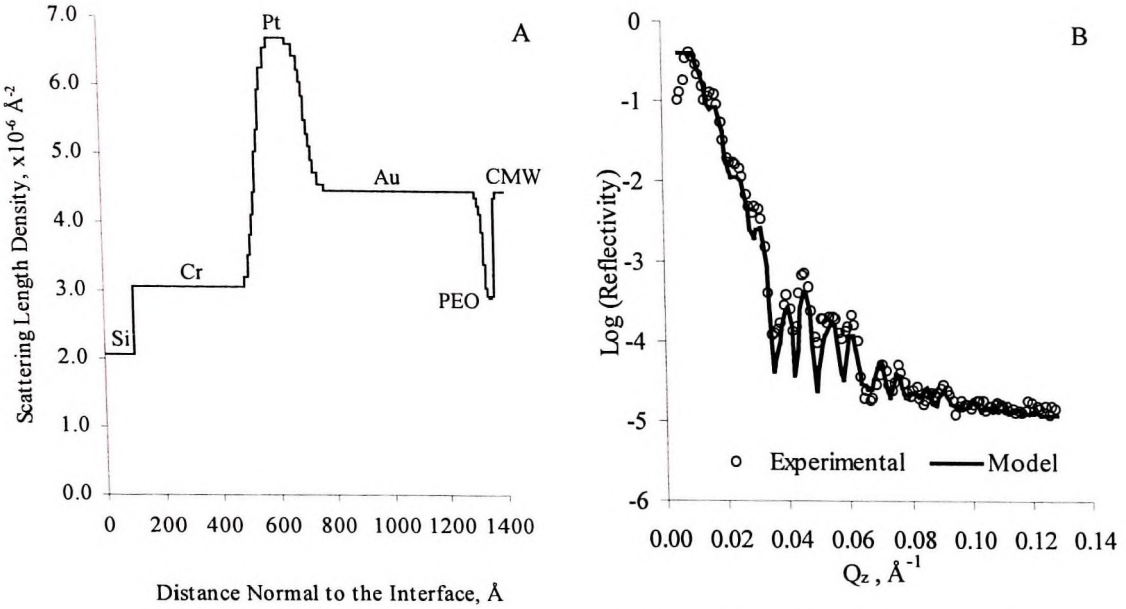

Figure 4. A. The SLD profile model obtained by neutron reflectivity for the 750 MW PEO layers formed under low solubility conditions for 0.5 h. The layer order is Si/Cr/Pt/Au/Carbonaceous Contamination (CC)/CMW from zero to high z values. Zero on the distance axis is 100 Å within the silicon. B. Neutron reflectivity profiles showing agreement between the observed (circles) and calculated (curve) values (χ^2=9.2).

TABLE 2. Model parameters for the films formed under low solubility conditions after chemisorption times of 0.5, 4 and 11 h, as illustrated in Figure 4. Errors given in parentheses are ± 1 s.d. (last digit of parameter value), and the parameters held constant during refinement are listed without errors.

Layer	Thickness (Å)			SLD × 10^{-6} (Å^{-2})			Interface width (Å)		
	0.5 h	4 h	11 h	0.5 h	4 h	11 h	0.5 h	4 h	11 h
Si	∞	∞	∞	2.07	2.07	2.07			
							Sharp	Sharp	Sharp
Cr	431.1(3)	431.1	431.1	3.064(3)	3.064	3.064			
							29.6(9)	29.6	29.6
Pt	172.8(2)	172.8	172.8	6.704(2)	6.704	6.704			
							37.4(3)	37.4	37.4
Au	622.0(2)	622.0	622.0	4.526(2)	4.526	4.526			
							18(1)	18.0(4)	18.0(5)
PEO/CC	34(2)	34.5(3)	32.8(2)	2.90(3)	2.13(2))	2.12(2)			
							3(7)	3(2)	2(1)
CMW	∞	∞	∞	4.526	4.526	4.526			

As indicated above the refinements leading to the data in Tables 1 and 2 were carried out with the parameters for the metal layers and the inner interfaces held constant

at the values obtained for the "clean" gold sample. The PEO layer parameters and the roughness of the gold-PEO interface were allowed to vary, even though the latter should in principle remain constant. However, the best fit always returned the same value of roughness thereby showing the validity of the model. The width of the gold/PEO interface in the refined models was 18 Å (within error) in all cases. This value is in agreement with the roughness of the gold surface as determined prior to chemisorption. While the thickness and SLD of the PEO layers varied depending on chemisorption conditions and time, the outer surface (PEO-aqueous interface) was surprisingly sharp in all cases. The general shape of the SLD profile of the PEO films (Figures 3 and 4) appears very different from that of the contamination layer (Figure 2) supporting the conclusion of Troughton et al. [18] that chemisorption is a "self-cleaning" process.

The "space" beyond the gold layer is occupied by either PEO or CMW which has the same SLD as gold, thus allowing determination of the volume fraction of PEO as a function of distance z from the gold-PEO interface. The volume fraction, $\phi_{PEO}[z]$, is given by:

$$\phi_{PEO}[z] = \frac{(\rho b)_{obs}[z] - (\rho b)_{Au,CMW}}{(\rho b)_{PEO} - (\rho b)_{Au,CMW}} \qquad (2)$$

where $(\rho b)_{obs}[z]$ is the experimentally observed SLD (Figures 3 and 4). $(\rho b)_{Au,CMW}$ was taken as 4.526×10^{-6} Å^{-2}, the value given by least-squares fitting; $(\rho b)_{PEO}$ was estimated as 0.56×10^{-6} Å^{-2} using a density of 1g/mL for the polymer.

The volume fraction profiles normal to the plane of the interface are shown in Figure 5 for the PEO layers formed under high solubility conditions. The data suggest

that the layers are fully formed after 0.5 h. The PEO volume fractions and effective PEO layer thicknesses (estimated from the height and FWHM of the profiles in Figure 5) for the 0.5 and 11 h layers were similar at 32% and 29 ± 3 Å. In experiments using the surface forces apparatus, Efremova et al. [14] observed thicknesses of 25 ± 5 Å for 750 MW PEO layers coupled to mica *via* a supported lipid bilayers, ie in good agreement with the values found in this work. For our high solubility conditions a value of effective monomer length a = 4 Å was used to calculate the chain densities, and values of ~ 0.56 and 0.59 chains/nm^2 were found for chemisorption times of 0.5 h and 11 h respectively, similar to a previously reported value of ~ 0.39 chains/nm^2 obtained using ellipsometry for 750 MW PEO layers formed after 4 h of chemisorption [11].

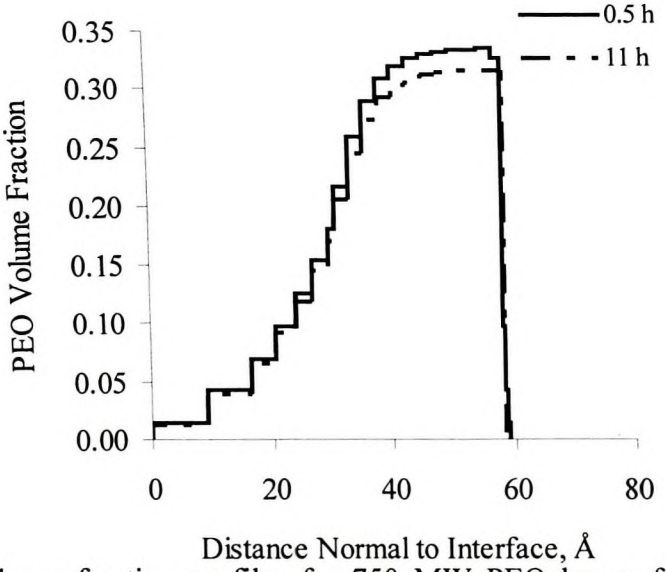

Figure 5. PEO volume fraction profiles for 750 MW PEO layers formed under high solubility conditions after 0.5 and 11 h chemisorption times. Zero on the x-axis is the gold-PEO interface.

As shown in Figure 6, layers formed under low solubility conditions require longer than 0.5 h to reach saturation; there is little change in PEO volume fraction (and probably in conformation) after 4 h. The volume fraction increases from 39% at 0.5 h to a limit of about 57% at longer chemisorption times. As expected, the volume fractions under low solubility conditions are greater than those under high solubility (maximum, 32%). The PEO layer thicknesses (FWHM) were determined to be 34 ± 2, 37.5 ± 3 and 35.8 ± 2 Å after 0.5, 4 and 11 h, respectively. Again, similar to these data, Efremova et al. [14] observed a maximum thickness of 31 ± 6 Å for 750 MW PEO layers in the brush regime. Given the FWHM layer thicknesses and an effective monomer length of 4 Å, the average chain density for the layers formed at 0.5, 4 and 11 h under low solubility conditions may be estimated as ~ 0.99, 1.32 and 1.17 chains/nm^2, respectively. These values for the hydrated layers are less than the previously reported value of 1.8 ± 0.9 chains/nm^2 (4 h chemisorption) determined for the dry layers using neutron reflectometry [11]. The "dry" and the "wet" NR chain density values appear to be similar, within error. Greater precision is expected for the *in situ* experiments as opposed to *ex situ* experiments, as previously discussed [11]: (1) there is a large error associated with NR measurements on thin (< 1 nm) dry PEO layers due to the low contrast between dry PEO and air; (2) the measured thickness of the dry-state 750 PEO layer was 10.0 ± 8.0 Å. This may be considered at the limit of the method since the ΔQ range needed to fully describe such a layer is 0.63 Å^{-1}, whereas the ΔQ captured for the *ex situ* work was only 0.1. The combination of these two difficulties, leads to high errors in the estimates of chain density in the dry state.

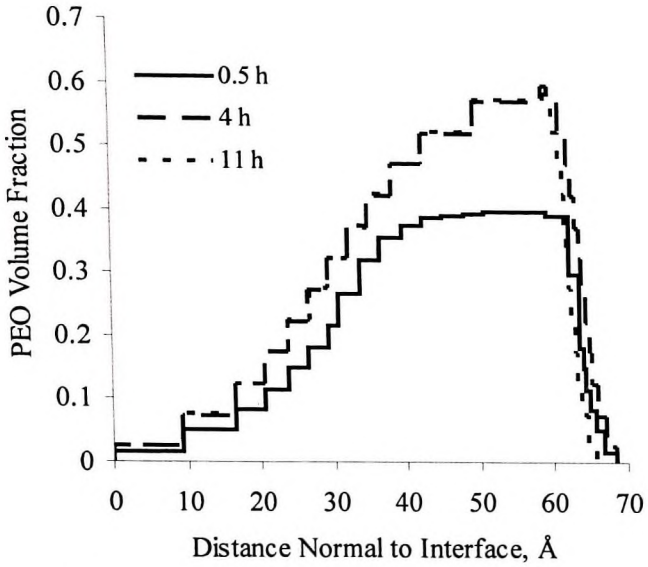

Figure 6. PEO volume fraction profiles for 750 MW PEO layers formed under low solubility conditions after 0.5, 4 and 11 h chemisorption times. Zero on the x-axis is the gold-PEO interface.

It should be pointed out for the *in situ* experiments that, although the PEO volume fraction for the films formed under low solubility increases by a factor of 1.5 from 0.5 to 4 h incubation time, the calculated chain densities remain relatively the same. This may be due to the fact that the effective monomer length is held constant in the calculations whereas it probably decreases with increasing chain density, so that chain densities in the high range may be underestimated.

Of interest is the upper limit on PEO volume fraction of ~57% for layers formed under low solubility conditions. It is interesting to note that the solubility limit for PEO in water is ~60% (v/v); at higher concentrations the polymer begins to precipitate [19]. The similarity between these values suggests the possibility that as the layer increases in density, a phenomenon akin to precipitation involving extensive chain-chain interactions,

begins to occur. If the entire layer phase separated a sharp decrease in overall PEO layer thickness, as a direct result of dehydration due to increased hydrophobic interactions, would be expected, a result that was not observed (Figure 6). Nonetheless it seems likely that at ~60% volume fraction, the layer is, on average, approaching the PEO solubility limit and may begin to develop local regions where the solubility limit is exceeded such that regional phase separation may occur. This would imply that the PEO layer is heterogeneous with a spatial distribution of densities, and that the mechanism for precipitation of PEO in aqueous solution is similar to that for the interactions of end-tethered chains at high concentration. Given that the neutron reflectometry data are averages over the entire beam footprint it is not unreasonable to suggest that local heterogeneity exists. Although the mechanism of precipitation of PEO in solution is not fully defined, it is thought that it arises from the loss of the hydration shell and the subsequent increase in hydrophobic interactions (both inter- and intra-molecular) between polymer moieties [20]. It does not seem likely that tethering at the solid-liquid interface would interfere fundamentally with this mechanism. If regions of phase separated PEO are indeed formed at high chain density, resulting in the presence of hydrophobic patches within the PEO layer, then this may explain why protein resistance at high chain densities begins to decrease as observed previously [15].

An interesting feature of the volume fraction profiles is the sharpness of the PEO-CMW interface. It would be expected that the roughness of the underlying gold would be replicated through the fairly thin PEO layer and would be evident at the PEO-CMW interface. The fact that this is not the case for any of the systems studied is surprising.

The most likely reason is a Q-dependent signal attenuation leading to over-estimation of reflectivity at high Q. This, in turn, would cause the interface roughness parameter to converge to an unrealistically small value in the least-squares refinement.

In previous work [15] we showed that for low solubility conditions, fibrinogen adsorption is greater on the 4-h layer than on the 0.5-h layer. The present NR investigation of these layers shows that the PEO volume fractions were 0.39 and 0.57, respectively, suggesting that there is an optimal PEO volume fraction for protein resistance (possibly of the order of 0.4). The data also suggest that the observed increase in adsorption at higher chain density may be due not only to reduced PEO mobility, but also to the formation of hydrophobic patches which form as the effective PEO concentration in the layer exceeds the solubility limit.

Acknowledgements

Financial support by the Natural Sciences and Engineering Research Council of Canada (NSERC) and the Canadian Institutes of Health Research (CIHR) is gratefully acknowledged.

References

1 Kingshott, P., Griesser, H.J., 'Surfaces that resist bioadhesion.' *Curr Opinion Solid State Mater. Sci.* **4**, 403 (1999).

2 Kingshott, P., Thissen, H., Griesser, H.J., 'Effects of cloud-point grafting, chain length, and density of PEG layers on competitive adsorption of ocular proteins.' *Biomaterials,* **23,** 2043 (2002).

3 Brash, J.L., 'Exploiting the current paradigm of blood-material interactions for the rational design of blood-compatible materials.' *J. Biomater. Sci. Polymer Ed.,* **11**, 1135 (2000).

4 Harris, J.M. "Introduction to Biotechnical and Biomedical Applications of Poly(ethylene glycol)," In Poly(ethylene glycol) Chemistry: Biotechnical and Biomedical Applications; Harris, J.M., Ed.; Plenum Press: New York, 1992: pp. 1-14.

5 Tosatti, S.; De Paul, S.M.; Askendal, A.; Vandevondele, S.; Hubbell, J.A.; Tengvall, P.; Textor, M., '*Peptide functionalized poly(L-lysine)-g-poly(ethylene glycol) on titanium: resistance to protein adsorption in full heparinized human blood plasma.*' *Biomaterials*, **24**, 4949 (2003).

6 Morra, M., 'On the molecular basis of fouling resistance.' *J.Biomater.Sci.Polymer Edn.* **11**, 547 (2000).

7 Malmsten, M., Emoto, K., van Alstine, J.M., 'Effect of chain density on inhibition of protein adsorption by poly (ethylene glycol) based coatings' *J. Coll. Interfacial Sci.,* **202,** 507 (1998).

8 Szleifer, I., 'Protein adsorption on surfaces with grafted polymers: a theoretical approach.' *Biophys. J.,* **72**, 595 (1997).

9 Ostuni, E., Grzybowski, B.A., Mrksich, M., Roberts, C.S., Whitesides, G.M., 'Adsorption of proteins to hydrophobic sites on mixed self-assembled monolayers.' *Langmuir* **19**, 1861 (2003).

10 Vogler, E.A., 'Water and the acute biological response to surfaces.' *J. Biomater. Sci. Polymer Ed.,* 10, 1015 (1999).

11 Unsworth, L.D., Tun, Z., Sheardown, H., Brash, J.L., 'Chemisorption of thiolated poly(ethylene oxide) to gold: surface chain densities measured by ellipsometry and neutron reflectometry.' *J. Colloid Interface Sci.,* **281**, 112 (2005).

12 Alexander, S., 'Adsorption of chain molecules with a polar head a scaling description.' *J. de Physique,* **38**, 983 (1977).

13 Anne, A., Demaille, C., Moiroux, J., 'Terminal Attachment of Polyethylene Glycol (PEG) Chains to a Gold Electrode Surface. Cyclic Voltammetry Applied to the Quantitative Characterization of the Flexibility of the Attached PEG Chains and of Their Penetration by Mobile PEG Chains.' *Macromolecules,* **35**, 5578 (2002).

14 Efremova, N.V., Sheth, S.R., Leckband, D., 'Protein-Induced Changes in Poly(ethylene glycol) Brushes: Molecular Weight and Temperature Dependence.' *Langmuir*, **17**, 7628 (2001).

15 Unsworth, L.D., Sheardown, H., Brash, J.L., 'Protein resistance of surfaces prepared by sorption of end-thiolated poly(ethylene glycol) to gold: effect of surface chain density.' *Langmuir*, **3**, 1036 (2005).

16 Lu, J.R., Li, Z.X., Smallwood, J., Thomas, R.K., Penfold, J., 'Detailed Structure of the Hydrocarbon Chain in a Surfactant Monolayer at the Air/Water Interface: Neutron Reflection from Hexadecyltrimethylammonium Bromide.' *J.Phys.Chem.*, **99**, 8233 (1995).

17 Ankner, J. F., Majkrzak, C. F., *Proceedings of the Society of Photo-Optical Instrumentation Engineers,* **1738**, 260 (1988).

18 Troughton, E.B., Bain, C.D., Whitesides, G.M., Nuzzo, R.G., Allara, D.L., Porter, M.D., 'Monolayer films prepared by the spontaneous self-assembly of symmetrical and unsymmetrical dialkyl sulfides from solution onto gold substrates-structur, properties, and reactivity of constituent functional groups.' *Langmuir*, **4**, 365 (1988).

19 van Oss, C.J., Interfacial Forces in Aqueous Media. Marcel Dekker, Inc., New York, New York, 2003.

20 Dormidontova, E.E., 'Role of Competitive PEO–Water and Water–Water Hydrogen Bonding in Aqueous Solution PEO Behavior.' *Macromolecules*, **35**, 987 (2002).

11.0 SUMMARY AND CONCLUSIONS

To investigate the effect of the surface chain density of PEO on protein adsorption, model surfaces comprising end-tethered PEO were prepared and characterized. Thiolated PEO was surface-tethered by chemisorption to gold-coated silicon wafers. Since PEO exhibits unique inverse temperature dependence of solubility in water, such that at higher temperatures and/or higher solution ionic strength solubility decreases and precipitation occurs (cloud point), it was possible to vary graft density by manipulation of both temperature/ionic strength and chemisorption time. Therefore, solution conditions were designed for various PEO species (600-OH, 750-OCH_3, 2000-OCH_3 and 5000-OCH_3) such that PEO solubility was close to, or far from, cloud point conditions.

The chemisorbed PEO layers were characterized using water contact angles, XPS, ellipsometry and neutron reflectometry. Ellipsometry and neutron reflectometry techniques were employed for the specific purpose of determining film properties (chain density, film thickness, PEO volume fraction) with high precision for correlation to protein adsorption data. The objective was to elucidate the mechanistic role of PEO chain density in the inhibition of protein adsorption. Since lysozyme and fibrinogen are of widely different size, are expected to have different "footprints" when adsorbed on a surface, and to have different ability to penetrate a given PEO layer, they were used to probe further the mechanism of protein resistance of the PEO films.

Western blot analysis was used to determine qualitatively the relative amounts and types of proteins adsorbed to the PEO-modified surfaces in contact with plasma.

Quantitative measurements of fibrinogen adsorption from plasma using radiolabeled protein were used to evaluate the effectiveness of the PEO layers in inhibiting the transient adsorption of fibrinogen (Vroman effect).

The chemisorption of thiolated PEO to gold coated silicon under different solution conditions proved an effective method of producing surfaces with variable chain density. The chain densities obtained were not only among the highest reported for these systems, but also the achievable chain density ranges were wide for all PEO molecular weights studied. Determination of PEO chain density from ellipsometry data obtained *in situ* involves fewer assumptions than from data obtained after drying (*ex situ*), and was found to be a more reliable procedure. Chain densities determined by neutron reflectometry and ellipsometry generally agreed within experimental error.

Neutron reflectometry studies yielded novel information about the structure of layers formed by 750 MW PEO under high and low solubility conditions. PEO volume fraction, film thickness and chain density were 0.33, 28 Å, and 0.56 chains/nm^2 respectively after 0.5 h of chemisorption, and 0.31, 28.5 Å, 0.59 chains/nm^2 respectively after 11 h, suggesting that layer formation is complete after 0.5 h for films formed under high solubility conditions. For low solubility conditions, the corresponding values were 0.39, 34 Å, and 0.99 chains/nm^2 after 0.5 h; 0.57, 37.4 Å, and 1.32 chains/nm^2 after 4 h; and 0.57, 35.9 Å, and 1.17 chains/nm^2 after 11 h. These data suggest that at high chain densities there may be regions within the PEO film that are effectively at concentrations above the solubility limit of PEO in aqueous solution, and are thus "forced" out of solution forming hydrophobic patches that facilitate increased protein adsorption.

Initial single protein adsorption experiments showed that resistance to fibrinogen passed through a maximum as chain density increased and that at a common chain density of ~0.5 chains/nm^2 protein adsorption was equally suppressed (80% decrease in adsorption compared to unmodified gold) for both 750 and 2000 MW PEO layers. The PEO-modified surfaces were also found to be resistant to lysozyme adsorption with fractional reductions similar to, if somewhat less than, those for fibrinogen. Further study of single protein adsorption using *in situ* ellipsometry showed trends similar to those observed using radiolabeled proteins. Thus minima in the adsorption of fibrinogen and lysozyme on the 750 and 2000 MW surfaces were of a similar magnitude and occurred at similar chain densities.

The observed trends in fibrinogen and lysozyme adsorption suggest that chain density, not molecular weight, is the major determinant of protein resistance. Furthermore, at chain densities of about 0.5 chains/nm^2 protein resistance seems to be independent of protein size. It is suggested that at high chain density, the chemisorbed PEO becomes dehydrated yielding a surface that is less protein resistant: a conclusion that is substantiated by neutron reflectometry data.

Adsorption of fibrinogen from plasma was investigated on surfaces determined to be 'optimal' in reducing adsorption in single protein systems. PEO layers formed from solutions near the cloud point adsorbed the lowest amount. Layers of 600-OH MW PEO showed almost complete suppression (versus controls) of the Vroman peak. Respective Vroman peak amounts for 600-OH, 750-OCH_3 and 2000-OCH_3 were 20 ± 1, 70 ± 20, 50 ± 3 ng/cm^2. Amounts adsorbed at higher plasma concentration were, respectively, 6.7 ±

0.6, 16 ± 9 and 12 ± 3 ng/cm^2. Fibrinogen adsorption from plasma was not significantly different for surfaces prepared with PEO of molecular weight 750 and 2000 when the chain density was the same (~0.5 chains/nm^2) supporting the conclusion that chain density may be the key property for suppression of protein adsorption. Furthermore, it was found that at a chain density of ~0.5 chains/nm^2, layers of PEO with terminal hydroxyl groups adsorbed less fibrinogen than those with terminal methoxy groups, suggesting that the "hydroxyl" surface inhibits fibrinogen and/or facilitates its displacement more effectively than the "methoxy" surface.

SDS-PAGE and immunoblotting were used to identify proteins eluted from these surfaces after plasma contact and showed that a number of proteins were adsorbed, including fibrinogen, albumin, C3 and apolipoprotein A-I. However, the blot responses were zero or weak for all four proteins of the contact system; some complement activation was observed on all of the surfaces studied.

The careful determination of PEO layer properties and corresponding protein adsorption behaviour as carried out in this research leads to the conclusion that chain density is *the* most important property of tethered PEO layers for inhibition of non-specific protein adsorption.

12.0 RECOMMENDATIONS FOR FUTURE WORK

Although gold coated silicon is an appropriate choice as a model surface for investigation of PEO chain density effects on protein adsorption, the surfaces used in this work were not optimal, in particular with respect to roughness at the gold-air interface. This is particularly important when using surface analysis techniques such as neutron reflectometry where nanometer scale substrate roughness increases the difficulty of interpreting the data. This situation could be improved by depositing thinner gold layers directly on polished Si wafers. Moreover, while the investigation of PEO modified surfaces using neutron reflectometry is amenable to nanometer level resolution of film properties in the z-dimension, this requires careful experimental setup and sophisticated equipment.

From this work it seems apparent that to further elucidate the mechanisms involved in PEO-mediated protein repulsion it will be necessary to determine the film structure, including hydration, at the nanometer scale. To obtain this information, experiments will have to be carefully designed, possibly using surface sensitive techniques such as neutron reflectometry, spectroscopic ellipsometry and TOF-SIMS. Future work should focus on understanding the hydration state of the PEO layer as it is formed (*in situ*) and as protein adsorption/repulsion occurs. Also, it would be interesting to evaluate the evolution of the hydration state of the protein (including orientation of bound water) during adsorption to the PEO layer. Efforts to determine the surface force profiles during layer formation and during the adsorption of selected peptides and

proteins using the surface force apparatus (or a modified AFM) would also be valuable in understanding protein-PEO repulsion mechanisms.

Finally much more work remains to be done to investigate and understand the behaviour of PEO-modified surfaces in complex biological systems like blood. The present work represents only a beginning in this regard.

APPENDIX A: EXPERIMENTAL PROCEDURES

In this work, gold coated silicon wafers were modified by chemisorption of thiolated PEO. To determine whether the solubility properties of PEO affect its interaction with the gold substrate, the adsorption of 750, 2000 and 5000 MW PEO was carried out under various solubility regimes. Herein, the protocols for all experimental procedures are detailed.

A.1 THIOLIZATION REACTION

Thiolization of the PEO was carried out by reaction of HO-PEO-OMe with mercaptoacetic acid in toluene at 80°C for 3 hours (Figure A-1). Mercaptoacetic acid was stored at 4°C. Poly(ethylene glycol) methyl ether (HO-PEO-OMe) with molecular weights of 750, 2000 and 5000 was stored in a sealed container under ambient conditions. 25 mL of toluene was preheated in a round bottom flask, with a magnetic stir rod. 5 g of the appropriate PEO, a drop of sulfuric acid, and a stoichiometric amount (1:1, OH:COOH) mercaptoacetic acid were added dropwise. A condenser water trap was used to drive the reaction forward by removing the evolved water. The solution was precipitated into 300 mL of isopropyl ether, and vacuum filtered. The precipitate was further purified by redissolving in dichloromethane and reprecipitated in isopropyl ether three times. Once purified, the reaction product was dried under vacuum at room temperature for two days. Proton NMR in deuterated chloroform with a drop of tetramethylsilane (TMS) as internal standard was used to characterize the reactants and the resulting products.

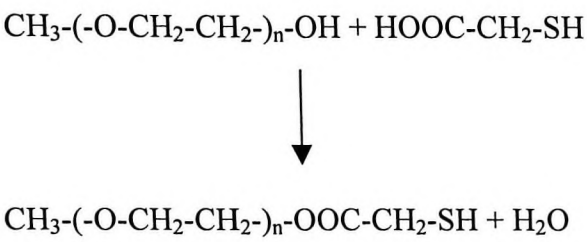

Figure A-1. Thiolization reaction mechanism.

A.2 GOLD COATING OF SILICON WAFERS

Gold layers, 1000~2000 Å thick, were thermally deposited on both sides of double polished, p doped, silicon wafers with the aid of a chromium/titanium adhesion layer ~500 Å thick by Koral Labs (Flint, Michigan). The product was tape tested on both sides to verify adhesion of the gold substrate. The wafers were then scored into 0.5 cm^2 samples, and stored in a sealed container.

A.3 IN SITU ELLIPSOMETRY SAMPLE CALCULATIONS

Sample calculations for the adsorption of protein are discussed herein; a similar procedure is followed for the adsorption of any molecule. As discussed in section 5.3 after PEO modification and prior to protein adsorption, polarizer (P) and analyzer (A) angles were obtained every 5 s for >30 min (incidence angle of 70°) for substrates in 19 mL of PBS. Protein (1 mL, 10 mg/mL) was introduced such that the final protein concentration was 0.5 mg/mL and mixed thoroughly. Adsorption data (P and A) were collected at an incidence angle of 70° every 5 secs for greater than 3 h, yielding a P vs. A plot as illustrated in Figure A-2.

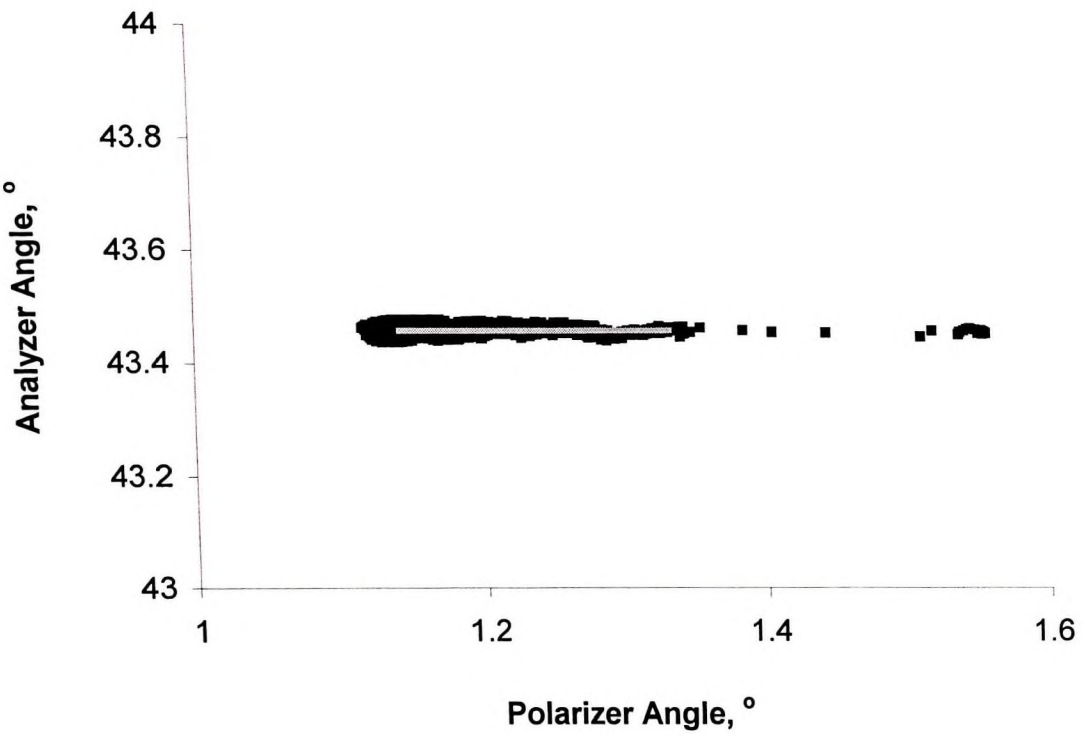

Figure A-2. Representative lysozyme adsorption plot of polarizer angle and analyzer angle as a function of time. Line represents modeled layer of adsorbed lysozyme.

From this dataset, it is obvious that as time progressed the polarizer angle decreases from around 1.38 to 1.12°. Using a protein film refractive index of 1.37 it was possible to construct a layer model, as outlined in Table A-1 and summarized by the line in Figure A-2.

Table A-1: Summary of model used to evaluate the layer properties of adsorbed lysozyme. The incident angle was 70°.

	n	k	Thickness, A
Ambient	1.33	0.0	
Lysozyme layer	1.37	0.0	40
Substrate	0.2	3.37	

Using equation 5-5, and refractive index increment of 0.188 cm^3/g, it is possible to calculate an adsorbed lysozyme amount of 0.085 $\mu g/cm^2$.

A.4 PROTEIN LABELING

Protein adsorption experiments were carried out using phosphate buffered saline spiked with NaI (PBS-NaI) at a pH of 7.4 and an NaI concentration of 5 mol%. Fibrinogen was labeled with ^{125}I using the ICl method. The ICl methods uses three vials: Vial 1 - 60 μL glycine buffer and 5 μL fresh ^{125}I; Vial 2 - 1.0 μL ICl; Vial 3 - 0.2 mL glycine buffer and 1 mg fibrinogen. Vials 1 and 2 were mixed with a pipette for one minute and then the mixture was transferred to vial 3, and mixing continued for two minutes. It was found that bubble formation during mixing increases the percent free iodide or the amount of unbound radioactive iodide in the preparation. Reduction of the free radioactive iodide level to below 1% is crucial as the unbound ^{125}I has a high affinity for gold. Clearly the uptake of free ^{125}I results in overestimates of adsorbed fibrinogen. Free iodide was removed by dialysis (SLIDALYZER® cassette) for 3 h at 25°C, and 16 h at 4°C, against PBS-NaI, with two changes of dialysate. The solution was removed from

the dialysis cassette, and the cassette was rinsed twice with 0.4 mL of PBS-NaI. Free iodide present in the labeled protein solution was measured by TCA precipitation of the protein. In all experiments, the free iodide content was between 0.4 and 0.6%. Cold NaI was added to the buffer to minimize uptake of free radioiodide by the surface.

The working solutions containing 1% labeled Fg were diluted with PBS-NaI to give total Fg concentrations of 1, 0.5, 0.3, 0.1 and 0.001 mg/mL. Modified gold surfaces (in triplicate) were incubated in 250 μL solution at each concentration for 3 h at room temperature. The samples were dip rinsed in 250 μL of PBS-NaI three times for 10 min each time. The radioactivity for each sample was determined using a gamma counter and the amount of adsorbed fibrinogen (μg/cm^2) was determined using the following equation,

$$Fg = \frac{(CPM_{total} - CPM_{background}) * [Fg]_A}{A_t * CPM_{solution}} \quad \textbf{(A-1)}$$

where CPM is the counts per minute in total less the background, $[Fg]_A$ is the fibrinogen concentration, and A_t is the total surface area of the sample.

A.5 SDS-PAGE AND WESTERN BLOT PROCEDURE

Polyacrylamide gel preparation (12% separating gel, 4% stacking gel)

The acrylamide/bis solution is prepared by dissolving the following reagents in distilled water, diluting to 100 mL and filtering the final solution:

Acrylamide/Bis	29.2 g
N,N'-Methylenebisacrylamide	0.8 g

The reagents for the 12 % separating gel were mixed and degassed for 15 min at room temperature:

12% SeparatingGel:

Distilled water	3.35 mL
1.5M Tris-HCl, pH 8.8	2.5 mL
10% (w/v) SDS stock (room temp)	0.1 mL
30% (w/v) Acrylamide/Bis	4 mL

Immediately prior to casting the gel, the following reagents are added to initiate polymerization in the above mixture:

10 % ammonium persulfate (fresh)	50 μL
TEMED	5 μL

Casting plates were cleaned with distilled water and ethanol (95%), dried and inserted into the casting assembly. The assembly was secured to the casting stand. The gel plates were filled using a syringe with polymer solution, leaving enough space to add stacking gel later. After 2 min a small amount of water was layered over the gel. Allow the separating gel to polymerize for 1 hour before adding stacking gel.

The reagents for the 4% stacking gel were mixed and degassed for 15 min at room temperature:

Distilled water	3 mL
0.5M Tris-HCl, pH 6.8	1.2 mL
10% (w/v) SDS stock (room temp)	100 μL
Acrylamide/Bis (30% stock)	0.65 mL

Immediately prior to casting the gel, the following reagents are added to initiate polymerization in the above mixture:

10 % ammonium persulfate (fresh)	25 μL
TEMED	5 μL

Using a syringe, the remainder of gel plates was filled with stacking (4%) polymer solution. The appropriate comb was added and the gel was allowed to polymerize for 1 hour before use.

Sample Preparation

The sample buffer used in sample preparation consists of the following reagents, mixed and stored at 4°C in 225μL aliquots:

Distilled water	4 mL
0.5M Tris HCl, pH 6.8	1.0 mL

Glycerol	0.8 mL
10 % (w/v) SDS	1.6 mL

Immediately prior to use, the following reagents were added to an aliquot, yielding tracking dye (TD):

2-Mercaptoethanol	30 µL
0.05% (w/v) Bromphenol blue	30 µL

Samples and standards used for SDS-PAGE only are prepared as follows:

0.5µL SDS-PAGE MW Standards, Low Range, 10µL TD
10 µL Protein sample, 10µL
7.5 µL Prestained SDS-PAGE Standards, Low Range

Samples and standards used for immunobloting are prepared as follows:

1µL SDS-PAGE MW Standards, Low Range, 10µL TD
80-150 µL Protein sample, 10 µL TD
7.5 µL Prestained SDS-PAGE standards, Low Range

Once mixed, the samples are placed in a 95oC water bath for 7.5 min.

Electrophoresis

Gently remove combs and rinse wells with distilled water. Remove gels from casting stand, and place into clamp assembly. Place clamp assembly into buffer chamber. A 5X stock solution of electrophoresis buffer was prepared by mixing the following reagents in distilled water and diluting to 1L (Note: pH of this solution should be 8.3 +/- 0.3, do not adjust with NaOH or HCl).

Tris Base	15 g
Glycine	72 g
SDS	5 g

Just before use dilute to 1X strength. Fill upper buffer chamber to 3 mm below outer long glass plate with electrophoresis buffer. Fill lower buffer chamber until 1 cm of gel is covered with electrophoresis buffer. Add samples onto gels. Operate power pack at 200 volts for approximately 45 min of electrophoresis. Layer a small quantity of Pyronin Y dye (in sample buffer) into wells just before the tracking dye (TD) reaches the bottom of the separating gel. Continue the electrophoresis until the Pyronin dye has just reached the top of the separating gel.

Gel Equilibration

Transfer buffer was prepared by mixing the following reagents in distilled water and diluting to 1L (Note: pH of this solution should be 8.3 +/- 0.3, do not adjust with NaOH or HCl).

3.03 g Tris
14.4 g glycine
200 mL methonal

Gels were equilibrated in fresh, cold transfer buffer for 15-20 minutes upon removal from assembly.

Electrophoretic Transfer

Immobilon PVDF transfer membrane were cut to gel-size, prewetted in methanol (1-3 s), water (1-2 minutes) and soaked in transfer buffer (15 min). The gels and membranes were loaded in the transfer cassettes according to specifications and placed in the transfer chamber. The chamber was then filled with transfer buffer so that the entire gel surface was covered. A potential difference of 100V (200mA) was applied for 1 h.

The membranes can then immediately be stained with colloidal gold or dried and used for immunoblot analysis.

Gold Staining

The PVDF membranes were washed 2X's in phosphate buffered saline (PBS), pH 7.4. PBS was prepared by mixing the following reagents in distilled water, adjusting the pH to 7.4 and diluting to 1 L:

Na_2HPO_4	1.32 g
NaH_2PO_4-H_2O	0.342 g
NaCl	8.5 g

The membranes were then incubated in 0.3% (v/v) Tween 20 solution in PBS for 1 h at 20°C to block unbound membrane sites. This was followed by 3 further washings of 5 min with this blocking solution. The membranes were then rinsed in water 3 times for 1 min each.

Western Blotting

Molecular Weight Determination: Remove marker lanes and small portion of sample lane (which covers the remainder of the blot) to be stained with the gold stained procedure described above.
Block Unbound Membrane Sites: Cut remainder of blot into 3 mm wide strips. Wet strips with 100% methanol, rinse with distilled water, and place into plastic wells. Block unbound membrane sites and prevent non-specific adsorption by incubating the strips for 1h, with gentle agitation, in 5% w/v nonfat dry milk in TBS, pH 7.4. This procedure blocks the areas of the membrane devoid of bound proteins so that nonspecific binding of antibodies to these areas will not occur. Wash strips 3 times for 5 minutes in 0.1% (w/v) nonfat dry milk in TBS.

Incubate with primary antibody: Incubate for 1h in 1 mL 1% (w/v) nonfat dry milk, 0.05% (v/v) Tween 20 in TBS containing the first antibody to the protein of interest. We typically use a 1/1000 titre for the majority of first antisera. Strips were then rinsed 3X's for 5 min each in 0.1% (w/v) nonfat dry milk in TBS.

Incubate with second antibody: Incubate strips for 1h in 1% (w/v) dry skim milk in TBS and 0.05% (v/v) Tween 20 in TBS with a 1/1000 dilution of the with the alkaline phosphatase conjugate secondary antibody. Strips were again rinsed 3X's for 5 min each in 0.1% (w/v) nonfat dry milk in TBS.

Detection: The strips were incubated for up to 4 h with a solution to develop the colour reaction for the detection of the bands. The buffer for this solution is prepared by dissolving the following reagents in distilled water, adjusting the pH to 9.8 and diluting to 100 mL:

NaHCO3	840 mg
MgCl2-6H2O	20 mg

The final reaction is prepared by mixing 1mL nitroblue tetrazolium (NBT) stock and 1mL 5-bromo-4-chloro-3-indolyl phosphate (BCIP) in 100 mL buffer: This reaction was stopped by rinsing with distilled water twice for 5 min each.

The following is a list of pertinent solutions:

TBS

50 mM Tris
150 mM NaCl
Adjust pH to 7.4

Carbonate Buffer

20 mg $MgCl_2$ $6H_20$
840 mg $NaHCO_3$
fill to 100 mL with ddH_20
pH with NaOH to 9.8

NBT & BCIP

dissolve 30 mg NBT in 300 µL H_20, 700 µL DMF
dissolve 15 mg BCIP in 1000 µL DMF
add above reagents to 100 mL of carbonate buffer just before use.
Note: these reagents are light sensitive with a maximum working time of 1 hour.

Please note that the water used in the preparation of all reagents is Milli-Q Plus water (18 megohm-cm resistivity). It meets or exceeds all ASTM, CAP, ACS, and NCCLS standards for purity.

Resistivity	18 megohm-cm
Total Organic Carbon	< 10 ppb
Particle Free	< 0.22 µm
Total dissolved solids	< 20 ppb
Silicates	< 0.1 ppb
heavy metals	< 1 ppb
Microorganisms	< 1 cfu/mL